Caps – Turns – Loops:

Designing Better β-Hairpins

Jordan M. Anderson

A dissertation

submitted in partial fulfillment of the

requirements for the degree of

Doctor of Philosophy

University of Washington

2017

Reading Committee:

Niels Andersen, Chair

Dustin Maly

Stefan Stoll

Program Authorized to Offer Degree:

Department of Chemistry

University of Washington

Abstract

Caps – Turns – Loops:

Designing Better β-Hairpins

Jordan M. Anderson

Chair of the Supervisory Committee:

Professor Niels H. Andersen

Department of Chemistry

As protein engineering promises advances in almost every field of science and medicine, a greater understanding of the protein folding problem is necessary to make these innovations a reality. This thesis examines one type of folded structure, the β-sheet. By designing several new peptide systems, the thermodynamics and kinetics of folding were examined quite thoroughly. Some of these include; a disulfide dimer "turnless" system used to investigate different β-capping strategies, an extensive residue search of [4:6] β-turns and a system to examine long flexible loops (> 20 residues), in which the loop connects β-strands that are in excess of 80% in a folded state. Lastly a conformational pH switch was developed, controlling the folded state of β-sheets. With these improvements, β-sheet design can become quite routine, hopefully expanding the usefulness of these ubiquitous structures.

Table of Contents

List of Figures

List of Tables

List of Abbreviations

CCD: Circular Coordinate Descent

CD: Circular Dichroism

COMU: (1-cyano-2-ethoxy-2-oxoethylidenaminooxy)dimethylamino-morpholino-carbenium hexafluorophosphate

CSD: Chemical Shift Deviation

CSDb: Chemical Shift Database

DIC: N,N'-diisopropylcarbodiimide

DIEA: N,N-diisopropylethylamine

DMF: dimethylformamide

DMSO: dimethyl sulfoxide

DSS: 2,2-dimethyl-silapentane-5-sulfonic acid

EtF: Edge-to-Face

Fmoc: fluorenylmethyloxycarbonyl

HBTU: N,N,N',N'-tetramethyluronium hexafluorophosphate

HDX: Hydrogen-Deuterium Exchange

HOBt: 1-hydroxybenzotriazole hydrate

NMP: N-methylpyrrolidine

NMR: Nuclear Magnetic Resonance spectroscopy

NOE: Nuclear Overhauser Effect

NOESY: Nuclear Overhauser Effect SpectroscopY

PPI: Protein-protein Interaction

ppm: parts per million

PyAOP: (7-azabenzotriazol-1-yloxy)trispyrrolidinophosphonium hexafluorophosphate

RD-NMR: Relaxation Dispersion NMR

RP-HPLC: Reverse Phase High-Performance Liquid Chromatography

SPPS: Solid Phase Peptide Synthesis

TFA: trifluoroacetic acid

TIPS: triisopropylsilane

T_m: Melting temperature

TOCSY: TOtal Correlation SpectroscopY

TTET: Triplet-triplet Energy Transfer

UV-Vis: Ultraviolet-Visible Light

Chapter 1. Introduction

1.1 Protein Structure and Composition.

At the root of nearly every motion and chemical transformation that the natural world undergoes, exists a protein. The function of each of these proteins is determined by its unique three-dimensional structure, which is completely encoded by the ordering and composition of each amino acid. Amino acids act as building blocks (monomers) of the larger polymeric protein. Although nature mostly uses only 20 different amino acids (Appendix A), the combination of these can create practically infinite different structures.

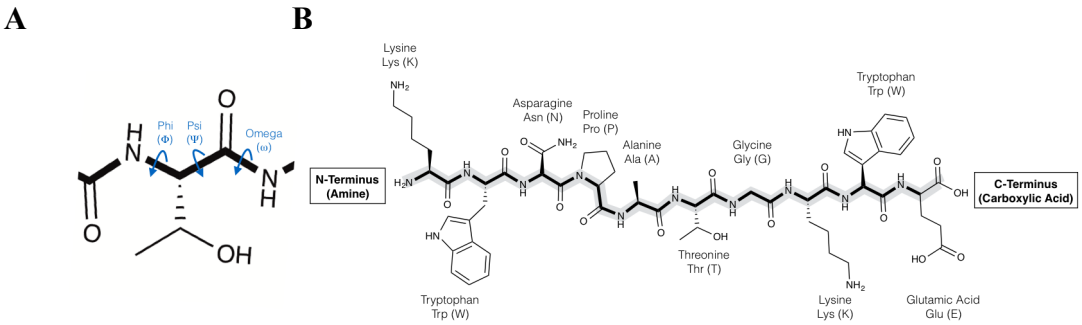

Figure 1.1. *An example peptide sequence. Each amino acid is labeled with the full name, and three and one letter abbreviations, with the backbone in bold. The sequence is KWNPATGKWE, in one letter abbreviation.*

Although amino acids share the same starting structure, linking together to create the backbone of the protein, they differ in the side chain that protrudes from each residue. These side chains add the functionality to the protein chain and determine the structure that the chain adopts, accomplished by varied size and functional group. By changing the side chain's size, the conformational entropy of the bond angles of the backbone around that position is modulated. Take for example the two extremes of this, glycine and proline. Glycine has no side chain, and thus has the least restricted conformational entropy of angles phi and psi (Figure 1.1A). At this position, the protein chain is able to move in almost any direction. Proline, in contrast, has a side chain that forms a 5-membered ring between the Cα and H_N atoms. With this, the

conformational space allowed is heavily restricted, as it turns out, this creates a kink in the backbone. These variations in restraints to angles phi and psi create local structuring which is designated as secondary (2^{o}) structure. These backbone restraints form structures such as α-helices, β-strands, and β-turns. Secondary structures are determined by the residues immediately before and after in sequence, and their backbone dihedral angles.

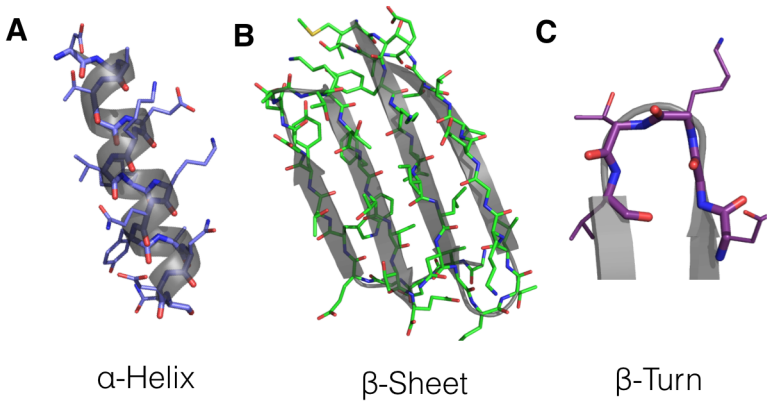

Figure 1.2. *Classes of secondary structure in proteins.*

The main classes of structure (in order of complexity – turns, β-sheets, and α-helices) are characterized by the phi/psi angles that are adopted by each residue after structuring. These angles are reinforced by additional interactions such as H-bonding, hydrophobic contacts and coulombic interactions (salt bridges). It is important to note that these classes of structures are the most commonly found ranges of phi/psi angles and are in no way the only structures that can be adopted. Since the two angles are within a single amino acid and the omega angle is a highly-restricted amide bond, it is more important to think of the two angles as changing at the same time instead of independently. Therefore, they are listed as a pair for each residue, typically not individually.

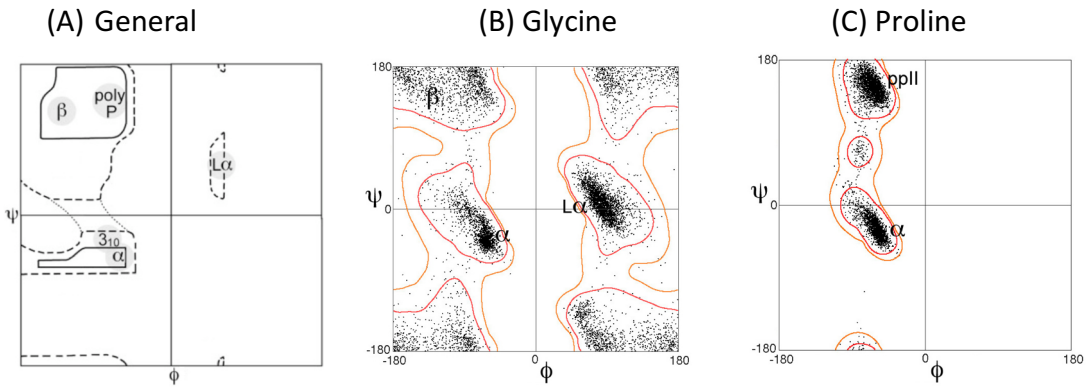

Figure 1.3. *Ramachandran plot. (Figure adapted from Richardson and co-workers* (Lovell et al. 2003)*)*

The most common way to visually represent the combination of angles phi and psi that are favored energetically is using the Ramachandran plot (Ramachandran, Ramakrishnan, and Sasisekharan 1963) (Figure 1.3). It plots the psi (ψ) angles from -180 to +180 on the vertical axis, and phi (ϕ) on the horizontal axis. The areas are described by borders showing favored regions, fully describing the torsion angle differences between the secondary structures mentioned earlier. This also allows for a complete identification of the differences in the allowed regions for different amino acids. In addition to the general Ramachandran plot shown in Figure 1.3, the amino acid specific plots for glycine/Gly and proline/Pro are shown (Lovell et al. 2003). This illustrate the significant difference in preferred phi/psi angles of the most and least flexible amino acids, respectively. Also, laying the basis for one of the energetics forcing a backbone into a specific structure, conformational entropy.

In addition to conformational restraints made by the side chains, long range contacts can also be made. The different amino acid side chains can interact with each other in many ways, including: coulombics (charge-charge), H-bonding and by hydrophobic forces. These can stabilize secondary structures present and act as a driving force for completing the protein folding process. Structures that are formed by such sequence-remote contacts are called tertiary

structures (3^o). Because of this β-sheets, composed of specifically aligned β-strands, should be considered 3^o structures, even though many regard them as secondary structures.

1.2 Forces of Folding

Considering how entropically-unfavored constraining a single residue to a single conformation would be, during folding this entropic penalty must be overcome by enthalpically favorable interactions (Sheu et al. 2000). Because proteins are in a constant equilibrium between the folded and unfolded states, the only covalent interactions between the residues are the amide bond and disulfides between Cys residues. The most important interactions that stabilize the folded states are the hydrophobic effect *(next section)* and a quite large collection of relatively small polar interactions (Sheu et al. 2000), differing in strength and distance dependence including; van der Waals, hydrogen bonding, salt bridges (charge-charge) and aromatic interactions. Although the nature of all polar interactions is electrostatic, the convention is to only refer to contacts between full positive and negative charge as such.

1.2.1 Hydrophobic Collapse

The main driving force for protein folding is thought to be hydrophobic collapse (Tanford 1962, 1997). This is the process of changing the solvation shell, the layer of water surrounding the protein, to optimize water's contacts. Because of water's highly polar structure, pure water exists as an ever-changing lattice of H-bonded water molecules. When a nonpolar molecule is incorporated into this lattice (Figure 1.4A), a void in the lattice structure must be made to accommodate the molecule, this disrupts the ability of water to H-bond with each other. If there are multiple nonpolar molecules near each other in water the lowest-energy solution is for the

nonpolar molecules to bind together and form a single void (Figure 1.4B). For example, if you were to whisk oil into pure water and let the solution settle, since oil is a nonpolar molecule that has no possible H-bonding interactions with water, all the oil molecules will find each other and separate from water – forming a single solvation surface. Polar molecules on the other hand can incorporate into this H-bonding lattice formed by the water (Figure 1.4C). Thus, a collection of ethanol molecules will stay in solution with water after mixing.

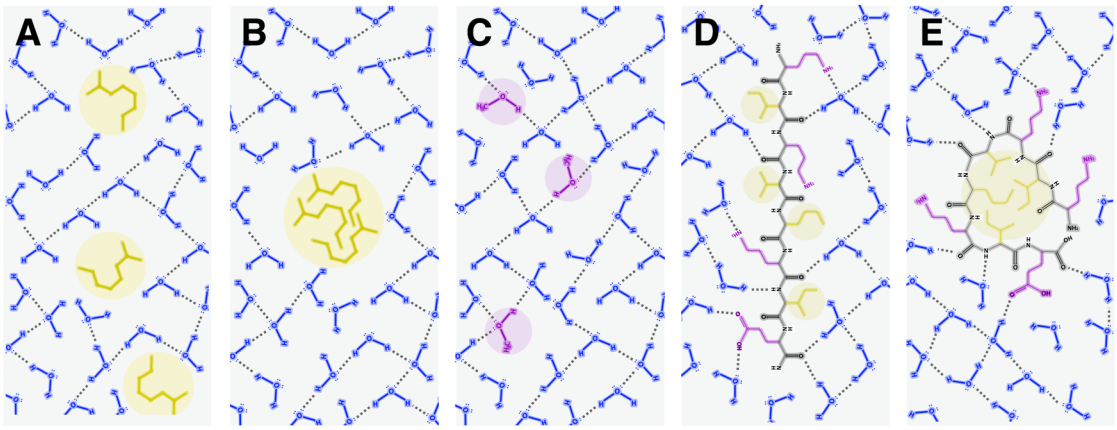

Figure 1.4. *Cartoon Representation of Hydrophobic Collapse. (**A**) Multiple hydrophobic molecules in water tend to exclude water and come together (**B**). (**C**) Hydrophilic molecules stay separated in water because they can participate in the H-bonding network created by water. (**D**) Unfolded peptide. (**E**) Folded peptide.*

In a polypeptide chain, different residues have different affinities for water, causing the apolar, hydrophobic residues to bury inside of the structure together. Since the polar (hydrophilic) residues can participate in hydrogen bonding, they help to solvate the folded structure (Figure 1.4D). This process of burying the nonpolar side chains is known as hydrophobic collapse (Figure 1.4E). Although this is by no means the only force favoring folding, it is commonly regarded to be the largest force for protein folding. In short, protein folding is a process where water forces a string of varying amino acids, which have practically

infinite conformations, into a single structure, spontaneously, quickly, *almost* always in the same way.

1.2.2 Van der Waals Forces

Van der Waals forces, (more appropriately London dispersion forces) are an attractive force which is a result of the fluid and polarizable nature of electronic clouds of non-polar groups. When two electron clouds become close, the repulsion reveals the positively charged nucleus, creating a temporary dipole, and thus a dipole-dipole attraction. After the initial hydrophobic collapse, van der Waals are arguably the most important force to stabilize a protein. Although individually they are short range and only provide ≤4 kJ/mol in stabilization (Petsko and Ringe 2004), there are so many of these, largely from amino acids with hydrophobic sidechains, that the sum is substantial.

1.2.3 Hydrogen Bonding (H-bonding)

Hydrogen bonding results from an electrostatic interaction in the polar bond that results from a hydrogen atom bonded to a highly electronegative atom (usually nitrogen, oxygen, fluorine or sulfur) and a non-bonding electron pair. The group containing the proton is referred to as the hydrogen bond donor, and the group containing the non-bonding electron pair, the acceptor. H-bonds can occur between the polar sidechains, but most importantly occur between different positions in the protein backbone. H-bonds are linear, in that there is a straight line intersecting the heteroatom of the donor, the proton, the non-bonding orbital and the acceptor heteroatom. Ranging in strength from 2-6 kJ/mol (Petsko and Ringe 2004), the collection of how various H-bonds twist and stabilize the backbone of the polypeptide, determines much of

the structure. β-Sheets have an alternating pattern of cross-strand H-bonds, and α-helices produce a pattern of i, i+4, with the backbone carbonyl H-bonding to the amide H_N 4 residues later in sequence.

1.2.4 Salt Bridges

In proteins, short range electrostatic interactions are referred to as salt bridges. They can take place between the sidechains of acidic and basic residues, but also to the charged termini of the backbone. These generally provide between 12-20 kJ/mol of stabilization, but can be as large as 30 kJ/mol when buried in the interior of the protein (Petsko and Ringe 2004). There is strong evidence that during the folding process salt bridges may serve a vital role. The other interactions listed are over short distances, and reduce quickly with distance. For comparison, van der Waals reduce by $1/r^6$ while electrostatics only reduce by 1/r (where r is the distance between the two interacting atoms); indeed, this may be why most protein termini are found in close proximity in the folded structure.

1.2.5 Aromatic Interactions

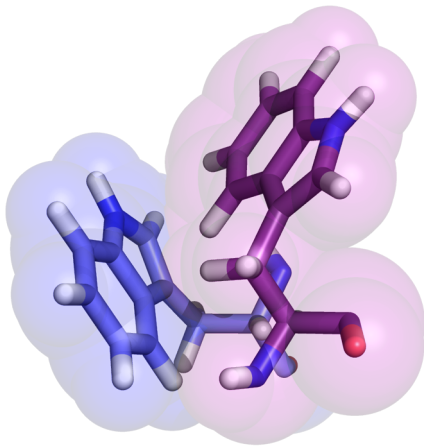

***Figure 1.5**. Trp/Trp Aromatic Cluster*

The aromatic amino acid's (phenylalanine, tryptophan, tyrosine and histidine) side chains can participate in a number of highly stabilizing interactions. In addition to producing hydrophobic contacts, the delocalized pi system of the rings creates a quadrupole with a negatively charged top and bottom and a positively charged ring periphery. Taking advantage of this,

aromatic clusters are produced by stacking of two rings, usually in an angled T-shaped edge to face orientation (EtF) (Jordan M. Anderson et al. 2016), shown with tryptophan in Figure 1.5. The strength of these interactions can vary in magnitude depending on the orientation and side chain type. There is much more information on this interaction in Chapter 3.

Charged side chains and H-bond donating groups can also interact with the quadrupole of aromatic side chains, usually in the form of Arg or Lys cation interacting with the negatively charged face of the aromatic, referred to as a cation-π interaction. In the same way, a H-bond acceptor uses a pair of non-bonding electrons, the pi electrons of an aromatic ring can also work as H-bond acceptors (Riemen and Waters 2009).

1.2.6 Disulfide Bonds

Cysteine sidechains end in a thiol group, which under mildly oxidizing conditions, can form a disulfide bond (-S-S-) with another cysteine. The S-S bond is a relatively weak covalent bond, and thus is also freely broken in reducing conditions. In nature, highly stable proteins can contain many disulfides, which form during or after the folding process. They may also present the problem of a kinetic trap if formed incorrectly. In laboratory settings, much care must be taken to avoid dimerization, or disulfide scrambling (the process of creating non-native disulfides during folding), especially in large proteins (Chang, Li, and Bulychev 2000). In general, the disulfide stabilizes structure by increasing the entropy of the unfolded state, thus increasing the ΔG of folding (Pace et al. 1988).

1.3 Folding Theory

Protein folding is a spontaneous and reversible process; thus, it is generally described as a single or series of equilibria. Because of the diversity of the natural world, no one model can be used to describe all folding pathways, but generally folding can be simplified to a two-state model. In an ensemble of proteins, there is only considered to be fully folded and unfolded molecules present. This is true because in most proteins there is one dominant transition state of significant free energy that nucleates the largest folding event, termed the nucleation-condensation theory of protein folding.

1.3.1 Energy Diagrams of Folding

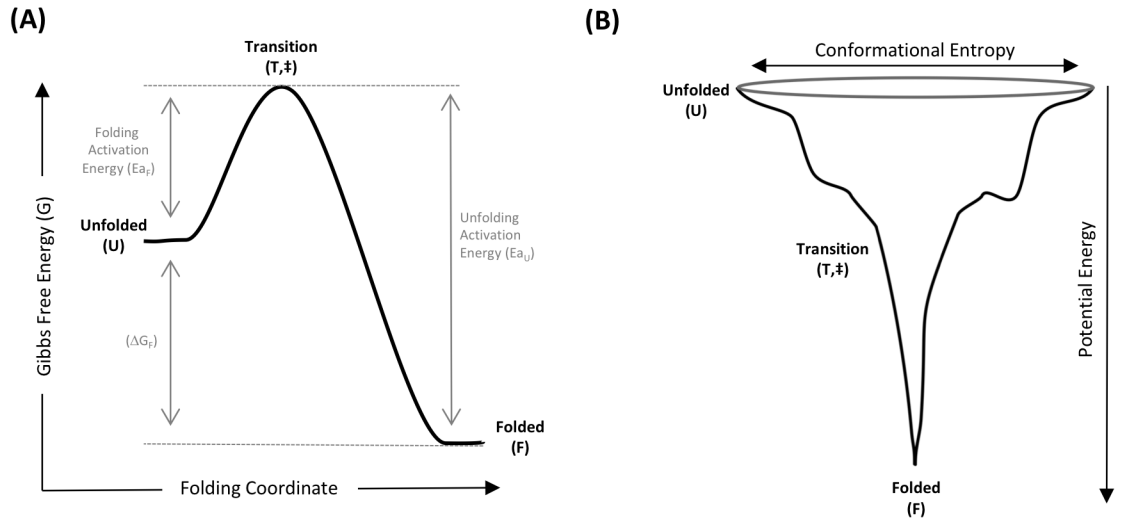

***Figure 1.6**. (**A**) Standard energy diagram representation of folding. (**B**) Folding funnel representation of folding.*

Folding is generally thought of in terms of Gibbs Free Energy (G), with ΔG_F and ΔG_U relating to the change in free energy for the folding and unfolding process, respectively. In a pure two-state model (Jackson and Fersht 1991; Zwanzig 1997) as ΔG_F decreases, the mole fraction of the folded state (χ_F) increases. This can be visualized by graphing G versus a folding

coordinate (Figure 1.6A), with the large hump (T) representing the transition state. Because of the large number of states possible with so many bonds a more correct version of this graph is the folding funnel (Clark 2004; Dill and Chan 1997) (Figure 1.6B), where energy is graphed against configurational entropy, in a 3D manner. The top of the graph there are many possible structures that would contain the same energy, and during folding there is a transition (T) which then nucleates a deep well in the funnel towards the native state (F).

Although the folding funnel is more correct, the first 1D representation easily demonstrates the relation between folding kinetics and thermodynamics. As the three states (U, F and T) are changed the kinetics of the folding and unfolding process change. In general terms, the energy distance between U and F determines the mole fraction in the folded state (χ_F), but the distance between U and T (folding activation energy, Ea_F) determines the rate at which folding will take place, with a larger barrier resulting in a slower folding rate.

Phi-value analysis takes advantage of these relationships to gain information on the transition state (Petrovich et al. 2006; Merlo, Dill, and Weikl 2005). Since this is what dictates much of a folding pathway, stabilizing or destabilizing this transition can have drastic effects on the protein. In Phi analysis, a mutation is made in a protein, and both ΔG_F and Ea_F are measured. If there is only a change in ΔG_F then that mutated site is not folded at the transition state, but if both ΔG_F and Ea_F change by a similar amount that site is a folded feature of the transition state.

Although most of the work presented here concerns the folding transition, in large proteins there are many other motions that occur in the folded state. One should always avoid thinking of a folded protein as a single conformation, most of function of a protein happens due to motions after, and in concert with folding.

1.3.2 Folding of the β-sheet

All the work presented in this thesis regards the folding of β-sheets or β-hairpins. The only difference between a β-hairpin and β-sheet is in what connects the sequential β-strands. A β-hairpin is connected, in sequence, β-strand, β-turn, β-strand, the turn being a defined organized structure. β-Sheet can refer to either a collection of more than 3 β-strands, or to a β-strand, loop, β-strand sequence, with a loop referring to an unorganized connecting piece, lacking any defined structure.

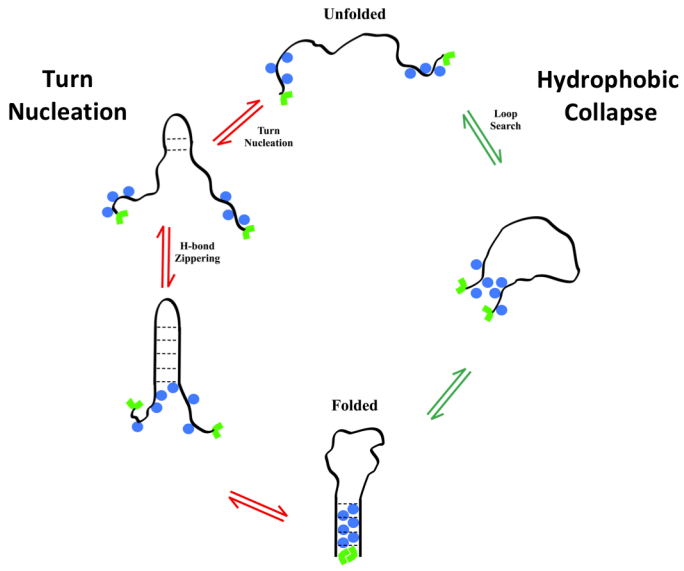

Figure 1.7. *β-Hairpin Folding Mechanisms.*

Traditionally, β-hairpins can be referred to as folding in two different mechanisms; either turn nucleation (Muñoz et al. 1997) or hydrophobic collapse (Dyer et al. 2004). Originally there was debate between these two mechanisms, and which one was correct, but now it is generally believed that hairpins can fold by either, depending on their composition. The difference between the two mechanisms is the extent to which turn formation is nucleating. Unlike α-helices, which can nucleate from any site and form the same fold, β-sheets must form in a specific way to form a specific inter-strand H-bonding register. This causes β-sheets to be much slower folding than α-helicies. One method of creating the order to align these strands is to use a nucleating turn (Lewandowska et al. 2010;

Huang, Larsen, and Chan 2012). A nucleating turn is a sequence of amino acids which have a collective preferred phi/psi angles that reverses the strand (Anderson et al. 2016), usually in concert with a number of local interactions (much more on this in Chapter 4). During the turn-nucleation mechanism, the turn is formed first, followed by a zippering of the residues away from the turn. Alternatively, the hydrophobic collapse mechanism starts using hydrophobic contacts between the strands, followed by an alignment of the strands which finally pushes the turn into a fixed orientation. Large β-sheets in proteins have been shown to contain a nucleating β-hairpin, which then leads to the orientation of the rest of the strands.

1.4 Misfolding and Aggregation

Many people study folding not to figure out what happens when everything goes right, but also why sometimes folding goes haywire. Protein misfolding diseases are a class of disorders where a protein in the body folds into a different structure, typically causing aggregation, forming fibrils or plaques which are toxic to the surrounding cells. Because free energies of aggregation are very negative, this last step is generally regarded as irreversible, which in return skews the equilibrium of this protein in the body. Examples include Alzheimer's, Parkinson's and Type 2 Diabetes, with the proteins involved being Aβ, α-synuclein and amylin respectively. With so many people affected by these deadly misfolding diseases, a better understanding of how this process happens, could result in a significant improvement in human life.

Aggregation is a process in which proteins form an oligomeric state, usually using non-covalent interactions, in an irreversible manner. Most oligomers of misfolding diseases are of a highly-ordered fibril state, but aggregation is a problem protein chemist work with in a more

general sense as well. As stated earlier, the exclusion of water during hydrophobic collapse is the driving force of protein folding. When hydrophobic sites make intermolecular contacts, oligomeric states can be produced, which can then form insoluble aggregates. This is a constant problem during the development of protein and peptide therapeutics. Similar to solubility, aggregation is concentration dependent, with more concentrated protein solutions more aggregate prone. Conversely, aggregation is more susceptible at higher temperature. Mechanistically, this is due to the unfolded state being more occupied at higher temperature, as temperature is increased the hydrophobic inside of the protein is exposed to the solution, allowing for intermolecular contacts to be made.

In the biologics industry, since aggregates are held so tightly in an inactive form, not designing with off pathway folding in mind can kill a product. Many protein drug formulations must be kept in a strict cold chain from production to administration, making many biologics unusable for neglected tropical diseases (G. Wang et al. 2013; Schlehuber et al. 2011). The problem is that commercial formulations must be kept at a high concentration, thus to keep the unfolded state from aggregating, must be kept refrigerated. A good example of this is Hubalek and co-workers (Vinther et al. 2015) at Novo Nordisk, who developed a disulfide-rich insulin analog that promises to help millions without proper access to refrigeration.

1.5 Peptide Therapeutics

Traditional drug design has largely been focused on the use of small molecules to target deep hydrophobic binding sites. This is usually done using the huge combinatorial libraries that drug companies have amassed. Small molecules are good candidates for the preferable orally available drugs for the market because they tend to be stable to the digestive tract and can move

through the body by passive diffusion. Unfortunately, most protein-protein interactions (PPIs) occur over large areas (1500 – 3000 $Å^2$) (Smith and Gestwicki 2012) which contain many "hot spots" of binding, instead of a deep cavern (London, Raveh, and Schueler-Furman 2013). This might be why the number of small-molecule drugs approved each year has remained unchanged (Albericio and Kruger 2012). Peptide therapeutics are ideal to mimic PPIs, due to their large size and ease of functionalization. Many natural peptides are already drugs such as: insulin, oxytocin and cyclosporine (Marx 2005). Using protein design techniques, chemists can take known peptide inhibitors or a piece of the native protein, and add fold stabilizing features. Typically, peptides in nature don't necessarily fold into a fixed structure until in the bound form. By stabilizing the folded state using helical stables, β-caps, cyclization or macrocycles, the entropic cost of folding to the bound form is reduced, thus increasing binding affinity. This discovery, together with the significant advancements in peptide synthesis, has caused a dramatic increase in the number of peptides entering the market over the last 10 years (Tsomaia 2015). Peptides have the added advantages of being less expensive to produce, more stable at room temperature and more easily penetrating tissues than recombinantly manufactured proteins. Additionally, since peptides are made synthetically, the introduction of novel functionalization is relatively easy, leading to a possible greater diversity in chemical space than proteins. In short, the future of peptide chemistry is bright.

1.6 Protein Folding Prediction

Within the folding of even a small protein, most of the interactions demonstrated so far can be found. This leads to an excessively complicated computational problem; evidenced by the fact that after the protein folding question was proposed 60 years ago (Dill et al. 2007), we

still cannot definitively predict a protein structure from a given amino acid sequence. Protein fold prediction can be broken down into two main categories, template based or *ab initio.* Template based fold prediction such as comparative modelling (Ginalski 2006) and threading (Rost, Schneider, and Sander 1997), use to some extent a sequence searching of databases of known structures or pieces of structures to produce the folded state. As the Protein Data Bank (PDB, http://www.rcsb.org/pdb) continues to grow past 100,000 structures, homology modeling of sequences can be quite good at producing the class of structure which a sequence contains. This is driven by the idea that there is a much small number of fold types that nature uses, compared to sequences, which are changed by evolution.

Ab initio structure prediction (Ding et al. 2008) is based on creating the ability to fold a protein from a somewhat extended or random coil state, mostly based on the physical bases of interactions (mentioned earlier). This requires an interplay between two functions, with most different programs using different versions of these functions. First, since the prediction is starting from some type of random-coil structure, a mechanism must be in place to choose direction and motion of each bond movement. Next, there must be a type of scoring function to determine whether that motion was advantageous or deleterious. Usually this scoring function is related to a theoretical free energy of the system. As the backbone and sidechains move, different possible structures are made, with the best-scored structure being taken as the solution.

Taken together, these methods work quite well in predicting the secondary structures of segments of a protein sequence. However, the most challenging aspect of prediction can be determining how the tertiary contacts are made, because these contacts are far in sequence, there are so many possibilities, and the number of bond rotations to get from one possibility to another is large.

Chapter 2. Materials and Methods

2.1 Solid Phase Peptide Synthesis (SPPS)

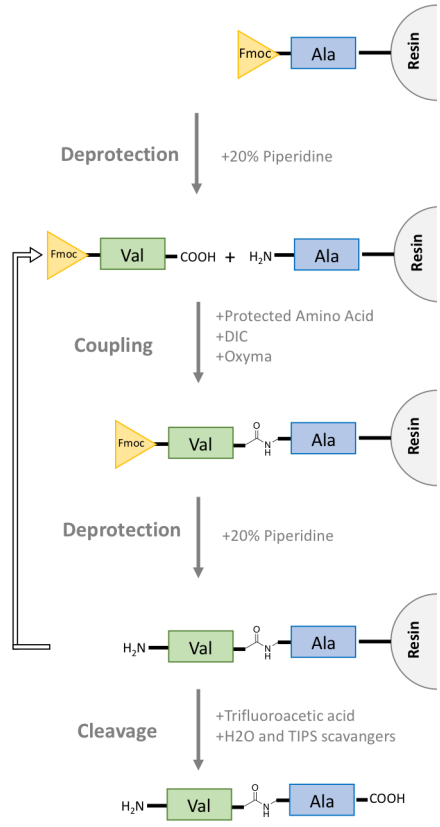

Figure 2.1. Schematic representation of a typical SPPS cycle.

The most valuable advancement in peptide sciences has been the invention of solid phase peptide synthesis by Merrifield, leading to his Nobel prize in 1984. (Mitchell 2008) Later advancements into automated synthesis and eventually microwave and conventionally heated synthesizers, has brought the cost and ease of making peptides to a new level.

Although the reagents have changed slightly to increase efficiency, the Merrifield synthesis concept hasn't changed since 1963. (Merrifield 1963) This method synthesizes a peptide by serially adding protected amino acids, to the resin-bound C-terminus, allowing for reagents to be quickly rinsed away, without need for purification between steps. This starts with preloaded resin, swelled in DMF (Dimethylformamide). Fmoc (Fluorenylmethyloxycarbonyl) deprotection is accomplished using a nucleophilic base such as piperidine or piperizine, revealing a free amine. After washing, the next Fmoc-protected amino acid can be added, typically using coupling agents DIC (N,N'-Diisopropylcarbodiimide) /Oxyma or HOBt (1-hydroxybenzotriazole hydrate) / HBTU (N,N,N',N'-tetramethyluronium hexafluorophosphate) and DIEA (N,N-Diisopropylethylamine), creating an activated carboxylic acid which couples

with the free amine on resin to create the peptide bond. This process can then be repeated to create the sequence of a desired peptide. After that sequence is completed, the peptide can be cleaved from the resin using a strong acid (trifluoroacetic acid) with radical scavengers. More hindered or difficult couplings can be accomplished using stronger coupling reagents such as PyAOP ((7-Azabenzotriazol-1-yloxy)trispyrrolidinophosphonium hexafluorophosphate) or COMU ((1-Cyano-2-ethoxy-2-oxoethylidenaminooxy)dimethylamino-morpholino-carbenium hexafluorophosphate). Additionally, there are several different commercial resins available to change the C-terminus, such as amidating the terminus (Rink-Amide resin) or releasing a fully protected peptide (2-Cl-Trityl resin) which can then be cyclized or further derivitized.

Advances to this basic procedure, along with the additions of pseudoprolines and orthogonal protecting groups for conjugate chemistry, synthesis of peptides up to 50 residues has become quite routine. Even peptides greater that 100 amino acids have been synthesized in this manner. With the improvements made to automated peptide synthesizers, the price of this has also come down substantially. (Behrendt, White, and Offer 2016)

2.1.1 General method for SPPS

For the present study, peptides were synthesized using microwave-assisted, automated SPPS (Liberty Blue synthesizer, CEM), using Fmoc-protected, preloaded Wang resin (0.3-0.4 mmol/g) for acid termini and Fmoc-protected Rink-Amide resin for amidated C-termini. For a 0.1 mmol synthesis, coupling is accomplished using 5 eq of DIC, Oxyma, and Fmoc-amino acid in 5 mL DMF at 75 ^{o}C for 10 min. Deprotection was accomplished using 4 mL of 20% v/v of piperidine/DMF at 75 ^{o}C for 5 min. After the synthesis was completed, the peptide was sidechain-deprotected and cleaved from resin by mixing in a cleavage cocktail of TFA:TIPS:H_2O

(Trifluoroacetic acid : Triisopropylsilane : water) (38:1:1) for 1 hr at room temperature. The resulting solution was concentrated and crashed out with cold ether. After centrifugation and washing two additional times, the crude product was purified by reverse-phase HPLC (10 – 90% H_2O/acetonitrile, 0.1% TFA, C18 column). The purified peptide was lyophilized before use.

Larger peptides were synthesized on preloaded PEG-matrix resin at a loading of 0.2 mmol/g (Tentagel R resin, Rapp Polymere GmbH), this prevents aggregation on the resin. Peptide sequences containing -DG- or -NG- were synthesized using piperazine (10% w/v in 90:10 NMP (N-methylpyrrolidine) : ethanol), to reduce aspartimide formation. Cys and His residues were coupled at a temperature of 50 ^{o}C for 10 min, to reduce epimerization.

2.2 Circular Dichroism (CD)

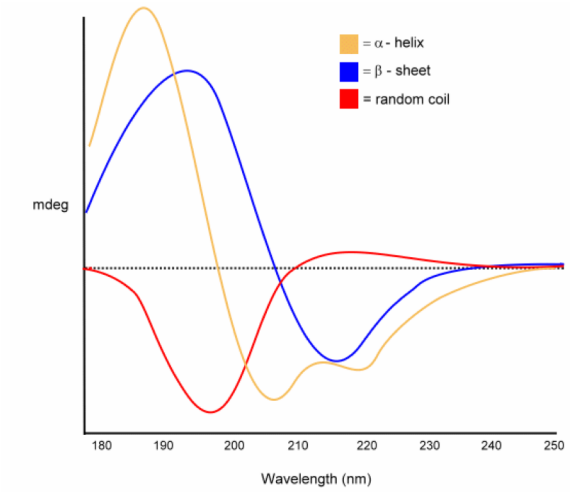

Figure 2.2. *Example CD spectra of typical secondary structure.*

With respect to proteins, circular dichroism (CD) usually refers to far-UV CD (180-250 nm). A CD spectropolarimeter works by measuring the differential absorption of the left and right circularly polarized light of a sample. Since peptides are, by nature, chiral (and thus optically active), CD can report of the orientation of the different electronic transitions of the amide bond, which absorbs in this region. And because the position and intensity of the electronic transitions are bond angle dependent, CD reports on the secondary structure of the protein backbone. (Kelly, Jess, and Price 2005) Figure 2.2 shows

idealized spectra of α-helix, β-sheet and random-coil structures. Each spectrum is made up of the combination of $\pi \rightarrow \pi^*$ and $n \rightarrow \pi^*$ transitions centered around 190 and 220 nm respectively. (Whitmore and Wallace 2007) β-Sheet protein spectra have a $\pi \rightarrow \pi^*$ maximum at 196 nm and a $n \rightarrow \pi^*$ minimum at 218 nm. The α-helix spectra contain a $n \rightarrow \pi^*$ transition with a negative peak at 222 nm and a large positive peak at 192 nm and a smaller negative peak at 209 nm due to exciton coupling of the $\pi \rightarrow \pi^*$ transition. Finally, a random-coil spectrum contains a small positive $n \rightarrow \pi^*$ peak at 212 nm and a negative $\pi \rightarrow \pi^*$ peak at 195 nm. Additionally, transitions involving the various bands of aromatic chromophores can also show up in this region (more in section 2.4.1). The main experimental advantages of CD are that it can be done at a low concentration (μM), over a large temperature range, and can report on the secondary structures of proteins and peptides where other methods can fail.

2.2.1 General Method for CD data collection

Stock solutions of purified and lyophilized peptide were made at ~ 200 μM peptide concentration in 20 mM potassium phosphate buffer, with the peptide concentration verified using the UV absorption of Trp or Tyr residues ($\varepsilon_{280\ nm}$ = 5690 and 1280 $M^{-1}\ cm^{-1}$ respectively), which was then diluted to 30 μM. CD spectra were acquired (JASCO 720 spectrophotometer) at 10 ^oC intervals from 5 – 95 ^oC, using a scanning rate of 100 nm/min from 190 – 270 nm at 8 iterations.

2.3.0 Nuclear Magnetic Resonance (NMR)

Nuclear Magnetic Resonance (NMR) at its simplest description uses a large magnet to look at little magnets. In the present case, the "little magnets" are hydrogen nuclei, and the big magnet is a superconducting 14-tesla electromagnet. When the spin-active proton is placed in a magnetic field, the magnetic moment of the nuclei will align with the field in two ways, with (in-line), or against the field. Because one of these states is at higher energy, it is less populated based on the Boltzmann distribution, thus causing a macro magnetic vector in-line with the magnetic field. During an NMR experiment, as a radio frequency pulse (RF) is applied, this vector will be rotated by 90^{o}, and then will precess around the field axis (Lamor precession), relaxing back to the orientation of the magnet. The frequency of this precession is based on the electronic environment of that the proton is experiencing. The signal produced by this can allow the chemist to investigate the structure and kinetics of a peptide's folding and interactions.

Unlike many biophysical techniques, NMR is uniquely suited to be able to report over the entire peptide molecule. Because ^{1}H NMR detects all protons in solution, a very complete understanding of what is happening is capable. Assignment of the peptide sequence is possible using a combination of TOCSY and NOESY pulse sequences. TOCSY (Braunschweiler and Ernst 1983) (TOtal Correlation SpectroscopY), is most closely related to the COSY pulse sequence. It allows for the two-dimensional correlation of spins which are participating in, through bond, scalar coupling. COSY is restricted in the distance this bond network can be, typically protons will not produce any correlation cross-peaks more that 4 bonds (4J) away. To overcome this, TOCSY uses a repeated 180^{o} pulses to extend the effective distance. Commonly termed Hartmann-Hahn coupling, the pulses during the mixing period causes the polarization to

spread out over the entire spin system, thus causing correlation between all protons in said system.

NOESY (Nuclear Overhauser Effect SpectroscopY) produces correlation cross-peaks, using the Nuclear Overhauser Effect (NOE). NOEs are dipole-dipole couplings of the magnetic moments and are not constrained by communication through bonds. These are purely distance dependent, with the correlated peak intensity growth rate reflecting the distance between the protons by a $1/r^6$ relationship, where r equals the distance between the nuclei. (Friebolin 1998) This is a powerful technique to investigate protein structures, because although many protons may be far in sequence (invisible to TOCSY) they can still be close in space (visible to NOESY).

Assignment of a peptide backbone can be accomplished using these two techniques. Unsurprisingly, a single residue's H_N and Hα creates a strong peak in the TOCSY experiment, but because the carbonyl of the amide bond breaks the spin system, no TOCSY cross-peaks appear between sites in separate residues. NOESY on the other hand, creates a strong peak between the H_N of i and the Hα i-1 and between Hα of i and H_N of i+1. By combining these experiments, a chemist can sequentially walk up or down the peptide backbone, additionally using the TOCSY spectra to verify that each H_N or Hα is attached to the correct side chain spin system.

2.3.0.1 General Method for 2D NMR data collection

Starting with a purified and lyophilized peptide, NMR samples were made at ~ 1 mM peptide concentration in 20 mM potassium phosphate solution with 1 mM DSS (4,4-dimethyl-4-silapentane-1-sulfonic acid) present as an internal standard and 10% D_2O as a lock solvent. TOCSY (pulse = dipsi2esgpph) and NOESY (noesyesgpph) spectra were acquired on Bruker AV

series instruments (500, 700 or 800 MHz). Data was processed using NMRPipe (https://www.ibbr.umd.edu/nmrpipe), and assigned using Sparky (https://www.cgl.ucsf.edu/home/sparky). The assigned chemical shifts were then transferred to the CSDb (an in-house database and analysis software, available publically at: http://andersenlab.chem.washington.edu/CSDb) (Niels H. Andersen et al. 1997; N H Andersen, Cao, and Chen 1992). All the peptides in this thesis are listed with their CSDb ascension name in Appendix B. Full proton assignments can be found for each peptide in Appendix C.

2.3.1 Chemical Shift Deviations (CSDs)

The chemical shift can tell a spectroscopist a lot about the chemical environment of protons in a peptide. Although inductive effects of bonding can be informative in some circumstances, such as the presence of a disulfide bond, or H-bonding, anisotropic effects of different functional groups causes the greatest shifts upon structuring. Also, unlike in small-molecule NMR, the absolute chemical shift is less useful, because different amino acids have different inductive effects, especially at the H_N and Hα sites, and we are more interested in what chemical shift changes as result of structuring. Therefore, chemical shifts are typically cited as Chemical Shift Deviations (CSDs) where a reference chemical shift, of where that proton is expected to be in at the random-coil structure, is subtracted from the observed chemical shift. This allows for the reporting of the change in chemical shift associated with folding. For the most part, two functional groups are responsible for CSDs, the amide backbone and aromatic side-chains.

The amide bond produces a field of magnetic anisotropy, due to the pi bonding system between the carbonyl and the nitrogen of the backbone amide. When in the magnetic field of the

NMR, the group is shielding above and below the plane of the amide, while deshielding in the plane of the amide. This causes the backbone protons to have significantly different chemical shift depending on the phi/psi angles of the neighboring, or even cross-strand, residues. For example, β-sheets produce an elongated structure, causing the Hα and H_N to be in the same plane as the amide. Additionally, cross-strand, the Hα and H_Ns are in the same plane as both the local backbone, but also the cross-strand backbone. This causes these protons to be de-shielded (CSD > 1 ppm), with the protons sequestered between two strands, more deshielded than those on the exterior. On the other hand, during the formation of a β-turn, because the plane of the amides, must be closer to orthogonal to each other, to accomplish a turn, there are areas where the protons of the backbone are highly shielded (CSD < -1 ppm). The collection of these CSDs over the entire backbone can lead to a diagnostic verification of the folded structure.

When an aromatic ring is placed into a magnetic field, the electrons in the pi system create a ring current, which produces a magnetic field opposite to the external magnetic field. This magnetic anisotropy results in shielding above and below the plane of the aryl ring, and de-shielding in the plane of the ring. In proteins, aromatic rings will produce significant changes in chemical shift, depending on the specific orientation and proximity.

2.3.2 Fraction Folded

Since the folded structure of proteins or peptides can be thought of as an equilibrium between the folded and unfolded states, if this equilibrium is fast the chemical shift reports on the population weighted average of these two states, CSDs can also be converted into a molar fraction folded (χ_F). With the CSDs already corrected for the chemical shift of the proton at χ_F=0, if the CSD of the proton at a known χ_F is available, the relation is stated in equation **1**.

$$\chi_F = \frac{CSD_{obs}}{CSD_{ref}} \chi_{F\,(ref)} \qquad [\mathbf{1}]$$

Using the relationship between the equilibrium constant ($K_{eq} = \chi_F/(1-\chi_F)$) this can also be used to calculate a change in Gibbs Free Energy (ΔG), shown in equations **2** and **3**.

$$\Delta G_U = RTlnK_{eq} \qquad [\mathbf{2}]$$

$$\Delta G_U = RT\ ln\frac{\chi_F}{1-\chi_F} \qquad [\mathbf{3}]$$

The CSDs associated with specific χ_F are usually verified by another technique, such as hydrogen-deuterium exchange (HDX), but can also be inferred by the slope of the melting curve of the CSDs.

2.3.3 Hydrogen-Deuterium Exchange (HDX)

Hydrogen-deuterium exchange (Dempsey 2001) (HDX) is a valuable technique to determine the amount of sequestration of exchangeable protons in a protein. When an amide H_N proton is hydrogen bonded in the folded state, it will only have an opportunity to exchange with solvent in the unfolded state. Thus, if a protein is highly folded there is less time for the amide proton to interact with the solvent, because the protein is spending less time in the unfolded state. In HDX by NMR (Dempsey 2001), this phenomena is taken advantage of by placing a fully protonated protein into deuterated solvent (D_2O), and then monitoring the decrease of the amide protons over time. The rate at which these protons decreases in intensity, is directly correlated with the χ_F of the structure.

2.3.3.1 General Method for HDX

Hydrogen-Deuterium Exchange (HDX) samples were made at ~ 1 mM peptide concentration from lyophilized peptide in 20 mM potassium phosphate buffer with 1 mM DSS.

The sample was then frozen and lyophilized. Chilled D_2O was then added, the sample was mixed, and followed immediately by the collection of 1D ^1H (pulse = zgesgph, receiver gain set for the first experiment then copied for each additional time point) spectra in increments of 30 sec for the first 10 min, then 1 min for the next hour, then 15 min for the next 6 hours, then 30 min for the next 6 hours. After all data were collected, the pH of the sample was measured and recorded. Data was processed in Topspin (Bruker), then the decay of the relative heights of exchangeable backbone protons was calculated.

2.3.4 Structure Elucidation

In addition to NMR giving a sense of rate of exchange between the folded and unfolded state, it is also possible to elucidate a three-dimensional structure from NMR data. NOEs are distance dependent by $1/r^6$ (where r equals the distance between the two nuclei), if a large enough collection of NOEs are produced, using computational models, there are only a small number of solutions where these distance restraints can all match and the backbone connectivity's stay correct. Usually this is accomplished by modeling the peptide starting from an elongated structure then cooling gradually, with the experimentally-determined restraints becoming increasingly tighter. This, in combination with a force-field to model the interactions of a protein's atoms, results in a useable structure. Coupling constants of backbone H_N protons, which depend and thus report on the phi angle, can provide additional constraints, using the Karplus relationship of the $^3J_{HN\text{-}Ha}$ coupling (Li et al. 2015). NMR structure elucidation has a major advantage over X-ray crystallography, because crystals do not need to be formed, which can be a significant obstacle. Also, due to additional possible contacts between proteins in the crystal, the structure may differ from that in solution,

2.3.5 Relaxation Dispersion NMR (RD-NMR)

Again, consider that the position of a signal observed during NMR is a population weighted average of the positions of the folded and unfolded states. This is because the exchange rate ($k_{ex} = k_F + k_U$) between the two states is much faster than the change in frequency of the signals associated with the two states ($k_{ex} >> \delta\nu$). If this exchange rate is significantly slower than $\delta\nu$, the two states will appear as separate sets of peaks, known as slow exchange. As this exchange rate is increased, the two peaks will begin to move closer together and begin to broaden until they coalesce at the weighted average ($k_{ex} \approx \delta\nu$). This regime is known as the intermediate exchange region. Between this and the fast region, the signals will appear as one peak, but broadening will occur with respect to the rate of the exchange between the two states.

Several different factors affect the observed linewidth (Δ^{obs}) of a signal in an NMR spectrum. These can be split into two groups; (Δ^{o}) the intrinsic linewidth of the spectra or (Δ^{ex}) linewidth broadening due to exchange between the two states (equation **4**).

$$\Delta^{obs} = \Delta^{o} + \Delta^{ex} \qquad [\mathbf{4}]$$

Intrinsic linewidth is largely effected by experimental conditions (i.e. viscosity, field inhomogeneity…) and the intrinsic T_2 of the proton, whereas Δ^{ex} is from the rate of the exchange between the folded and unfolded states. Using a reference of a similar proton that experiences no chemical shift change between the two states, Δ^{o} can be subtracted from Δ^{obs}, leaving only Δ^{ex}. The relation between this linewidth broadening and the exchange lifetime (τ_{ex}) is shown in equation **5**, where χ_F and χ_U are the molar fractions of the folded and unfolded states, respectively, and $\delta\nu$ is the frequency distance between the two states.

$$\Delta^{ex} = 4\pi\, \tau_{ex}\, \chi_F\, \chi_U\, (\delta_\nu)^2 \qquad [\mathbf{5}]$$

This can also be described as rate constants of folding (k_F) and unfolding (k_U), in equations **6a** and **6b**, respectively.

$$k_F = 4\pi\,(\chi_F)^2\,\chi_U\,(\delta_\nu)^2(\Delta^{ex})^{-1} \qquad [\mathbf{6a}]$$

$$k_U = 4\pi\,\chi_F(\,\chi_U)^2\,(\delta_\nu)^2(\Delta^{ex})^{-1} \qquad [\mathbf{6b}]$$

The actual Δ^{obs} values can be calculated in a number of different ways, but usually involves some form of data fitting to a mathematical model. These models involve simulating the peak of interest with a collection of Lorentizian expressions, placed at the distance and intensities relating to the various J couplings which the proton is involved in. More complete simulations, such as MEXICO (Bain, Rex, and Smith 2001) and Bruker's TOPSPIN DNMR (a version of TEDDY (Rohonczy 1992)), can also simulate second-order effects by including the distance the simulated coupled protons are from each other. This can be especially useful when dealing with systems with small broadening.

The use of a reference signal is incredibly helpful during RD-NMR calculations, due to the simplifications allowed, stated above. This assumes both the observed and reference signals are clear of other proton signals, which can be difficult as the peptide becomes larger, and broadening of other protons occur. However, if there are two shifted signals, experiencing broadening from the same motion, and this broadening is much larger than the difference in intrinsic linewidth they may have, this can be sufficient to calculate the dynamics of the process.

Consider two protons, *a* and *b*, which are shifted due to the same motion, the exchange broadening of each would relate to the rate constant of the motion in the following equations.

$$\Delta_a^{ex} = \frac{4\pi X_U X_F^2 \Delta\nu_a^2}{k_F} \qquad [\mathbf{7a}]$$

$$\Delta_b^{ex} = \frac{4\pi X_U X_F^2 \Delta\nu_b^2}{k_F} \qquad [\mathbf{7b}]$$

With each lineshape broadening due to exchange (Δ_a^{ex} and Δ_b^{ex}) relating in the following ways.

$$\Delta_a^{ex} = \Delta_a^{obs} - \Delta^o \quad [\mathbf{8a}]$$

$$\Delta_b^{ex} = \Delta_b^{obs} - \Delta^o \quad [\mathbf{8b}]$$

Since the signals are experiencing the same experimental environment, all the broadening effects due to field inhomogeneity will be the same. The only difference between the two Δ^o is a small difference in the intrinsic T_2 of each signal. If these signals are assumed to be similar in nature, and this ΔT_2 intrinsic is much smaller than the broadening due to exchange, Δ^o of *a* and *b* can be assumed to be equal. As stated before, because this is due to the same motion, k_F and fraction folded (χ_F), will be the same for both *a* and *b*. Thus, the reference signal can be subtracted from the calculation resulting in equations **9a** and **9b** for k_F and k_U, respectively.

$$k_F = 4\pi\chi_U\chi_F^2 \frac{(\Delta\nu_a^2 - \Delta\nu_b^2)}{(\Delta_a^{obs} - \Delta_b^{obs})} \quad [\mathbf{9a}]$$

$$k_U = 4\pi\chi_F\chi_U^2 \frac{(\Delta\nu_a^2 - \Delta\nu_b^2)}{(\Delta_a^{obs} - \Delta_b^{obs})} \quad [\mathbf{9b}]$$

2.3.5.1 General method for RD-NMR data collection

RD-NMR samples were made by dissolving lyophilized peptide in 0.6 ml of 20 mM potassium phosphate buffer with 1 mM DSS to produce a ~ 1 mM solution. This sample was then frozen and lyophilized, and dissolved in pure D_2O. 1D ^1H NMR spectra (pulse = zgesgp) were collected at a variety of magnet field strengths (Bruker AV series 300, 500, 700 and 800 MHz) at temperatures ranging from 275 – 330 K. Spectra were processed in Topspin (Bruker) and lineshape fitting was accomplished using Topspin's DNMR program, assuming the coupling constants found in Appendix D. Further description of the data analysis can be found in the previous section of this chapter.

2.4 Diagnostics of the β-Cap

As mentioned earlier, aryl-aryl clusters can stabilize the fold of β-sheets and hairpins by 7-9 kJ/mol. One basis of this stabilization is the quadrupole-quadrupole edge-to-face (EtF) interaction. The most stabilizing of which is the tryptophan-tryptophan EtF, shown in figure 2.4. This has been found to be especially stabilizing at the termini of a β-hairpin, which will be present in many of the systems used in this thesis. This arrangement of aromatic rings produces a number of spectroscopic diagnositcs; these are presented and discussed in the following paragraphs.

2.4.1 CD

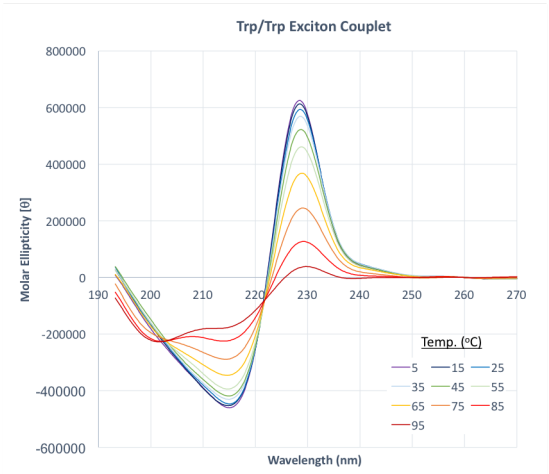

Figure 2.3. *CD spectra of a Trp/Trp exciton couplet.*

In CD spectra, the Trp/Trp aromatic cluster appears as an exciton couplet with a maximum at 228 nm and a minimum at 215 nm (Figure 2.3). This is usually the dominating feature in each spectrum due to the molar ellipticity of a folded couplet often being as large as ~ 600,000 deg mol^{-1} cm^{-1}. The temperature dependence of this feature serves as a good representation of the melting of the β-cap.

2.4.2 NMR

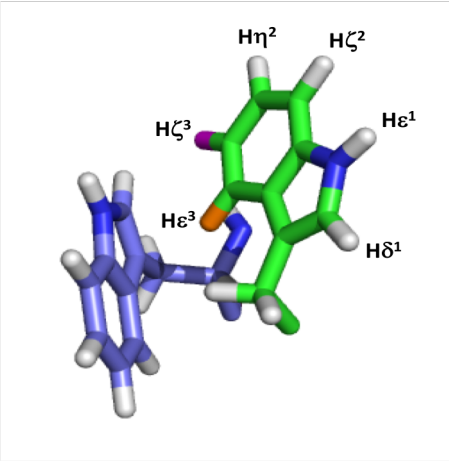

Figure 2.4. *The Trp/Trp EtF interaction*

Due to the significant ring current of the indole side-chains in the β-cap, the $H\varepsilon^3$, $H\zeta^3$ and $H\beta^x$ protons of the edge Trp are shifted significantly upfield in the folded state, by (CSD) -2.50, -0.65 and -0.30 ppm. This gives a large range of diagnostic proton signals; the aromatic signals are in a relatively uncomplicated region of a protein ^1H spectra. In the same peptide, the $H\varepsilon^3$ and $H\zeta^3$ protons of the "face" indole, are shifted less than 0.1 ppm in the folded state, providing reference peaks in RD-NMR (Section 2.3.5). In more complicated spectra, $H\delta^1$ and $H\zeta^3$ of the edge indole can also be used together to find the folding dynamics by the second method listed previously, equations **9a** and **9b**.

Chapter 3: β-Capping – An Optimized β-Cap Using Coulombic Interactions.

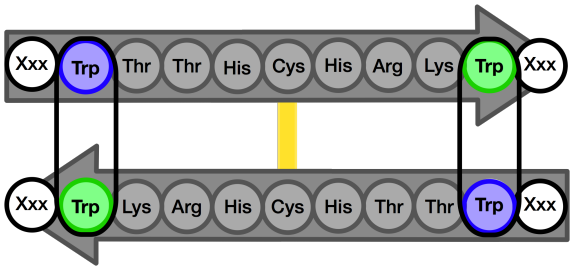

3.1 Introduction

The study of β-sheets has been hampered by a lack of systems that fully isolate β-strands from their protein contexts (Gellman 1998). Improvement in this situation have the promise to lead to the design of inhibitors, hydrogels and even catalysts. β-Hairpins were the obvious choice for these designs, but when excised from a larger β-sheet, natural β-hairpins have a tendency to be insoluble and unfolded. Some of the first attempts to obtain "stable" systems include the second hairpin of the B1 domain of protein G (GB1) (Blanco, Rivas, and Serrano 1994) and the N-terminal hairpin of Ubiquitin (Searle, Williams, and Packman 1995). Although these were massive improvements at the time, they were still only 40-60 % folded. The largest improvement in isolated hairpin stability came with the design of the "Tryptophan Zippers" by Cochran et al. (Andrea G Cochran, Skelton, and Starovasnik 2001) This design used a collection of 4 Trps arranged as two Trp/Trp aromatic clusters, with remarkable stability, this system yielded T_ms greater than 340 K in some cases. Unfortunately, these were small systems with most of the

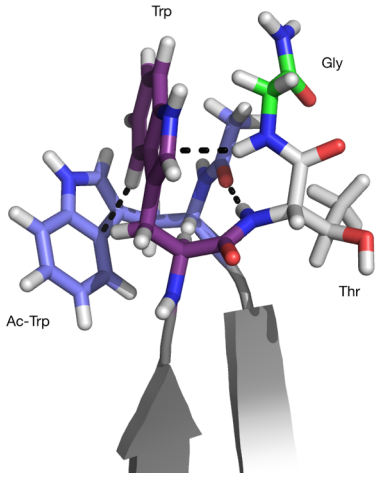

Figure 3.1. *The Kier β-Cap, relevant interactions presented in text shown with dotted lines.*

β-strands made up of Trps. Not optimal for the study of native hairpins, when this was reduced to one aromatic cluster the T_m dropped to 315 K. In this chapter, I describe hairpin systems with β-end-capping, which require minimal change at the termini to stabilize beta structure.

β-Capping was first introduced by Kier et al, (Kier et al. 2010) as a way to create highly stable β-hairpins without terminal fraying. It employed an Ac-W- N-terminus and a -WTG-NH_2 C-terminus, and these provided 6-9 kJ/mol of fold stability to a β-hairpin system. This designed motif incorporates a number of interactions (Figure 3.1), the most stabilizing of which is a Trp/Trp edge-to-face (EtF) interaction (see Section 2.4 for interesting spectroscopic consequences). The TG-NH_2 of the C-terminus, folds back on itself forming an aromatic-H-bond between the C-terminal Trp and the H_N of the glycine, causing this proton to be shifted > 2.7 ppm upfield. The carbonyl of the acetylated N-terminus also produces a strong H-bond with the H_N ***and*** the hydroxyl of the C-terminal Thr. Creation of this simple motif made the design of β-hairpins more folded than before quite routine, without the need for drastic redesign.

The original Kier β-cap is also very easy to functionalize at the N-terminus with essentially any carboxylic acid using standard coupling to the free amine, in place of the acetyl group. This can even be taken a step further, by using a di-carboxylic acid to create specific angles between β-strands, which in turn was found to be useful in creating larger ordered structures. (Kier and Andersen 2014b, 2014a) Additionally, some work by Waters (Cline and Waters 2009) demonstrated that the stability of a β-hairpin can

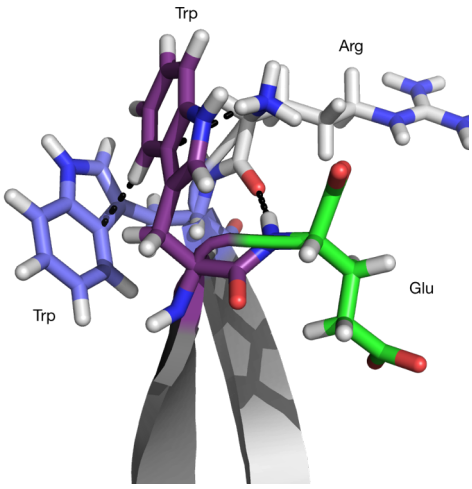

Figure 3.2. *The Coulombic Cap. Major interactions leading to fold stabilization shown with dotted lines.*

lead to reduced proteolytic activity, showing it may be useful for therapeutics. Even with these advantages, this β-cap is still limited since it terminates each strand, and displays some solubility problems.

In this chapter, the development of an alternative capping technique which continued the work of Kier, using complementary charged side-chains at the termini, is described. The best of these is the RW / WE pair (for the N and C termini respectively, Figure 3.2) pair. This motif is referred to as the *coulombic cap*. In common with the Kier β-cap, the Trp/Trp EtF interaction is central to the stabilization effect; there is also a H-bond between the two terminal residues, H_N of the C-terminal Glu and the carbonyl of the N-terminal Arg. The most significant difference is in the H_N-aromatic bond. In the prior β-cap this interaction is between the C-terminal Gly and the Trp, whereas in the coulombic cap, there is a H_N-aromatic interaction between the N-terminus and the C-terminal Trp. This creates more of a caged motif around the aromatic cluster. Terminal H_Ns are typically invisible by ^{1}H NMR due to exchange with the solvent. CSDs of the Hα of the terminus is always shifted upfield by > 0.5 ppm in a folded cap, when residues are extended on either side of this motif, this H_N is also observed > 1 ppm upfield. This evidence, in addition to NOE-derived structures of the cap, show that free N-termini is H-bonding into the ring of the C-terminal Trp.

3.2 System Design

XWTTHCHRKW**Z**
|
ZWKRHCHTTW**X**

Figure 3.3. *The Turnless Hairpin system.*

For the optimization of this coulombic cap, a specific peptide system was chosen to probe only the termini, with variable stability. A disulfide dimer, "turnless hairpin" system, was used with a scaffold of $(XWTTHCHRKWZ)_2$, where the central Cys creates a disulfide bond with another β-strand,

creating the dimer (Figure 3.3). Using this system, we avoid any effects of a turn, also exaggerating the effects of the Cap from having two per molecule. In the center of the peptide there are four His residues surrounding the disulfide. When designing highly folded systems these act to modulate the stability of the strand. When the pH of the solution is lowered unfavorable cross-strand repulsive charges destabilized the β-structure of the strand. A non-His version was also used, with the sequence $(XWTTVCIRKWZ)_2$. Occasionally, if the system is too folded, a better comparison is between the low-pH destabilized version. This system was first used by Kier, (Kier et al. 2010) who established that the (CH_3CH_2CO-W-TTVCIRK-WTGPK-NH_2) peptide has a $\chi_F = 0.985$ at 280 K, based on H/D exchange (HDX), which is reduced to $\chi_F = 0.72$ ($\Delta\Delta G_U = +7.54$ kJ/mol) upon N-terminal deacylation. An extended version of this design also showed the ability to created extended turn-less β-strands of up to 35 residues. (Kier et al. 2016)

3.3 Materials and Methods

Synthesis of these peptides was achieved using standard microwave assisted Fmoc SPPS. After synthesis of the monomers, dimerization was accomplished in a 1:1 mixture of DMSO and water under acidic conditions. Dimerization seemed to be folding dependent, with the more folded peptides forming dimers more readily. For the unfolded systems, it was necessary to use a 1:1 mixture of DMSO:1M HCl, to force dimerization. The peptides were then purified using RP-HPLC (~30% acetonitrile/water, gradient of 10-50% over 20 min.) after diluting 10fold with water and filtering. After lyophilization of the purified peptide, NMR and CD samples were made and characterized using the conditions outlined in Chapter 2. Dimerization was verified

using mass spectrometry, by presence of the +3 charge state of the dimer, and by NMR, the downfield shifted Hα and upfield shifted $H\beta^3$ of the central Cys residue.

Molar fraction folded values for this system were calculated using the diagnostic probes of W2Hα, $T3H_N$, T4Hα, R8Hα, and $K9H_N$. These were compared to the CSDs of peptide R-VCI-E, which was assumed to have a χ_F of 0.99 based on the lack of melting of the CSDs at pH 8. These CSDs agree within ± 2% to the CSDs found by Kier in the previously mentioned HDX experiment.

3.4 Results

Using the new -HCH- core structure, the coulombic cap remains more folded at both high and low pH ($\Delta\Delta G_U$ = 6.76, 4.84 kJ/mol at 300 K, pH 8, pH 2 respectively), compared to the Kier β-cap. There is a ~2 kJ/mol decrease in fold stability upon acidification. This can be from a variety of reasons, either a change in the charge state of the termini or the destabilization of the HCH core protonation. In the β-cap (peptide **2**) this is especially deleterious, with a loss of fold stability of ~ 5.5 kJ/mol at 300 K from pH 8 to 2.

Table 3.1. Coulombic capping vs. Kier β-Cap

	(X-HCH-**Z)$_2$**		**pH 2**			**pH 8**		
		T	**280**	**300**	**320**	**280**	**300**	**320**
1	**R-**HCH-**E**	χ_F	0.76	0.60	0.32	0.99	0.97	0.78
2	Ac-**W-**HCH-**W**TG-NH_2	χ_F	0.39	0.16	0.05	0.83	0.64	0.49

χ_F = Fraction folded

To further optimize the termini of the coulombic capping motif, a number of point mutations were made at the termini, and their respective fold populations were calculated from NMR at varying temperature and pH (Table 3.2). Mutating the N-terminus to a Lys (peptide **3**), had a minimal destabilizing effect at low temperature over all pHs, and only a 2 kJ/mol destabilization

at pH 8 and 320 K. Most charge-charge interactions prefer Arg, since the delocalized charged species can stay solvated while participating in a salt bridge. Unusually, the evidence suggests that complementary coulombic sidechains is preferred, but during the calculation of NOE-based structures no salt bridge is evident between the terminal side-chains. This may point to the charge attraction aiding in the folding process and not necessarily stabilizing the folded state.

Table 3.2. *Mutations of the Coulombic Capping Interaction of* $(XWTTHCHRKWZ)_2$

			pH 2			pH 5			pH 8		
	X---Z		**280**	**300**	**320**	**280**	**300**	**320**	**280**	**300**	**320**
1	**R---E**	χ_F	0.76	0.60	0.32	0.84	-	-	0.99	0.97	0.78
3	**K---E**	χ_F	0.66	0.48	0.27	0.83	0.77	0.55	0.98	0.94	0.63
4	**K---T**	χ_F	0.78	0.62	0.35	0.85	0.79	0.55	0.96	0.87	0.35
5	**K---A**	χ_F	0.63	0.28	0.15	0.78	0.60	0.33	0.93	0.83	0.56
6	**K---A**-NH_2	χ_F	-	-	-	0.61	0.43	-	0.90	0.80	0.62

Further mutations were made at the C-terminus to verify the preference of a negatively charged side-chain. When the C-terminus is mutated to Thr or Ala (peptides **4** and **5** respectively) a loss of 2.1 and 2.9 kJ/mol is found at pH 8, 300 K, suggesting a preference for the acidic side chain of Glu. Thr and Ala also have different structural propensities. Due to phi/psi preferences, Thr, with a β-branched sidechain, has high β propensity, whereas Ala is preferred in α-helices. This may be why at low pH, where the Glu side-chain will be fully protonated, Thr is preferred to both Glu and Ala by 1.4 and 3.6 kJ/mol respectively. The termini of the peptide could also form a possible coulombic attraction. Amidation of peptide **5** found this to be less important to the folded structure. Peptide **6** was insoluble at pH 2, at pH 8 there was almost no change to the molar fraction folded of between the amidated and non-amidated structures.

The original β-Cap had the disadvantage that no additional residues could be placed past the termini, due to their acetylation and amidation. By using the coulombic cap, this can be

circumvented, but it was found that it is necessary to have a spacer of one glycine on the N-terminus before this extension can be made.

Table 3.3. *Effects of residue extension at the termini of a Coulombic cap.*

			pH 2			pH 5			pH 8		
	X---Z		**280**	**300**	**320**	**280**	**300**	**320**	**280**	**300**	**320**
3	**K---E**	χ_F	0.66	0.48	0.27	0.83	0.77	0.55	0.98	0.94	0.63
7	TT-**K---E**-TT	χ_F	-	-	-	0.12	0.11	0.11	-	-	-
8	GG-**K---E**-GG	χ_F	0.73	0.42	0.20	0.84	0.71	0.40	0.94	0.87	0.56
9	TG-**K---E**-GT	χ_F	0.77	0.55	0.24	0.81	0.66	0.34	0.92	0.82	0.37
10	GT-**K---E**-GT	χ_F	-	-	-	-	-	-	0.06	0.08	0.11
11	TG-**K---E**-TG	χ_F	-	-	-	-	-	-	0.92	0.90	0.62

Table 3.3 contains a variety of 2-residue extensions made to the K-HCH-E (peptide **3**). With mutating extensions of two Thr's to each terminus, peptide 7 was only 10% folded at pH 5. When this is changed to mutations of two Gly's at each termini, the folded state is fully regained. Since allowing only Gly's at the termini would gravely limit applications of this motif, alternative mixtures of Gly and Thr were investigated, at pH 8. When the Thr residues are only on the exterior of the extensions, the peptide's fold regains most of the folded state, but still

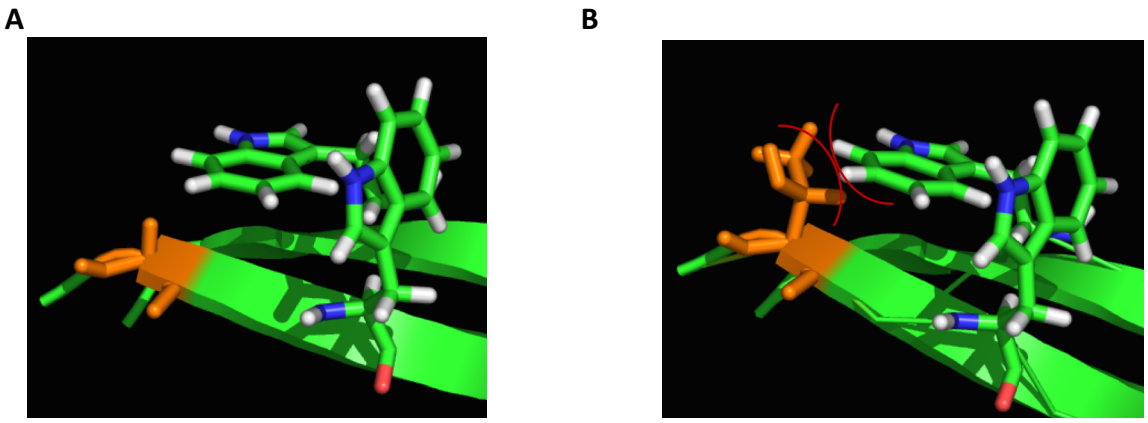

Figure 3.4. *Mockup structures of the residue extensions to the coulombic cap, with Gly (**A**) or Thr (**B**) in the N-terminal position.*

remains destabilized by 3 kJ/mol at 300K. Finally, if the Thr is on the interior of the N-terminus, fraction folded loss is reduced to near zero, but alternatively, the C-terminal version remains as folded as peptide **9**, even resisting melting more.

This was investigated further, by modeling these extensions. Upon further examination of a mockup structure, residues at the position S-1 to the Lys of the cap form a steric clash with the indole ring of the C-terminal Trp. Shown in Figure 3.4 in orange, Glycine (Fig 3.4A), with its lack of a side chain, does not exhibit this problem.

Further, the usefulness of this system in fold stabilization of an isolated β-hairpin from a native system was shown. The WW domain is a three-stranded β-sheet protein (More in Chapter 6). This simplified motif was used to stabilize the first hairpin of the Pin1 WW domain. (Jäger et al. 2001) Although this hairpin is known to be nucleating it is not stable when excised from the β-sheet. Figure 3.5 shows the Hα CSDs for this hairpin in three forms; (1) as a part of the larger WW domain structure (wtWW, blue) (2) as an excised β-hairpin (EXpin1, red) and (3) as a capped hairpin using RW/WD as a coulombic cap (Capped pin1, green). As can be seen by the CSDs, when excised from the greater β-sheet, the hairpin is mostly unfolded, but when the

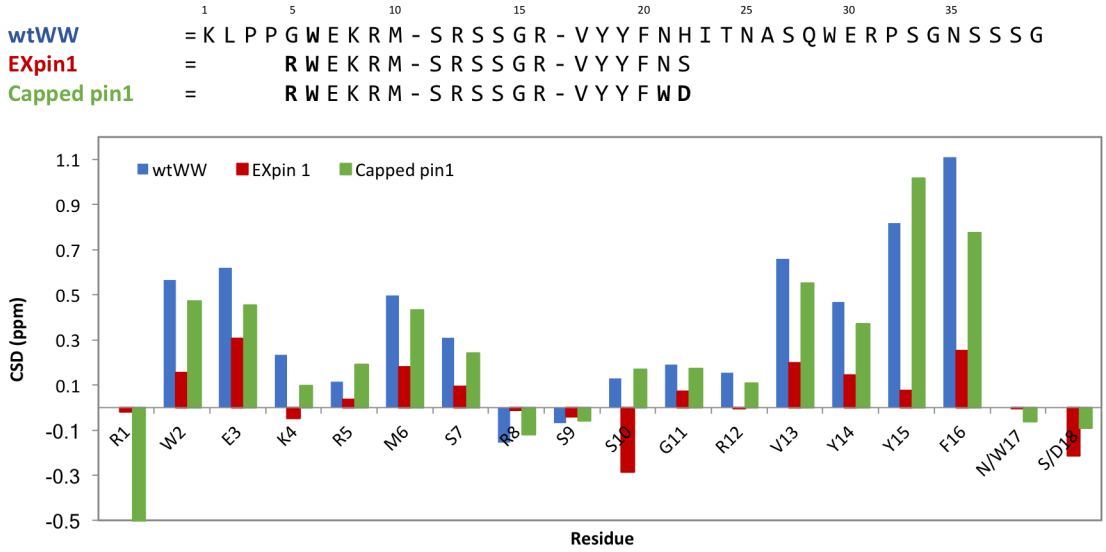

Figure 3.5. *β-Capping of the excised first hairpin of a WW domain.*

RW/WD cap is added, the fold is regained. Small differences in the CSDs are due to effects of the third strand.

3.5 Conclusions

Using this optimized **RW** - peptide – **WE** capping system, numerous peptide systems have been successfully stabilized, (Anderson et al. 2017; Anderson et al. 2016; Kier, Anderson, and Andersen 2015) remaining soluble over a wide pH range, showing a great improvement over the Kier system. Additionally, it was shown that residue extension of each termini is also possible. In this Thesis, the coulombic capping system will be used to stabilize peptides to investigate turn mutations (Chapter 4) and loop elongations (Chapter 5). It is our hope that this system will find even more use in the future, not only for the study of β-sheets, as we have done, but also in stabilizing functional peptides and proteins.

Chapter 4: Nascent Hairpins and β-Turn Optimization.

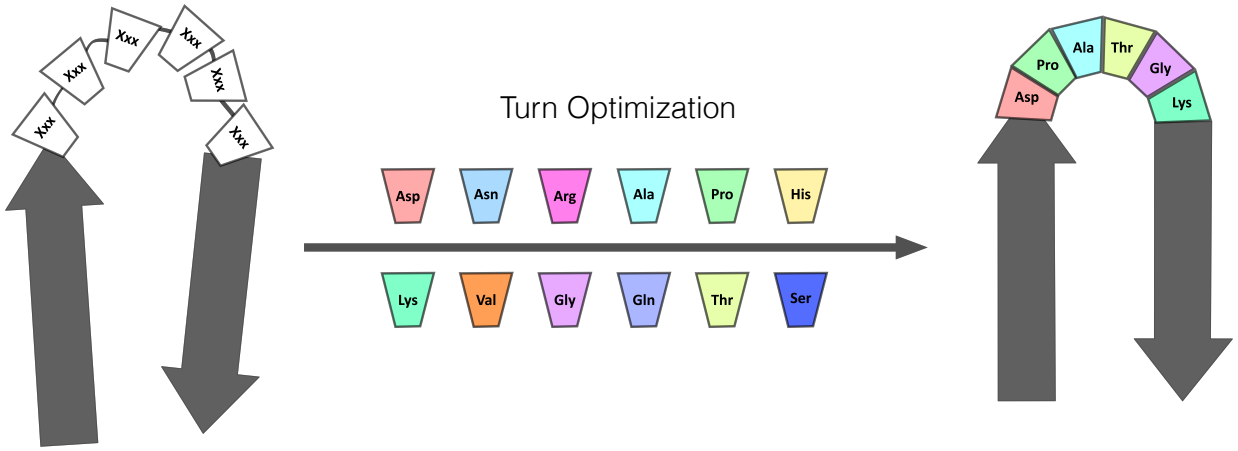

4.1 Introduction

Protein folding involves interactions over a variety of distances. Although it's tempting to think that the small organized pieces of the protein can stay folded when excised, this is generally not true. The framework of stabilizing interactions of the protein's larger structure can be the major force that locks residues, even far in sequence, together. A β-hairpin is the simplest possible β-sheet containing structure, containing two anti-parallel β-strands connected by a β-turn. β-Turns are short, organized sequences that reverse the backbone. When an α-helix folds, due to the local repeating interactions, if the fold is started from any point, the same helix will be formed. In contrast, β-hairpins fold using far-range sequence contacts, with the β-turn necessary to determine the H-bonding register of the β-sheet. Because of this, much more information is available for the folding of α-helices, compared to β-hairpins. Additionally, there are well known sequences which cap the helix to reinforce the macro-dipole produced by the alignment of the amide bonds in the helix. Due to these know forces, generally α-helixes are sub-microsecond folders (Kubelka, Hofrichter, and Eaton 2004). In contrast, β-hairpins fold using longer range contacts which have multiple options, think of the strands sliding against each-

other, forming the similar contacts. What determines the register is the turn, and not much is known about what is required for turn formation preferences.

In the context of protein folding, β-turns have been found to be nucleating folding events for the rest of the protein. Using phi-analysis, many proteins have been determined to contain nucleating hairpins, including: ubiquitin (Bofill et al. 2005), the B domain of protein G (Mccallister, Alm, and Baker 2000), and the well-known WW domain. (Jäger et al. 2006) During the development of the first isolated β-hairpins, it was discovered that these were still poorly folded without the rest of the protein. (Blanco, Rivas, and Serrano 1994) This, and the consideration that β-structures tend to be very hydrophobic and thus insoluble, made β-hairpins considerably more difficult to study. The first strategy to overcome this was to design the peptides with alternating hydrophobic and hydrophilic residues, creating a charged face and a hydrophobic face. Additionally, specific interactions can be added to stabilize the fold such as aromatic clusters, (Cochran, Skelton, and Starovasnik 2001) coulombic interactions, (Ciani, Jourdan, and Searle 2003) coulombic-aromatic interactions (Riemen and Waters 2009) or even disulfides. (Santiveri et al. 2008)

Since both nucleating and non-nucleating β-turns can exist in a protein, the prediction of the structures of β-sheet containing proteins from sequence alone can be difficult. If an algorithm can be created to determine which β-turns will form on there own thus forming nascent hairpins, it would greatly aid the solving of β-sheet containing structures. This can be simplified by asking, will this β-hairpin fold without the rest of the protein? If so, it's a nascent hairpin.

The turns of nascent hairpins require a sequence of residues with high turn propensity. Statistically, turns are shown to have a high percentage of both proline and glycine, these serve

opposite purposes. In addition to sidechain-sidechain interactions, the folding of a nascent β-turn is driven by preferred phi/psi space for each residue. Due to the differences in sidechains of amino acids, each residue has a slightly different preferred phi/psi space. The most constrained of this is proline, caused by the sidechain of forming a 5-membered ring with the backbone. In contrast, glycine is the least constrained residue, due to its lack of a sidechain altogether. In most nucleating β-turns, there are both residues. Due to proline's constraints, it has an ability to *kink* the backbone, but because reversing the backbone requires unusual phi/psi space to be occupied, glycine must be included to complete the turn. Designed β-turns can overcome the entropic cost of fixing glycine into one position, by placing a D and L amino acid next to each other, for instance pP (lowercase indicates D-proline) is an excellent turn locus.

The naming of β-turns has seen many different systems, with 4-residue turns getting the most attention. The most common system was started by Venkatachalam (Venkatachalam 1968) with Type I/I' and II /II' covering the most common types of 4-residue turns.

4.2 System Design

This study focuses on 6-residue turns, with the general sequence of RWTV-β-turn-ITWE. Using a coulombic cap of RW/WE (described better in Chapter 3), a Trp/Trp edge-to-face interaction leads to a great deal of stability (5-7 kJ/mol), allowing for the determination of turn-propensities of even relatively poorly folded turns. To determine the fraction folded (χ_F), the CSDs of W2 Hα, T3 H_N, I11 Hα, T12 H_N and W13 Hε3 were used, based on the extent of folding of the –NPATGK- parent sequence, (χ_F = 0.84, 300 K and pH 6.5). Additionally, CD spectra can afford the T_m of each peptide based on the changes in the exciton couplet maximum (further information can be found in Chapter 2).

4.3 Results and Discussion

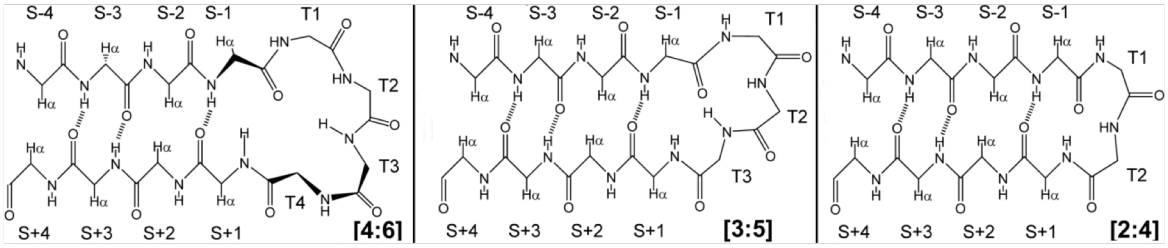

Figure 4.1. *Example turns labeled using the Andersen and Thornton designations.*

Although much of the work in β-turn design has been focused on 4-residue turns, 6-residue turns have been found to be very common and can produce β-sheet nucleation. The best example of this is found in the second hairpin of the B domain of protein G (GB1), with a DDATKT turn. (Kobayashi, Endo, and Munekata 1992; Blanco, Rivas, and Serrano 1994) Unlike the classic 4-residue turn types (I, I', II and II'), larger turns are more likely classified by the notation created by Thornton. (Sibanda, Blundell, and Thornton 1989) Shown in Figure 4.1, this classification uses the position of the first cross-strand H-bond and the number of residues that constitutes the turn locus (number of residues between the outer beta residues). For example, a [4:6] turn, contains 6 residues, with 4 residues between the first H-bond. The preferred numbering scheme to combine with this was developed in the Andersen lab, (Fesinmeyer, Hudson, and Andersen 2004) with β-strand residues designated by a S and turn residues by a T, example shown in Figure 4.1. Thus a [4:6] turn's residues would be labeled, S-1, T1, T2, T3, T4, S+1.

Design of optimized 6-residue turns generally started with bioinformatics residue searching. In 2004, both the Andersen (Fesinmeyer, Hudson, and Andersen 2004) and Honda (Honda et al. 2004) groups, created optimized versions of the GB1 sequence (DDATKT) using

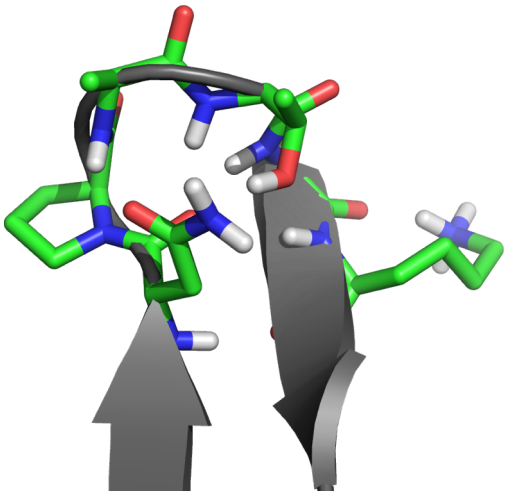

Figure 4.2. *Structure of the NPATGK Turn. Turn residues are shown with green carbons.*

statistics from protein segments to create the NPATGK and DPETGT turns, respectively. Later the NMR structure of the NPATGK turn was elucidated, (Niels H. Andersen et al. 2006) shown in Figure 4.2. Interestingly, this revealed that the structure can be thought of as a specific motif, where positions of the turn require specific residues, likely due to side-chain interactions. This data also lead to position specific phi/psi data designating the standard [4:6] turn motif by: $\beta - \alpha_R - \alpha_R - \gamma_R - \alpha_L - \beta$, for positions S-1 to S+1.

This chapter is a continuation on this work, calculating mutational $\Delta\Delta G_F$ values for the positions of the turn. This allows for the true determination of turn propensity of each sequence. As stated earlier, a nascent hairpin can fold without the structure of the rest of the protein. Bioinformatics studies cannot distinguish between nucleating and non-nucleating turns. This creates a problem when trying to determine a folding pathway or searching for β-turns within sequences. Starting with the NPATGK parent system, point mutations were made at each site. Additionally, double mutations were made in certain cases to better understand the single mutations. Since protonation states can affect residues at different positions, the data was also taken at pH 2.5, 6.5 and 8. Table 4.1 shows the bulk of this data, and the peptides investigated will be referred to using the turn sequence or the mutational reference (Column 1, Table 4.1). Appendix E contains a complete list of $\Delta\Delta G_U$ values for each point mutation.

Table 4.1. *Turn mutations to the parent peptide, RWTV-NPATGK-ITWE.*

Reference	*Turn Sequence*	*Fraction Folded (χ_F) at 300K* [a]			*T_m (^oC) CD at pH 6.5*
		pH 2.5	*pH 6.5*	*pH 8*	
1	**NPATGK**	**0.69**	**0.84**	**0.83**	**64.3**
2	DPATGK	0.64	0.81	0.94	72.7 (> 80)
3	HPATGK	0.04	0.59	0.90	[43-53]
4	CPATGK	0.46	n.d.	0.86 [c]	n.d.
5	SPATGK	0.38	0.71	0.48	48.0
6	QPATGK	0.20	0.45 *(0.56+)*	0.61	40.9 (44)
7	APATGK	0.18	0.47	0.46	27.1 (37)
8	GPATGK	*(0.23)*	*(~0.3)*	n.s.	15.8
9	IPATGK	0.29	0.68	0.49	39.7
10	TPATGK	0.13	0.55	0.35	30.7
1-2A	N**A**ATGK	0.55	0.77	0.83	53.5
1-2A,4A	N**A**A**A**GK	0.03	n.s.	n.s.	
1-2V	N**V**ATGK	0.49	0.88	n.s.	56.0
1-2G	N**G**ATGK	0.32	0.66	0.71	45.3
1-3V	NP**V**TGK	0.73	0.92	0.90	72.1
1-4N	NPA**N**GK	0.55	0.88	0.76	55.3
1-4D	NPA**D**GK	0.45	0.83	0.85	54.1
1-4H	NPA**H**GK	0.04	0.35	0.15	
1-4A	NPA**A**GK	0.05	0.15	0.07	< 5
1-4A,5T	NPA**AT**K	~0.05	≤ 0.04	0.02	<< 0
1-4G	NPA**G**GK	0.18	0.13	-----	
1-4V	NPA**V**GK	-----	0.30	0.26	< 0
1-6T	NPATG**T**	0.55	0.81	n.s.	63.2
1-6A	NPATG**A**	0.66	0.79	-----	65.5
1-6G	NPATG**G**	0.42	0.55	0.82	27.4
2-6R	**D**PATG**R**	0.63	0.82	0.96	73.9
2-3G	**D**P**G**TGR	0.42	0.68	*(0.96)*	57.4
2-4S	**D**PA**S**GK	0.40	0.63	0.90	53.8
2-4S,5T	**D**PA**ST**K	< 0.15	0.19	0.21	7.5
2-5N	**D**PAT**N**K	0.23	0.64	n.s.	45.9
1-5A	NPAT**A**K	-----	*(0.54)*	0.37	32.2
1-5H	NPAT**H**K	0.56	0.85	0.69	49.2
3-6R	**H**PATG**R**	0.04	0.23	0.84	52.0
3-4A,6R	**H**PA**A**G**R**	0.05	0.05	n.s.	

[a] Based on CSDs determined by NMR.

The studies by Andersen and Honda both showed a large preference for D or N at S-1, which was confirmed by this system. Asp is as folded as the parent at pH 5 and 2.5, but appears to be even better folded by 2.9 kJ/mol at pH 8. There appear to be several pH dependences to mutations, even with residues not containing charged sidechains. It is important to note that much of this is due to the coulombic interactions of the β-capping motif used in these peptides. Although there are also turns that show a dramatic change in respects to pH, beyond the cap. Peptide **3**, containing the HPATGK sequence, is 1.5 kJ/mol more folded than the parent at pH 8 and 9.9 kJ/mol less folded at pH 2.5, due to the protonation change of the His residue. This is explored further in Chapter 6, using this turn to create pH switchable β-sheets.

Proline is known to be used in β-turns as a *kink*, to help reverse the backbone. Surprisingly, position T1 was only marginally affected by mutations. Using A and G (peptides **1-2A** and **1-2G,** respectively) at this position, 1.1 and 2.5 kJ/mol of destabilization was found at pH 6.5, although NGATGK was only found to be 32 % folded at pH 8. Val was found to be as folded as the parent at pH 6.5, by not soluble at higher pH. Although not many mutations were made to the Ala in position T2, Val makes this quite a stable turn (peptide **1-3V**).

Position T3 was shown to have a high preference in nature for Thr, with almost twice the abundance over other residues. (Honda et al. 2004) The current data suggests that both Asp and Asn are well tolerated at this positon, but others are not. H, A, G and V all significantly reduced the foldedness of the peptides, many by more than 6 kJ/mol. Ser was found to do marginally well at this position, using comparison between peptides **2** and **2-4S.** H^0 and V (**1-4H** and **1-4V** respectively) were found to only exhibit ~30% foldedness at pH 6.5, while A and G were unfolded over all conditions (**1-4A** and **1-4G**, respectively).

Glycine is usually an essential position of a β-turn. Since turns are reversing the backbone, there is commonly a position that needs to be placed into an unfavorable phi/psi space. Glycine is the only residue that is allowed in this space (γ_R = -80/0°, in this turn), because of its lack of sidechain. In [2:4] turns the positioning of this glycine will determine the turn type. In example, trpzip; with ENGK (Cochran, Skelton, and Starovasnik 2001) exhibiting a I' turn, while EGNK (Wu et al. 2012) has a II' turn. This [4:6] system found that not many residues are tolerated at this, the T4 position. Even mutation to Ala (peptide **1-5A**) resulted in a peptide that was insoluble at pHs 2.5 and 5, and only 35% folded at pH 8. Since β-hairpins contain many hydrophobic residues, unfolded peptides demonstrate aggregation and solubility issues. Mutations to T and N were also incredible detrimental (**2-4S,5T** and **2-5N**), although His (**1-5H**) was found to be stable. Lastly, position S+1 was found to tolerate many amino acids, with Lys and Arg being the most folded.

4.4 Conclusions

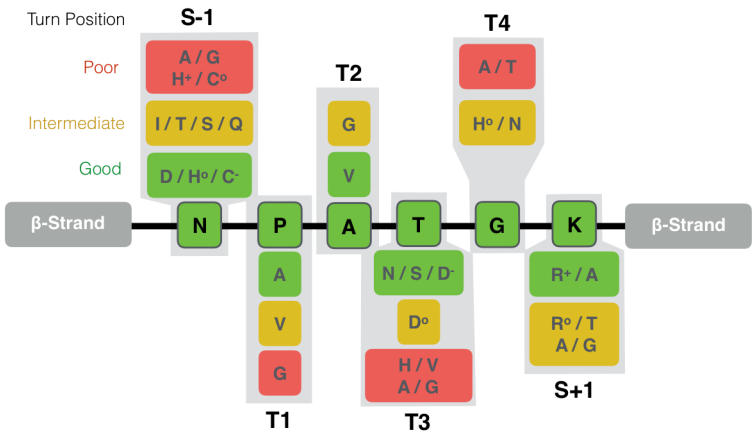

Figure 4.3. *Residue preferences for each position of the 6-residue turn.*

The data collected in this project has given greater clarity to the residue requirements for each position of a 6-residue turn, summarized in Figure 4.3. Although the ability to form a turn is largely determined by the allowed torsion angles of each residue, this data suggests that the formation of sidechain specific interactions is necessary to create this motif. Constraining

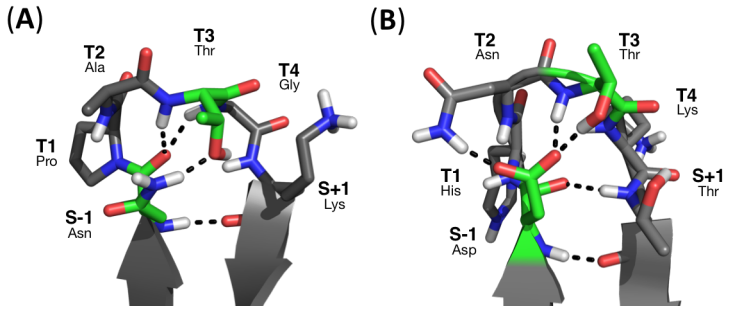

Figure 4.4. *Structure of the Turns NPATGK and DHNTKT (PBD entry = 2EVQ and 5AHT).*

any residue into a specific position is entropically unfavorable, these interactions can offset this. While turns are often imagined as a flat reversal of the backbone, the loop of the turn usually folds over onto itself. This arching causes the H_Ns of much of the backbone to point towards the S-1 position. This creates many possible H-bonding interactions with the S-1 backbone carbonyl, and polar sidechain. This incredible network of H-bonds that can be created in the turn, is proposed to be the reason for positions S-1 and T3 requiring polar sidechains. Figure 4.4 shows great examples of these H-bonding networks, within the parent turn, NPATGK, and turn 2 of the Nedd4-1 WW domain (Panwalkar et al. 2016), DHNTKT. In a short survey of different [4:6] β-turn structures, it was found that positions S-1 and T3 can act as both H-bond donors or acceptors. It was also found (Figure 4.4B) that bifurcated H-bonds to the S-1 backbone carbonyl and sidechain are possible.

While this dataset works nicely as a complete design guide to [4:6] β-turns, it has an even more promising and exciting potential. As advancements in high-throughput protein sequencing by MS has gigantically outpaced structural biologists, computational determination of a protein's structure only from the sequence will need to be relied on more. A major challenge of that is nascent hairpin identification. Improvements in this will also lead to better understandings of protein folding landscapes, pushing better design by incorporating greater thought into optimization of the protein folding pathway.

Chapter 5: Loops

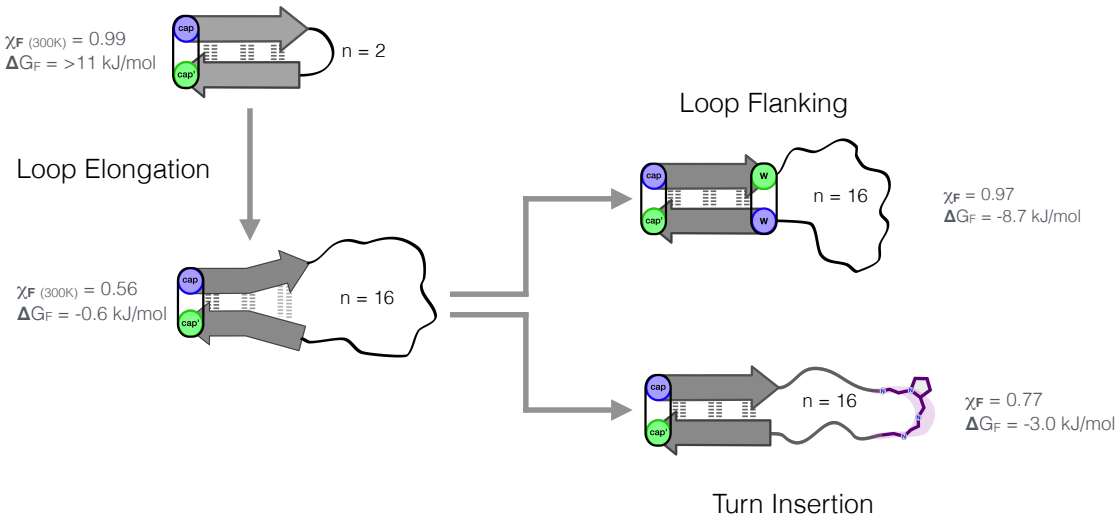

5.1 Introduction

Unlike β-turns, discussed in detail in Chapter 4, loops are unstructured sections of a protein which connect structured regions. Due to a loop's large number of possible conformations, study of them can be quite difficult. Commonly invisible to crystal structures, and convoluted in NMR studies due to signal overlap. Regardless of this, and possibly due to the attraction of studying the structured regions more, loops still make up a significant portion of the folding landscape of most proteins. In β-structures, loops are used for a number of purposes, the hydrophobic nature of β-sheets can be offset by the addition of hydrophilic residues in the loop region (Koebnik 1999). For instance, membrane proteins commonly contain highly charged loops in one region to keep one end of a β-barrel at the surface of the membrane, while the barrel itself is submerged into the hydrophobic fatty chains of the membrane.

Loops, as the connecting portions between β-strands, have a major use in the tuning of the flexibility of the β-sheet. As a loop is elongated between β-strands, the residual segmental

motion of the loop will perpetuate into the strands. The most noticeable effect of this in nature is found in the differences in loops between proteins contained in organisms that evolved in different environments (Scandurra et al. 1998). Proteins from organisms at high temperatures (Vieille and Zeikus 2001; Zeikus, Vieille, and Savchenko 1998) (thermophiles) are found to have smaller loops, while proteins from cold loving organisms (Modarres et al. 2015) (psychrophiles) are found to have larger loops. This intimately reveals the interplay between motion and function. Although a protein's structure determines its function, both binding and catalytic activity requires a certain amount of flexibility to the structure.

Although the loops are a major factor in solubility and overall motion, they can also play a key role in a protein's activity. Significant roles are as binding motifs and active-site gates, two areas where flexibility can be an advantage. For example, the strongest small molecule-protein interaction known is the binding of biotin to streptavidin (Song et al. 2015). One of the reasons this binding is so strong is due to a loop that binds to biotin, closing this pocket, encompassing the substrate completely. In catalysts, such binding initiated loop motions, cause a larger structural change, which is linked to function or catalytic rate (Malabanan, Amyes, and Richard 2010).

Loops also act to bind over large areas, especially protein-protein interactions (PPIs). Antibodies are an excellent example of this (Ekiert et al. 2012; Ramsland et al. 2000). Antibodies, also known as immunoglobulins, are proteins produced by the immune system to neutralize pathogens (antigens) in the body either by blocking the active site of the pathogen or by signaling phagocytosis. Binding to the antigen, by an antibody, is accomplished by a collection of variable loops. The fact that small mutations in these loops does not result in a large change to the structure of the antibody, is why your body can produce so many different

antibodies in a relatively short time. Antibodies, although very specific binders, can be poor therapeutics due to their large size and poor solubility (Tsomaia 2015). This has lead peptide chemists into the antibody mimetics field, where the loops are constructed and then placed onto a smaller protein scaffold (Woodman et al. 2005; Pluckthun 2015), or a small-molecule hub. (Heinis et al. 2009; Robinson et al. 2008)

Since protein backbones have such a large number of degrees of freedom, computational determination of specific features associated with loop closure has proven to be difficult. Additionally, sequence homology fails to locate loop regions; there is little evolutionary pressure for specific features in "loops". (Messih, Lepore, and Tramontano 2015; Yarnitzky, Levit, and Niv 2010) As a result, other methods have been required to model the allowed phi/psi space of each residue and find a solution that meets these (Deane and Blundell 2000) consistent with loop closure. *Ab initio* methods with a variety of scoring functions and structural perturbation algorithms such as "random tweak" (Fine et al. 1986; Shenkin et al. 1987) and circular coordinate descent (CCD) (Canutescu and Dunbrack 2003; L. C. T. Wang and Chen 1991) have made advances, with help from models for robotic arm movements (L. C. T. Wang and Chen 1991), some of which state an accuracy of 90% in correctly predicting loop conformations of loops of ≤ 8 residues. (Fiser and Sali 2003) But an understanding of how loop length and "stiffness" affect folding landscapes still largely eludes us. (Nagi and Regan 1997; Wright et al. 2004)

Most of the non-computational research into loop closure dynamics has used a variety of fluorescence measurements. Using triplet-triplet energy transfer (TTET), Fierz and coworkers (Fierz et al. 2007) used a model of a $(GS)_n$ polypeptide loops with xantone and napthylalanine on the termini, concluding that loop closure, even as n approaches 12, was on the sub-microsecond

scale. Models such as this, however, do not link the loop closure to a structuring event, using as a 'closure probe' a transfer that could be over large distances (5Å) in a short time (ps). Larger protein models are not able to isolate this motion from the many other motions in a folding pathway. Using the model systems in this chapter, the loop closure dynamics are linked to a single β-sheet association step.

5.2 Peptide Design

The peptide system used in this Chapter shows how fold stabilizing the improved coulombic cap (from Chapter 3) is. The chapter is divided into three main sections (1) Short Loops, (2) Long Loops and (3) Loop Composition Effects. In this, we refer to loops shorter than 10 amino acids as short and greater than 10 as long loops. It also signifies a break in the system design. The general system is cap - β – loop – β' – cap' motif where β and β' are potential β-strands. A system such as **RW**ITVTI – loop – KKIRV**WE** is representative, with the caps shown in bold. In the short loop series, the loop is an increasing number of glycines from 2-10 residues (G_n), whereas in the long loop system, two lysines must be place at every four glycines for solubility, $(G_4K_2)_n$. This allows for the system to be extended to loops of 28 residues without solubility problems. Both systems were verified to be monomeric at the concentrations used, by monitoring the NMR and CD at concentrations much higher and lower than the measurements, shown in Appendix F. Along with adding significant fold stability to the system, the EtF Trp/Trp interaction allows for the measurement of accurate thermodynamic and kinetics of folding.

5.3 Materials and Methods

The peptides in this Chapter were synthesized using standard Fmoc microwave assisted solid-phase peptide synthesis (SPPS). Synthesis cycles were accomplished using piperidine (20% in DMF) at 75^{o} C for deprotection and DIC/Oxyma (5 eq in DMF, with 5 eq Fmoc-amino acids) at 75^{o} C for each amino acid coupling. Most syntheses were done on a 0.1 mmol scale, using preloaded Wang resin, or Rink amide resin for the carboxylic acid or amide terminus respectively. Peptides were purified using RP-HPLC (Agilent ZORBAX Prep-HT SB-C18, or Millipore Chromolith SemiPrep RP-C18 columns, using a gradient of 10-50 % acetonitrile/water over 20 min.), and concentrated and lyophilized before use. The mass of the peptides was verified by mass spectrometry (ESI-Ion trap, Bruker Esquire), and characterized using the NMR methods found in Chapter 2). It was found, because of the large serial synthesis of these peptides that impurities of ± Gly within the loop was reduced by keeping the temperature during synthesis at 75^{o} C, and by changing to a high swelling PEG resin. Peptides with loops larger than 10 amino acids were synthesized on preloaded TentaGel R PHB resin (RAPP polymere GmbH). Samples for NMR and CD were prepared in accordance to Chapter 2.

5.4 Short Loops

The peptides examined herein have a RWITVTI-G_n-KKIRVWE sequence with RWITVTI designated as β-strand 1 (β) and KKIRVWE as β-strand 2 (β'), with the loop region (G_n) being the only part varied. The naming of these peptides - **G2**, **G3**, **G4** etc. - indicate the number of glycines in the "loop" at n > 4. The **G2** – **G4** examples however could have well defined turn structures in which Ile and Lys are part of the turn: **G2** as a type I/II' β -turn, G3 as a [3:5], and G4 could form a [4:6]. As a result, it is not clear what to designate as the actual

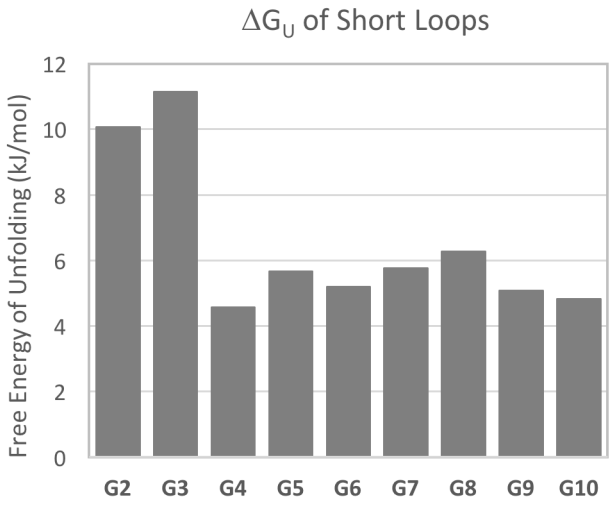

Figure 5.1. *Free energy of unfolding for peptides* ***G2-G10*** *at 300 K.*

"loop length". We employ all glycine loops, to allow modeling of only the protein backbone connected to β-strands, without contributions from or constraints associated with sidechains.

It was found that increasing the loop size sequentially revealed a more complicated relationship between loop length and fold stability than initially hypothesized, defining the difference between an organized turn and an unstructured loop. As the loop was increased from **G2-G10** there are clear distinctions between these two classes. From **G2-G4**, there is a dramatic decrease in ΔG_F at **G4** of 5 kJ /mol (Figure 5.1). To reverse a protein backbone, at short loop sizes it is necessary to constrain the phi/psi space of each residue into specific angles. This causes the dramatic decrease in free energy of fold stability noted at **G4**. As each loop residue is constrained, the entropy loss is regained by enthalpy gains of the β-strands, or the turn motif itself.

Specific conformations are also evidenced by NMR structuring shifts. Large negative, structure-specific CSDs are shown in the glycine's of **G2** and **G3** revealing diagnostics of classic [2:4] and [3:5] turns (Appendix G). As the loop size is increased, although each residue requires more constrained space, more possible 'solutions' to the chain direction reversal problem arise, offsetting the entropy of additional amino acids. As the loop size continues to increase, this offset is overcome by increased segmental motion within the loop. This results in a net decrease in the fold stability of the β-strand-associated state. Comparing the H_N CSDs of Ile 3 and Ile 7

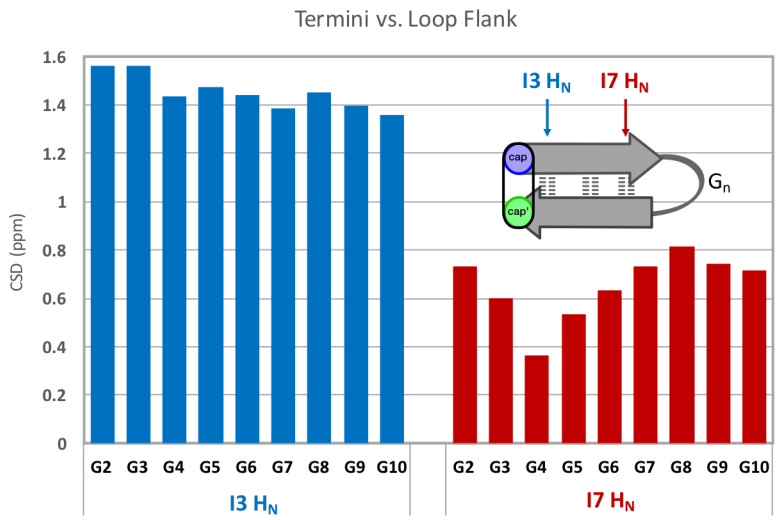

Figure 5.2. *Comparison of the CSDs of I3 and I7 HNs.*

can track these changes. As shown in Figure 5.2, even though the CSDs of I3 essentially at the chain termini and immediately adjacent to the Trp/Trp β-cap, change very little, the I7 CSDs at the loop flanking position reveal a clear minimum at the **G4** loop length, and a maxima at **G8**. This indicates a clear division point between a protein turn and loop, and is further verified by circular dichroism measurements, with both the maxima of the Trp/Trp exciton couplet and the melting points revealing this large decrease from **G2-G4** and regain at **G8** (Appendix H). As previously noted, the further decrease in β-state fold stability as the loop length is increased past eight residues (**G8-G10**) is likely due to increased segmental motion of the highly flexible loop region (Anderson et al. 2017) being transmitted into the loop flanking regions of the β-strands.

5.4.1 Short Loop Closure Dynamics

The dynamics of loop closure can reveal more information on what causes these changes in free energy of the folding equilibrium. Use of line broadening on the Hζ3 signal of the edge Trp in the β-cap as diagnostics, allows for rate measurements over a large temperature range. The peptides demonstrated Arrhenius kinetics and 2-state folding over the 280-320 K range, for which the rates and activation energies of folding and unfolding were derived (Table 5.1). At the

shortest length, 3 glycines (**G3**), that provided useable data, with relatively rapid folding ($1/k_F$ = 12.1 μs) coupled with the slowest unfolding rate observed ($1/k_U$ = 696.3 μs), see Table 5.1. A single glycine loop elongation, **G4**, increased both the folding and unfolding rate with the 10-fold decrease in the unfolding lifetime ($1/k_U$ = 60.3 μs) being particularly notable. As might have been expected, the entropy loss associated with forcing four glycines into the specific phi/psi values of a [4:6] turn, cannot be overcome by the enthalpy gain of β-strand association. As the loop is lengthened and more solutions to the strand reversal problem appear, there is less variation in the folding rates as the number of residues increases. Of note at **G7**, a relatively fast folding rate is coupled with a notably faster unfolding rate. These are, presumably, associated with an odd/even variation in activation energies in the intermediate loop size range.

Table 5.1. *Variations in the dynamics of loop closure with loop size for loops connecting antiparallel associated β-strands.*

		Folding Data			**Unfolding Data**		
Loop	**ΔG_F (kJ/mol)**	**Ln k_F**	**$1/k_F$ (μs)**	**Ea_F (kJ/mol)**	**Ln k_U**	**$1/k_U$ (μs)**	**Ea_U (kJ/mol)**
G3	-12.35	11.3	12.1	21.2	7.3	696.3	43.9
G4	-5.37	11.8	7.7	23.3	9.7	60.3	27.7
G5	-6.65	10.5	27.3	34.5	8.0	341.8	68.6
G6	-6.02	10.8	20.9	44.3	8.5	207.9	64.4
G7	-4.71	11.3	12.9	16.9	9.4	79.5	25.8
G8	-6.23	10.7	22.1	29.0	8.4	235.5	48.5
G9	-4.99	11.1	14.7	14.7	9.2	100.0	25.1
G10	-4.56	10.8	21.4	13.5	9.0	124.3	24.0

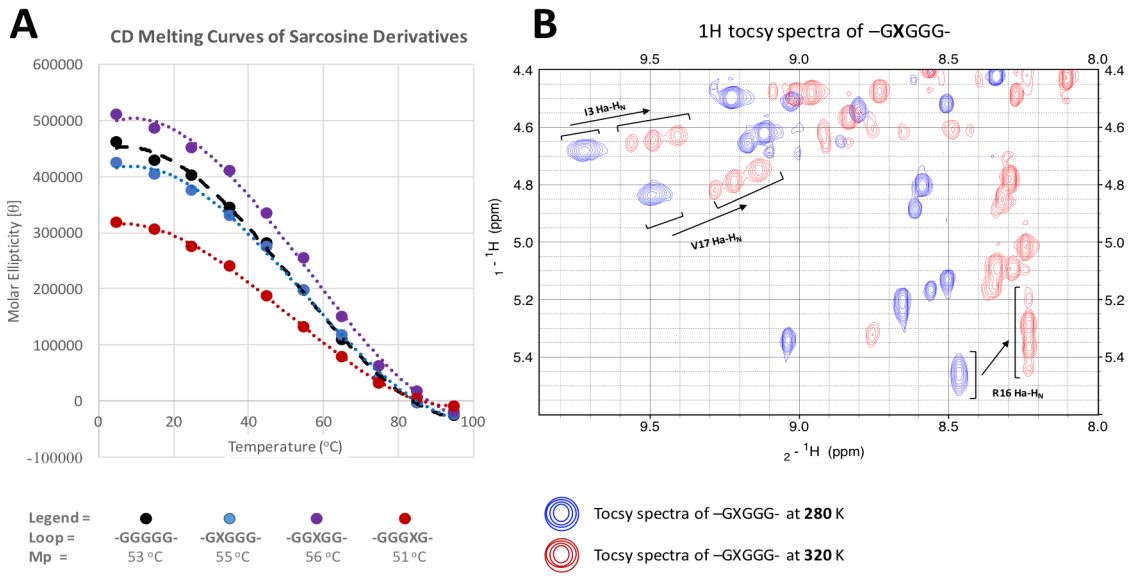

Figure 5.3. *Sarcosine derivatives (A) CD melting curves monitored at 228 nm, X = Sarcosine. (B) ^{1}H TOCSY spectra at 280K (blue) and 320K (red) of –GXGGG-, illustrating many turn conformations are in slow exchange.*

5.4.2 NMR Diagnostics of Loop Structuring at Glycines within the Loop

As mentioned previously, when a residue is fixed into a turn position, the CSDs can reveal the conformation. Although a specific residue's Hα and H_Ns can be downfield shifted due to the conformation, unlike in β-strand residues, large upfield shifted H_Ns and Hαs are also seen. It is also possible for H-bonding interactions to begin to stabilize a specific loop size and conformation. Chemical shift deviation data suggests that the turn formed by the **G5** is more stable than the **G4** turn. Because of the specific geometries required in the reversal of a peptide backbone, negative (upfield shifted) Hα CSDs are usually observed for the majority of turn residues. As these become conformationally averaged by the increased flexibility in most loops, these CSDs revert toward zero. For the turn glycines of **G4**, the largest negative CSD is for Gly11 H_N = -0.155 ppm, whereas the Gly12 H_N for the G5 peptide is -0.259 ppm. It is hypothesized that the large entropic cost of the ordering of the turn glycines is offset by the increase in the number of solutions to the chain-direction reversal problem for the **G5**.

To further investigate this, single-site sarcosine derivatives were synthesized. Sarcosine is the N-methylated derivative of Gly, and has a reduced allowed region in a Ramachandran plot ***and*** no ability to act as an H-bond donor. Figure 5.3A shows the CD melting traces for the Gly9, Gly10 and Gly11 to sarcosine mutations. Although there wasn't much change in the melting temperature there is an apparent preference for the Sar at the middle (Gly10) position, with the two other mutations slightly detrimental, implying there are specific preferences for each position.

The more surprising result was found during the NMR investigation. It is known that the N-methylation in sarcosine causes a slow exchange equilibrium between the cis and trans isomers of the omega (peptide) bond, commonly resulting in two sets of peaks in a NMR spectra. During the NMR of the derivatives stated above, typically three or more signals are observed for the most shifted H_N and Hαs of the β-strands, and for the Hε3 of the Trp18. The chemical shift differences for these multiple signals increase at the higher temperature (Figure 5.3B), presumably due to different degrees of unfolding. We hypothesize this is caused by an exchange between multiple turn conformations, exaggerated by slow cis-trans isomerization about peptide bonds involving the sarcosine. Unfortunately, lineshape broadening dynamics measurements were not possible for these peptides due to the overlapping of these multiple signals.

5.4.3 Short Loops Summary

In a simple system containing two β-strands connected by polyglycine loops of increasing size from 2-10 residues, it was found that the dynamics and fold stability can vary significantly with loop size. Although it may be expected that increasing the loop length would simply lead to a gradual decrease in fold stability due to increased loop size, with an incremental

decrease in folding rate, it was found that the folding dynamics changes can be more complicated, reflecting a more convoluted folding landscape. Peptides **G2-G4** must be considered as β-hairpins, with distinct defined turn geometries that must be used to reverse the backbone. The constraining of the large conformational entropy of each glycine leads to an increasingly less folded peptide from **G2-G4**. After **G5** this entropic cost can be offset by an increase in the number of loop conformations that allow chain reversal. It was found that at **G8** this offset is then overcome by increased segmental motion within the loop, since there are many conformations that each individual glycine can adopt. By using only glycine in these loops, the flexibility of the loop is exaggerated, exemplifying that the backbone itself has many different entropic concerns. In design, it is often thought that shorter loops lead to more stable β-sheets. This may be a simplification that needs detailed examination and re-evaluation in other cases as well. It is our hope that these data, combined with future residue specific information, will advance the field of loop closure prediction and lead to the design of proteins that can be fully tuned to an optimal dynamic structure.

5.5 Long Loops

After 10 residues, the connecting sequences can be confidently characterized as loops. Due to solubility problems, loops greater than 10 residues have two lysines added for every 4 glycines, resulting in a general sequence of RWITVTI $(GGGGKK)_n$ IRVWE, with the last two lysines of the repeated sequence part of the β-strand. Thus, n = 2 can be considered as a 10-residues loop, n = 3 as a 16-residue loop and so on. In this group there are two main systems, a system with a single endcapping coulombic cap (C2) and a system with an additional loop

flanking Trp/Trp aromatic cluster (C4). The specific sequences are shown in the Tables (5.2-5.4), with all "edge" oriented Trps colored in green and "face" oriented Trps in purple.

First, I'll show how loop size affects the thermodynamics of the folded state equilibrium. As shown in Table 5.2, unsurprisingly, as the loop is lengthened the molar fraction folded decreases. As in the previous study, the 2-residue loop (C2-2), is fully folded and was used as the control, for CSD comparisons. At 10 residues (C2-10) there is a loss of 6 kJ/mol in fold stability at the lowest temperature, with ΔG_U falling to 5 kJ/mol. As the loop is extended to 16 and 22 residues this is reduced to 2.1 and -1.7 kJ/mol, respectively at 280 K. This trend was confirmed by CD (Appendix I), with the T_m decreasing from 50 to 5 to < 0 ^oC for the 10, 16 and 22 residue loops, respectively. The majority of this can be attributed to the residual segmental motion of the loop propagating into the strands, causing a pulling apart of the peptide from within. This is confirmed by a large decrease in the CSDs of the residues near the loop, compared to those at the termini.

Table 5.2. *Thermodynamic data of Long loop system C2*

System	Loop Length	**Sequence** **cap** – β-strand – loop – β-strand – **cap'**	ΔG_U (kJ/mol)	***Fraction Folded*** (χ_F)	
			280 K	300K	320K
C2	2	**RW**ITVTI - GG - KKIRV**WE**	> 11	0.99	0.99
C2	4	**RW**ITVTI - GGGG - KKIRV**WE**	+ 5.8	0.88	0.74
C2	10	**RW**ITVTI - $(G_3GKK)GG_3$ - KKIRV**WE**	+ 5.0	0.84	0.59
C2	16	**RW**ITVTI - $(G_3GKK)_2GG_3$ - KKIRV**WE**	+ 2.1	0.56	0.38
C2	22	**RW**ITVTI - $(G_3GKK)_3GG_3$ - KKIRV**WE**	- 1.7	0.29	0.25

The dynamics data for these loops, measured by RD-NMR, was even more surprising. Previous studies had largely discounted loop search contributions, assuming that loop search was very fast during folding. Our results suggest that longer loops can affect the rate of folding significantly.

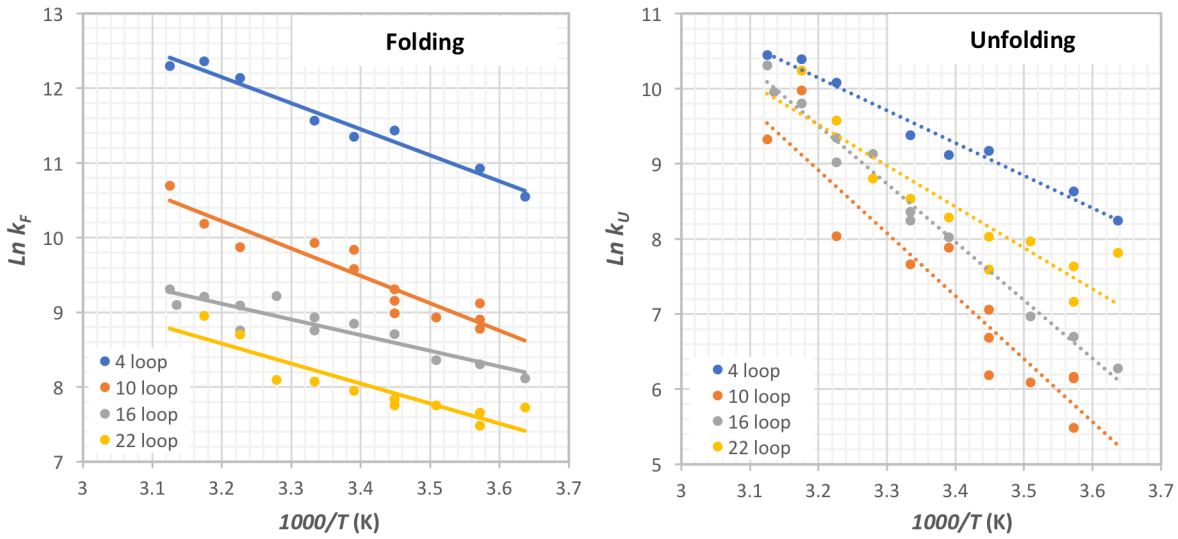

Figure 5.4. *Arrhenius plots of Loops C2 4-22*

Figure 5.4 shows the Arrhenius plots for the folding and unfolding kinetics for these long loop systems. As the loop is elongated, there is a significant decrease in the folding lifetime for β-strand association. β-Hairpins, containing nucleating turns, have been shown to be fast folders, with $1/k_F = < 4$ μs. Starting with the 4 loop (C2-4, which can be considered a loop due to entropy concerns discussed in Section 5.4), the folding lifetime ($1/k_F$) is 8.4 μs at 300 K. As the loop size is increased, to 10 residues, although there is only a 0.8 kJ/mol decrease in the folded equilibrium, the folding time increases to 59.3 μs. Upon increasing the length to 16 and 22 residues, further increases in the fold time are observed: to 145 and 320 μs, at 300 K. It's important to note that unlike previous measurements of loop closure, these are completely tied to the formation and association of the β-strands, a more pertinent model of protein folding. These

Arrhenius plots also contain information on the activation barrier for the folding and unfolding process, represented by the slope of the line (Slope = -Ea/R). A summary of this information can be found in Table 5.3.

	Folding			Unfolding		
	$Ln\ k_F$	$1/k_F$ (μs)	Ea (kJ/mol)	$Ln\ k_U$	$1/k_U$ (μs)	Ea (kJ/mol)
4 Loop	11.7	8.4	29.0	9.6	70.2	36.0
10 Loop	9.7	59.3	30.5	7.8	410.7	69.6
16 Loop	8.8	145.5	17.5	8.5	208.6	64.4
22 Loop	8.0	320.8	16.1	8.4	218.1	34.5

Table 5.3. *Folding and unfolding data for long loops.*

5.6. The Effects of Loop Flanking Trp/Trp

As shown in the previous section, loop elongation decreases the degree of folding and rigidity of the residues near the loop due to increased conformational entropy of these positions from motions of the loop. The most obvious way to overcome this, to produce more fold stable β-strands, is to add favorable enthalpic interactions between the two strands near the loop termini. This is another instance where the Trp/Trp aromatic cluster can be used. By placing Trp's at the loop flanking positions, the strands can be clamped down creating highly folded β-strands (system C4). This system was shown to be very well-folded even with loops of 28 residues.

Table 5.4. *Thermodynamic data for system C4.*

System	Loop Length	**Sequence** cap –β-strand–loop–β-strand–cap'	ΔG_U (kJ/mol)	Fraction Folded (χ_F)	
			280 K	300K	320K
C4	4[a]	RWITVRIW - IGGK - WKTIRVWE	> 11	0.99	0.99
C4	10	RWITVRIW - G_3GKKGG_3 - WKTIRVWE	> 10	0.98	0.95
C4	16	RWITVRIW- $(G_3GKK)_2GG_3$ -WKTIRVWE	+ 8.6	0.97	0.92
C4	22	RWITVRIW- $(G_3GKK)_3GG_3$ -WKTIRVWE	*+ 5.5[a]*	*0.84[a]*	*0.61[a]*
C4	28	RWITVRIW- $(G_3GKK)_4GG_3$ -WKTIRVWE	*+ 4.0[a]*	*0.77[a]*	*0.45[a]*

[a] Fraction folded values estimated by CD, values by NMR not possible due to line broadening.

The system used in this study had the general sequence of R$\mathbf{W^F}$ITVRI$\mathbf{W^E}$-loop-$\mathbf{W^F}$KTIRV$\mathbf{W^E}$E, containing both an end-capping and loop flanking Trp/Trp aromatic cluster. Which Tryptophan is the edge or face of the aromatic cluster is designated by a "$\mathbf{W^E}$" or "$\mathbf{W^F}$", respectively, and color–coded in Table 5.4. Confirmed by sidechain ^{1}H CSDs, as shown in previous studies of turn flanking aromatic clusters, the loop flanking Trp/Trp cluster contains the N-terminal Trp as the "edge" Trp and the C-terminal Trp as the "face" position. As in the previous system, the loop was elongated by using multiples of $(GGGGKK)_n$. Since cross-strand aromatic interactions are most stable at the non-H-bonded sites, the smallest peptide to use as a reference, for the fully folded peptide, is a loop of IGGK.

As seen in Table 5.4, the folding of this system is remarkably resistant to loop elongation; the additional strand length and loop-flanking W/W interaction adds >5 kJ/mol of fold stability to the equivalent loop length of the C2 system. This design technique also provides added thermal stability, with the C4-10 loop (Figure 5.4) maintaining $\chi_F = 0.95$ at 320K, while C2-10 loop (Figure 5.2) had a mole fraction folded of 0.59 at 320 K. This allowed for the synthesis of highly stable β-strands connected by flexible loops of 22 and 28 residues remaining 84 and 77 %

folded at 300K, respectively. A significant accomplishment, considering that the associated β-strands are connected by loops containing many more residues than in the β-strands.

Although these systems are incredibly fold-stabilized, it still appears that the peptides are very slow folders, as demonstrated by the previous C2 system. Unfortunately, with four tryptophans there is such significant overlap in the aromatic region of the NMR spectra, lineshape analysis could not be done. Still, there is significant line-broadening in the 22 and 28 residue systems, this also complicates assignment of the 2D NMR spectra. Despite this, CD measurements were still conclusive. Additionally, to ensure that the CD exciton couplet and NMR lineshape observed were not due to oligomer formation, measurements were done at high and low concentrations (NMR = 30-700 μM, CD 6.25-100 μM) with no difference in the respective spectra found (Appendix F).

5.7 Loop Composition

Table 5.5. *Thermodynamic data for long loops with turn insertions.*

System	Loop Length	**Sequence** cap – β-strand – loop – β-strand – cap'	ΔG_U (kJ/mol)	Fraction Folded (χ_F)	
			280 K	300K	320K
C2	6	RWITVTI-GGGGGG-KKIRVWE	+ 5.8	0.88	0.77
C2	6	RWITVTI - G**IpGK**G - KKIRVWE	+ 6.9	0.97	0.98
C2	6	RWITVTI - G**IPGK**G - KKIRVWE	+ 5.9	0.92	0.85
C2	10	RWITVTI-(G_3GKK)GG_3-KKIRVWE	+ 5.0	0.84	0.59
C2	10	RWITVTI - G_3**IpGK**G_3 - KKIRVWE	+ 6.4	0.93	0.86
C2	10	RWITVTI - G_3**IPGK**G_3 - KKIRVWE	+ 5.1	0.90	0.72
C2	16	RWITVTI-(G_3GKK)$_2GG_3$-KKIRVWE	+ 2.1	0.56	0.38
C2	16	RWITVTI - G_6**IpGK**G_6 - KKIRVWE	+ 4.2	0.77	0.57
C2	16	RWITVTI - G_6**IPGK**G_6 - KKIRVWE	+ 3.4	0.69	0.45
C2	16	RWITVTI – G_5**NPATGK**G_5 - KKIRVWE	+ 4.2	0.79	0.63

Up to this point all the loops examined have been homogeneously flexible. Loops in nature, on the other hand, commonly contain a wider variety of residues. One difference that interests us is what happens to loop search when a small structured element is placed into the loop. To probe this, loops were synthesized that contained β-turns. A common highly nucleating turn is the IpGK turn (p = D-Pro) (Stanger and Gellman 1998), which has a particularly high turn propensity. Turns have a number of effects on a peptide backbone. First of all, most turns contain a proline in order to "kink" the backbone, reducing the entropy difference between the folded and the unfolded states due to the highly-constrained nature of the conformational states around this residue. Additionally, the combination of residues in the turn creates a highly favored folded state. These two effects can be separated by comparison to the IPGK turn, which is a much less favored turn. Surprisingly both turns increase the fraction of the folded state, when placed in the center of the loop (Table 5.5). An added benefit of the placement into the center of the loop is that the nucleating turn can act to nucleate loop folding by determining the center of the loop. Table 5.5 shows the comparison between the 10 and 16 loops to their counter parts with IpGK and IPGK in

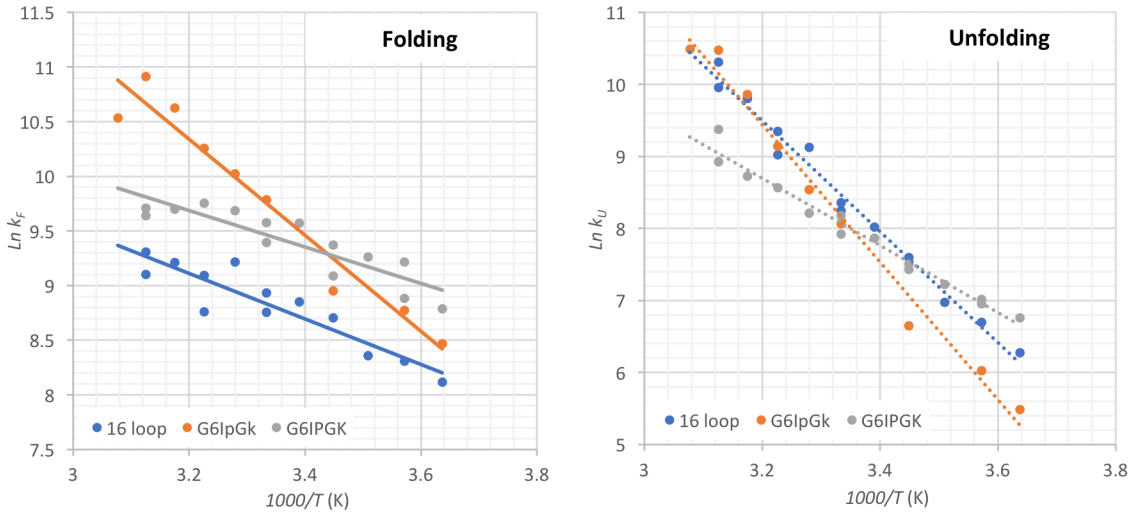

Figure 5.5. *Arrhenius plots of C2-16 with turn insertions: G/K loop (Blue), IpGK (Orange), IPGK (Grey)*

the center of the loop (i.e. 16 loop, -G_6IpGKG_6- and -G_6IPGKG_6-). It was found that the IpGK turn insertion added ~2.4 kJ/mol of fold stability to both the 10 and 16 loop systems, and the IPGK turn insertion only 0.2 and 1.4 kJ/mol of fold stability to the 10 and 16 loops systems, respectively. These were also investigated in the G6 system discussed in section 5.4 showing the same trend, but to a lesser extent likely due to the system already being very well folded. Additionally, a NPATGK turn (discussed in great detail in Chapter 4) was also placed into the 16 loop series (G_5NPATGKG_5) and showed a stability increase of 2.7 kJ/mol at 300K. This may be due to a greater entropy in the unfolded state due to a larger residue turn, but both the IpGK and NPATGK turns in the 16-loop system appear to be in the folded turn conformation to the extent of 30-40%, even being in the middle of unstructured glycine segments.

The dynamics of the folding process of the 10 and 16 residue loop systems was also investigated. Interestingly, the two systems act completely analogously. As noted previously the 10 and 16 residue loops have folding lifetimes of 48 and 146 μs, respectively. This is significantly decreased to 33 and 58 μs with the IpGK turn insert, even though there is an increase of 19 kJ/mol in the activation energy of the folding process (Table 5.6). In the

		Folding			Unfolding		
	ΔG_F (kJ/mol)	Ln k_F	$1/k_F$ (μs)	Ea (kJ/mol)	Ln k_U	$1/k_U$ (μs)	Ea (kJ/mol)
10 Loop	- 4.1	9.9	47.9	25.7	8.1	289.1	59.2
G_3-IpGK-G_3	- 6.4	10.3	33.2	45.5	7.4	641.3	82.0
G_3-IPGK-G_3	- 5.5	10.1	43.2	13.8	7.9	363.0	37.6
16 Loop	- 0.6	8.8	145.8	17.3	8.5	209.8	64.0
G_6-IpGK-G_6	- 3.0	9.8	58.1	36.5	8.2	283.1	79.4
G_6-IPGK-G_6	- 2.0	9.5	77.5	13.9	8.1	311.1	38.7

Table 5.6. *Folding and unfolding data for systems C2-10 and C2-16 with turn insertions. All ΔG_F and k_F measurements at 300 K.*

unfolding direction, there was an increase in the lifetime and an increase in the unfolding activation barrier of 22 and 15 kJ/mol for the 10 and 16 residue loops, respectively: unfolding is definitely retarded by the turn insertion. The IPGK turn insertion decreased both the folding lifetime and activation barrier by a smaller extent, but showed a decrease in the unfolding activation barrier by 22 and 25 kJ/mol for the 10 and 16 residue loops, respectively. Based on this information, we can begin to propose an energy diagram for these processes.

Since both the IpGK and IPGK sequences have the same restrictions in conformational space but varying propensities for turn reversal, a great deal of information can be obtained by comparing the Arrhenius plots for the folding and unfolding processes. When this information is combined with the thermodynamic data calculated from the mole fraction folded, the increase in Ea of folding of the IpGK

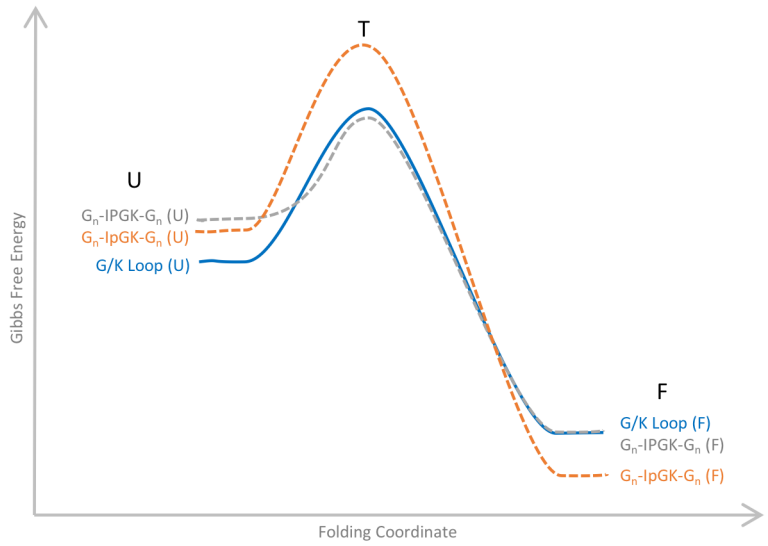

Figure 5.6. *Proposed energy diagram for long loops with turn insertion.*

derivative also has a decrease in ΔG_F. This is contrasted by the IPGK derivative, which displays a slight decrease in Ea of folding and less of a decrease in ΔG_F. By combining this with the unfolding data shown in Table 5.6, the proposed energy diagram can be seen in Figure 5.6. From the unfolded side, there is an increase in free energy, by the same amount, due to identical decrease in entropy from the confinement of the conformational space of the residues in the unfolded state. Now considering the differences in ΔG_F for each peptide, the ΔG_F for the flexible loop (G/K Loop) is the least favorable, followed by G_n-IPGK-G_n and finally G_n-IpGK-G_n with the most favorable folding thermodynamics. The activation barriers, from the Ea for folding and unfolding, reveal that there is a larger barrier for the IpGK derivative. Presumed to be related to the ordering of the turn in combination with the organization of the β-hairpin register, causing this dramatic increase in a folding barrier. This reveals that the added increase in fold stability, is mostly due to an increase in the unfolding barrier.

5.8 Conclusions

Although commonly thought of as simply connecting sequences between the structured regions of a protein, loops constitute an important feature in protein folding and dynamics, adding a level of flexibility not common in other structures. Since the most obvious way to study a piece of a protein is to isolate it by placing it in a smaller peptide system, the study of loops connecting β-strands has suffered because of a lack of appropriately designed systems. In this chapter I have demonstrated many systems which can stabilize and report on the dynamics and fold stability of loops connecting β-strands.

Chapter 6: pH Switchable β-sheets

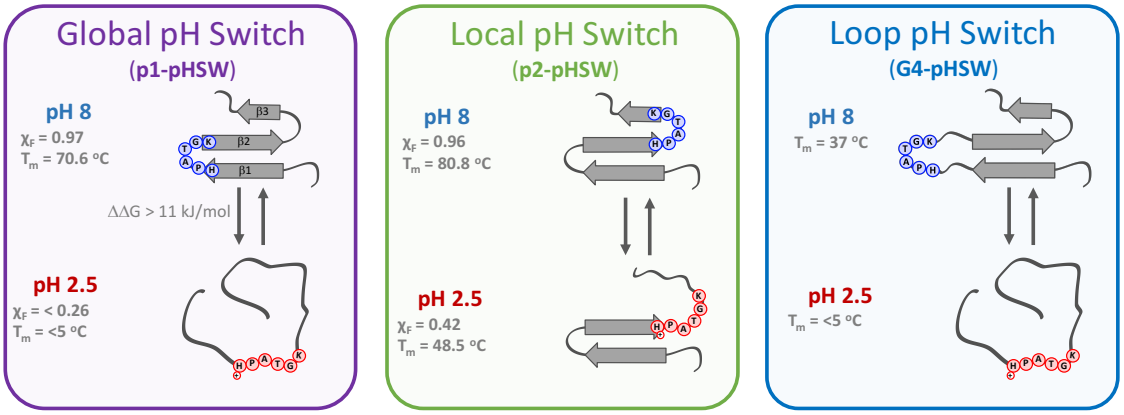

6.1 Introduction

The ability of a protein to perform its designated function requires several features to be fulfilled at the same time. Of course, the sequence dictates the 3D structure of the protein, it also determines the flexibility that the structure possess, which may consist of a number of different motions. As biotechnology promises advances though the use of proteins for new and exciting ways, methods to control when a protein is folded can find use.

Conformational switches (Lin and Scott 2012) are structural features which allows for control between two or more conformations of a protein, either between two folded states or between the folded and unfolded state. Switching between two structures can allow for the change between a biologically active and inactive state. Many such examples include structural redesign by placing charged residues in positions that are attracted or repealed under different conditions. Other options include backbone replacement (Renner and Moroder 2006), small-molecule conjugation (Dagliyan et al. 2013), natural post-translational modification (Bah et al. 2015), or the binding of metal ions (Cerasoli, Sharpe, and Woolfson 2005; Ambroggio and Kuhlman 2006), proteins or peptides (Johnsson and Varshavsky 1994; Magliery et al. 2005).

These switches have found use in bio-sensing (Frommer, Davidson, and Campbell 2009), drug delivery (Reja et al. 2016) and hydrogels (Haines et al. 2005; Schneider et al. 2002; Ozbas et al. 2004). A major problem with these options is that they may require drastic redesign of a protein and the use of unnatural amino acids, making the options less useful for proteins expressed recombinantly. In this chapter I will describe a small β-turn sequence which can lead to a pH-induced conformational switch in a β-sheet, using all natural amino acids and at mild conditions.

Unlike α-helices, the folding of a β-sheet requires long range interactions to form the correct register, with folding pathways often including a specific nucleating hairpin (Olsen et al. 2005; Mccallister, Alm, and Baker 2000). Since the ordering of this hairpin is necessary for the rest of the protein to fold, modifying this by modulating a nucleating turn could control the folding of the protein. (Much more about nucleating hairpins can be found in Chapter 4: β-Turn Optimization.)

	β1	T1	β2	T2	β3	χ_F from NMR (300K)		T_m (°C) from CD	
						pH 8	pH 2.5	pH 8	pH 2.5
Cntrl	= KG WEKRW	----NPATGR----	WYYY	NRITGK	RQWE	RPD-NH_2	0.96	0.89	76.9	48.7
p1- pHSW	= KG WEKRW	----HPATGK----	WYYY	NRITGK	RQWE	RPD-NH_2	0.97	<0.26	70.6	< 5
p2-pHSW	= KG WEKRW	----NPATGR----	WYYY	HPATGK	RQWE	RPD-NH_2	0.96	0.75[1]	80.8	48.5
G2_pHSW	= KG WEKRW	--GGHPATGKGG--	WYYY	NRITGK	RQWE	RPD-NH_2	0.87	----	51.1	7.9
G4_pHSW	= KG WEKRW	GGGGHPATGKGGGG	WYYY	NRITGK	RQWE	RPD-NH_2	----	----	36.9	< 5

Figure 6.1. *Sequences of WW domains used, with a summary of the thermodynamic data from NMR and CD.*
[1]Data shows the global foldedness.

6.2 System Design

The WW domain is a three-stranded sheet system commonly used in studies of β-sheet stability and dynamics (Jäger et al. 2006). The system used in this study is based on the hyper-stable WWst29 system (Kier, Anderson, and Andersen 2014), which contains a Trp/Trp aromatic cluster flanking hairpin 1, resulting in a diagnostic exciton couplet in CD (Anderson et al. 2016). A key advantage of the system is that hairpin 1 is nucleating while hairpin 2 is non-nucleating,

meaning hairpin 1 must form to stabilize the formation of hairpin 2 and the complete fold (Jäger et al. 2001). In this system, the sequence –HPATGK- was placed into both turn 1 and 2, with the stable control sequences being –NPATGR- and –NRITGK- respectively. Additionally to the diagnostics found in CD, there are a number of diagnostic NMR CSDs found in the ^{1}H NMR: the E4 H_N, W7 Hε3, Y15 H_N, Y16 Hα, Y16 H_N, Y17 H_N, N18 Hβ3, K23 H_N, R24 Hα, P29 Hγ3 and W26 Hε3 sites. These were used to calculated the χ_F, using the **Cntrl** peptide at 280 K as 0.99 mole fraction folded. In addition to a number of CSDs from structuring of the three β-strands, many are also from long-range interactions. Among these, the largest of include: the upfield shifted W7 Hε3 (-2.5 ppm), N18 Hβ3 (-3 ppm), upfield shifted P29 Hγ3 (-1.8 ppm) and downfield shifted W26 Hε3 (+0.5 ppm). A full list of the interactions can be found in Appendix J.

6.3 Results and Discussion

When the pH switch sequence (Anderson et al. 2016) (-HPATGK-) is placed into the first hairpin of the WW domain, because it is the nucleating hairpin of the β-sheet, a global pH switch is created (**p1-pHSW**). Although the control peptide (**Cntrl**) only went from χ_F = 0.96 to 0.89 for pH 8 and 2.5 respectively, a marginal loss of 2.7 kJ/mol at 300K, we observed a drastic > 11 kJ/mol decrease in fold stability for **p1-pHSW**. This was confirmed by the exciton couplet in CD (Figure 6.2), with a change in T_m from 70.6 to < 5 ^{o}C from pH 8 to pH 2.5 respectively. Proton NMR reveals that all the peptides prepared for this study display the same fold, with downfield shifted backbone protons in the β-strands and upfield shifted backbone protons in the turns (shown in Figure 6.3). This design required no additional changes, other than a turn

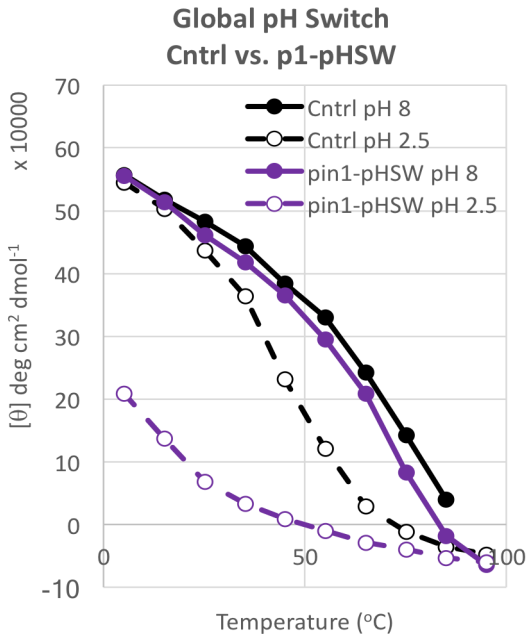

Figure 6.2. *CD spectra of* ***Cntrl*** *and* ***p1-pHSW*** *at pH 8 and 2.5*

mutation. Interestingly, it appears that the change in the structuring of this turn has exclusively to do with the protonation of the His residue. Most of the structuring change happens between pH 6 and 3. Since the lowest energy structure of the peptide is the His^0-folded state, the pKa of the His residue has been lowered to 4.8 (Appendix J).

If instead this turn sequence is placed in the second turn of the WW domain (**p2-pHSW**) a local pH switch is created instead of the global switch demonstrated in **p1-pHSW**. This exemplifies what mutation in the non-nucleating turn of a β-sheet can do. Although the CD spectra only reveals a change from 80.8 to 48.5 °C in the T_m of the peptide, NMR reveals that it is due to the third β-strand undocking from the β-sheet. Figure 6.4 shows that there is still structuring in the β1, β2 and T1, while T2 and β3 have minimal CSDs. The average change in χ_F is from 0.96 to 0.42 for pH 8 and 2.5 respectively. When the mole fraction folded is separated by β-strand, by only using CSDs within the same

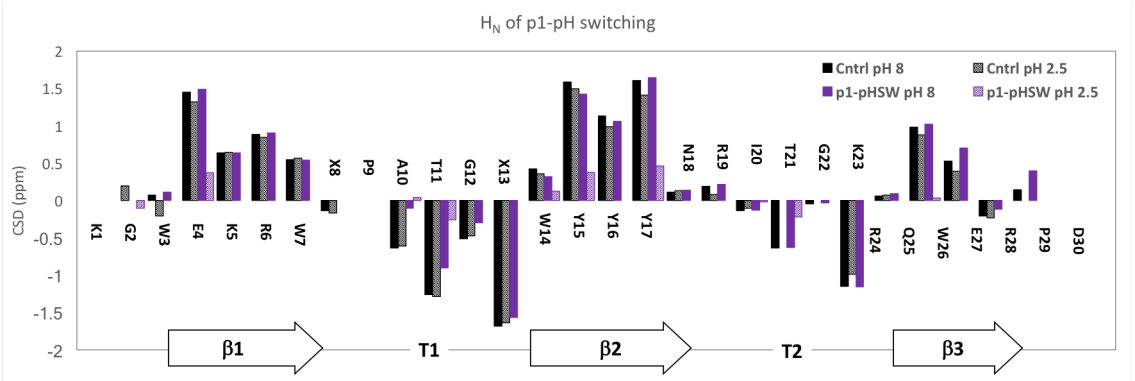

Figure 6.3. *H_N of* ***Cntrl*** *and* ***p1-pHSW*** *at pH 8 and 2.5.*

strand, it appears that χ_F = 0.75, 0.75 and 0.14 for β1, β2 and β3. The reduction in χ_F for the first two stands and change in T_m at pH 2.5 is due to cooperativity between the three strands.

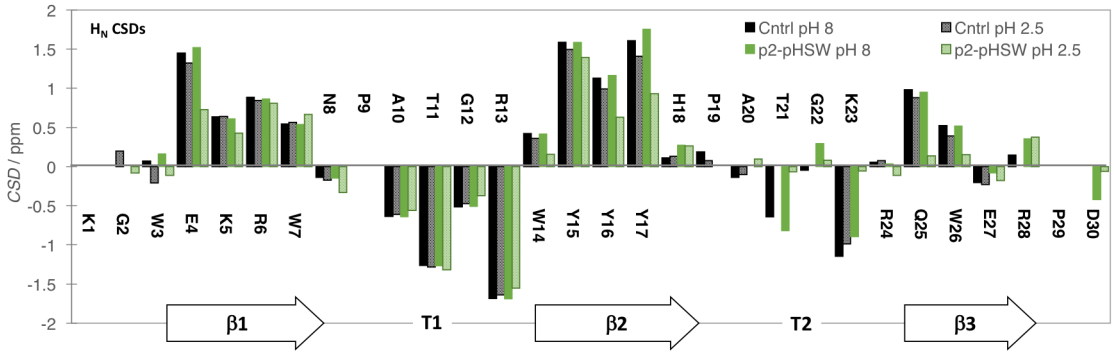

Figure 6.4. *H_N of **Cntrl** and **p2-pHSW** at pH 8 and 2.5.*

Up to this point the switch ability has been built on the use of a mutation into a structure already containing a [4:6] β-turn. As shown in Chapter 5, placing a highly-structured turn into an unstructured loop can affect the protein folding landscape dramatically, by aiding in the folding of the β-sheets they are connected to. Based on this finding, we synthesized a **p1-pHSW** version where two and four glycine's were placed on either side of Turn 1. These are labeled as **G2-pHSW** and **G4-pHSW** in the sequence list, Figure 6.1. Unfortunately, turn 2 did not tolerate loop elongation. Additionally, complete NMR assignments could only be obtained for the **G2-pHSW** at pH 8 due to extensive line-broadening for the unfolded low pH data, and the **G4-pHSW** at both pHs. At pH 8 for **G2-pHSW**, the NMR data indicates χ_F = 0.87, with a change in T_m by CD from 51.1 to 7.9 °C for pH 8 to 2.5 respectively (Figure 6.5). Even with the

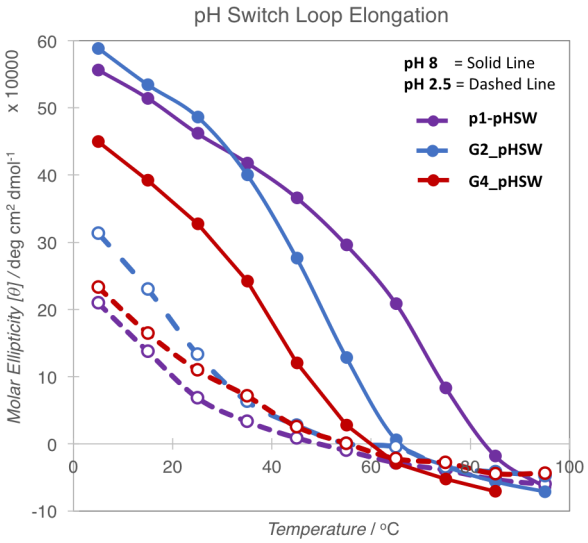

Figure 6.5. *CD spectra of pH switchable loop elongated WW domains.*

expected reduction in population of the folded state due to the loop elongation, **G4-pHSW** had a T_m of 36.9 ^oC at pH 8. This was reduced to < 5 ^oC at pH 2.5, showing the utility of this sequence.

6.4 Conclusions

In this chapter, I have described a pH switch β-turn which is fully folded at high pH and unfolded at low pH. This sequence -HPATGK- was found previously in a small β-hairpin system, Chapter 4. Unlike other conformational switches, this uses all natural amino acids and only requires mutations in the turn region of a protein. β-Sheets typically fold using a nucleating turn. In the WW domain test system this is turn 1 (T1), when the pH-switch is placed into T1, a global pH switch results. When this same sequence was placed into the non-nucleating turn (T2) of the system, a local pH switch was created. This corresponded to just undocking of the third β-strand and not a complete unfolding upon acidification. Finally, to demonstrate the utility of this sequence, the pH switch was also placed into the middle of loops of 10 and 14 residue length. This shows that this pH switch can be used in systems that are not [4:6] β-turns. It is our hope that this pH switch will add greater control to β-sheet and β-hairpin containing proteins, with the majority of the change in foldedness being in the physiological pH-range (Maurer et al. 2015). This has the ability to give the chemist control over the folded and thus the active state of a protein.

Bibliography

Albericio, Fernando, and Hendrik G. Kruger. 2012. "Therapeutic Peptides." *Future Medicinal Chemisty* 4: 1527–31. doi:10.4155/FMC.12.94.

Ambroggio, X. I., and B. Kuhlman. 2006. "Computational Design of a Single Amino Acid Sequence That Can Switch between Two Distinct Protein Folds." *Journal of the American Chemical Society* 128 (4): 1154–61. doi:10.1021/ja054718w.

Andersen, N. H., B. Cao, and C. Chen. 1992. "Peptide/Protein Structure Analysis Using the Chemical Shift Index Method: Upfield α-CH Values Reveal Dynamic Helices and a_L Sites." *Biochemical and Biophysical Research Communications* 184 (2): 1008–14.

Andersen, Niels H., Jonathan W. Neidigh, Scott M. Harris, Gregory M. Lee, Zhihong Liu, and Hui Tong. 1997. "Extracting Information from the Temperature Gradients of Polypeptide NH Chemical Shifts. 1. The Importance of Conformational Averaging." *Journal of the American Chemical Society* 119 (36): 8547–61. doi:10.1021/ja963250h.

Andersen, Niels H., Katherine A. Olsen, R. Matthew Fesinmeyer, Xu Tan, F. Michael Hudson, Lisa A. Eidenschink, and Shabnam R. Farazi. 2006. "Minimization and Optimization of Designed β-Hairpin Folds." *Journal of the American Chemical Society* 128 (18): 6101–10. doi:10.1021/ja054971w.

Anderson, Jordan M., Brandon L. Kier, Brice Jurban, Aimee Byrne, Irene Shu, Lisa A. Eidenschink, Alexander A. Shcherbakov, Mike Hudson, R. M. Fesinmeyer, and Niels H. Andersen. 2016. "Aryl-Aryl Interactions in Designed Peptide Folds: Spectroscopic Characteristics and Optimal Placement for Structure Stabilization." *Biopolymers* 105 (6): 337–56. doi:10.1002/bip.22821.

Anderson, Jordan M., Brice Jurban, Kelly N. L. Huggins, Alexander A. Shcherbakov, Irene Shu,

Brandon Kier, and Niels H. Andersen. 2016. “Nascent Hairpins in Proteins: Identifying Turn Loci and Quantitating Turn Contributions to Hairpin Stability.” *Biochemistry* 55: 5537–53. doi:10.1021/acs.biochem.6b00732.

Anderson, Jordan M., Alexander A. Shcherbakov, Brandon L. Kier, James K. Kellock, Irene Shu, Aimee Byrne, Lisa Eidenschink, and Niels H. Andersen. 2017. “Optimization of a β-Sheet-Cap for Long Loop Closure.” *Biopolymers* 107 (3): e22995. doi:10.1002/bip.22995.

Bah, Alaji, Robert M. Vernon, Zeba Siddiqui, Mickaël Krzeminski, Ranjith Muhandiram, Charlie Zhao, Nahum Sonenberg, Lewis E. Kay, and Julie D. Forman-Kay. 2015. “Folding of an Intrinsically Disordered Protein by Phosphorylation as a Regulatory Switch.” *Nature* 519 (7541): 106–9. doi:10.1038/nature13999.

Bain, Alex D., Darrell M. Rex, and Rashida N. Smith. 2001. “Fitting Dynamic NMR Lineshapes.” *Magnetic Resonance in Chemistry* 39 (3): 122–26. doi:10.1002/mrc.806.

Behrendt, Raymond, Peter White, and John Offer. 2016. “Advances in Fmoc Solid-Phase Peptide Synthesis.” *Journal of Peptide Science* 22 (1): 4–27. doi:10.1002/psc.2836.

Blanco, Francisco J., German Rivas, and Luis Serrano. 1994. “A Short Linear Peptide That Folds into a Native Stable β-Hairpin in Aqueous Solution.” *Nature Structural Biology* 1 (9): 584–90. doi:10.1038/367347a0.

Bofill, Roger, Emma R. Simpson, Geoffrey W. Platt, Maria D. Crespo, and Mark S. Searle. 2005. “Extending the Folding Nucleus of Ubiquitin with an Independently Folding β-Hairpin Finger: Hurdles to Rapid Folding Arising from the Stabilisation of Local Interactions.” *Journal of Molecular Biology* 349 (1): 205–21. doi:10.1016/j.jmb.2005.03.048.

Braunschweiler, L., and R. R. Ernst. 1983. “Coherence Transfer by Isotropic Mixing:

Application to Proton Correlation Spectroscopy." *Journal of Magnetic Resonance (1969)* 53 (3): 521–28.

Canutescu, Adrian A., and Roland L. Dunbrack. 2003. "Cyclic Coordinate Descent: A Robotics Algorithm for Protein Loop Closure." *Protein Science : A Publication of the Protein Society* 12 (3): 963–72. doi:10.1110/ps.0242703.

Cerasoli, Eleonora, Belinda K. Sharpe, and Derek N. Woolfson. 2005. "ZiCo: A Peptide Designed to Switch Folded State upon Binding Zinc." *Journal of the American Chemical Society* 127 (43): 15008–9. doi:10.1021/ja0543604.

Chang, Jui-Yoa, Li Li, and Alexey Bulychev. 2000. "The Underlying Mechanism for the Diversity of Disulfide Folding Pathways." *The Journal of Biological Chemistry* 275 (12): 8287–89. doi:10.1074/jbc.275.12.8287.

Ciani, Barbara, Muriel Jourdan, and Mark S. Searle. 2003. "Stabilization of β-Hairpin Peptides by Salt Bridges: Role of Preorganization in the Energetic Contribution of Weak Interactions." *Journal of the American Chemical Society* 125 (30): 9038–47. doi:10.1021/ja030074l.

Clark, Patricia L. 2004. "Protein Folding in the Cell : Reshaping the Folding Funnel." *Trends in Biochemical Sciences* 29 (10): 527–34. doi:10.1016/j.tibs.2004.08.008.

Cline, Lauren L., and Marcey L. Waters. 2009. "The Structure of Well-Folded β-Hairpin Peptides Promotes Resistance to Peptidase Degradation Hairpin Peptides Promotes Resistance to Peptidase Degradation" *Biopolymers* 92 (6): 502–7. doi:10.1002/bip.21266.

Cochran, A. G., N. J. Skelton, and M. A. Starovasnik. 2001. "Tryptophan Zippers: Stable, Monomeric B - Hairpins." *Proceedings of the National Academy of Sciences of the United States of America* 98 (10): 5578–83. doi:10.1073/pnas.091100898.

Cochran, Andrea G., Nicholar J. Skelton, and Melissa A. Starovasnik. 2001. "Tryptophan Zippers: Stable, Monomeric Beta-Hairpins." *Proceedings of the National Academy of Sciences* 98 (10): 5578–83. doi:10.1073/pnas.091100898.

Dagliyan, Onur, David Shirvanyants, Andrei V. Karginov, Feng Ding, Lanette Fee, Srinivas N. Chandrasekaran, Christina M. Freisinger, et al. 2013. "Rational Design of a Ligand-Controlled Protein Conformational Switch." *Proceedings of the National Academy of Sciences* 110 (17): 6800–6804. doi:10.1073/pnas.1218319110.

Deane, Charlotte M., and Tom L. Blundell. 2000. "A Novel Exhaustive Search Algorithm for Predicting the Conformation of Polypeptide Segments in Proteins." *Proteins: Structure, Function and Genetics* 40 (1): 135–44. doi:10.1002/(SICI)1097-0134(20000701)40:1<135::AID-PROT150>3.0.CO;2-1.

Dempsey, Christopher E. 2001. "Hydrogen Exchange in Peptides and Proteins Using NMR Spectroscopy." *Nuclear Magnetic Resonance Spectroscopy* 39 (2): 135–70.

Dill, Ken A., and Hue Sun Chan. 1997. "From Levinthal to Pathways to Funnels." *Nature Structural Biology* 4 (1): 10–19. doi:10.1038/nsb0197-10

Dill, Ken A., S. Banu Ozkan, Thomas R. Weikl, John D. Chodera, and Vincent A. Voelz. 2007. "The Protein Folding Problem: When Will It Be Solved?" *Current Opinion in Structural Biology* 17 (3): 342–46. doi:10.1016/j.sbi.2007.06.001.

Ding, Feng, Douglas Tsao, Huifen Nie, and Nikolay Dokholyan. 2008. "Ab Initio Folding of Proteins with All-Atom Discrete Molecular Dynamics." *Structure* 16 (7): 1010–18. doi:10.1016/j.str.2008.03.013.

Dyer, R. Brian, Shelia J. Maness, Eric S. Peterson, Stefan Franzen, R. Matthew Fesinmeyer, and Niels H. Andersen. 2004. "The Mechanism of Beta-Hairpin Formation." *Biochemistry* 43

(36): 11560–66. doi:10.1021/bi049177m.

Ekiert, Damian C., Arun K. Kashyap, John Steel, Adam Rubrum, Gira Bhabha, Reza Khayat, Jeong Hyun Lee, et al. 2012. "Cross-Neutralization of Influenza A Viruses Mediated by a Single Antibody Loop." *Nature* 489 (7417). 526–32. doi:10.1038/nature11414.

Fesinmeyer, R. Matthew, F. Michael Hudson, and Niels H. Andersen. 2004. "Enhanced Hairpin Stability through Loop Design: The Case of the Protein G B1 Hairpin." *Journal of the American Chemical Society* 126 (13): 7238–43. doi:10.1021/ja0379520.

Fierz, Beat, Helmut Satzger, Christopher Root, Peter Gilch, Wolfgang Zinth, and Thomas Kiefhaber. 2007. "Loop Formation in Unfolded Polypeptide Chains on the Picoseconds to Microseconds Time Scale." *Proceedings of the National Academy of Sciences of the United States of America* 104 (7): 2163–68. doi:10.1073/pnas.0611087104.

Fine, R. M., H. Wang, P. S. Shenkin, D. L. Yarmush, and C. Levinthal. 1986. "Predicting Antibody Hypervariable Loop Conformations. II: Minimization and Molecular Dynamics Studies of MCPC603 from Many Randomly Generated Loop Conformations." *Proteins: Structure, Function and Genetics* 1 (4): 342–62.

Fiser, András, and Andrej Sali. 2003. "ModLoop: Automated Modeling of Loops in Protein Structures." *Bioinformatics* 19 (18): 2500–2501. doi:10.1093/bioinformatics/btg362.

Friebolin, Horst. 1998. *Basic One- and Two-Dimensional NMR Spectroscopy*. 3rd ed. Weinheim: WILEY-VCH.

Frommer, Wolf B., Michael W. Davidson, and Robert E. Campbell. 2009. "Genetically Encoded Biosensors Based on Engineered Fluorescent Proteins." *Chemical Society Reviews* 38 (10): 2833–41. doi:10.1039/b907749a.

Gellman, S. H. 1998. "Minimal Model Systems for Beta Sheet Secondary Structure in Proteins."

Current Opinion in Chemical Biology 2 (6): 717–25. doi:10.1016/S1367-5931(98)80109-9

Ginalski, Krzysztof. 2006. "Comparative Modeling for Protein Structure Prediction." *Current Opinion in Structural Biology* 16: 172–77. doi:10.1016/j.sbi.2006.02.003.

Haines, Lisa A., Karthikan Rajagopal, Bulent Ozbas, Daphne A. Salick, Darrin J. Pochan, and Joel P. Schneider. 2005. "Light-Activated Hydrogel Formation via the Triggered Folding and Self-Assembly of a Designed Peptide." *Journal of the American Chemical Society* 127 (48): 17025–29. doi:10.1021/ja054719o.

Heinis, Christian, Trevor Rutherford, Stephan Freund, and Greg Winter. 2009. "Phage-Encoded Combinatorial Chemical Libraries Based on Bicyclic Peptides." *Nature Chemical Biology* 5: 502–7. doi:10.1038/nchembio.184

Honda, Shinya, Kazuhiko Yamasaki, Yoshito Sawada, and Hisayuki Morii. 2004. "10 Residue Folded Peptide Designed by Segment Statistics." *Structure* 12 (8): 1507–18. doi:10.1016/j.str.2004.05.022.

Huang, Joseph Jen-Tse, Randy W. Larsen, and Sunney I. Chan. 2012. "The Interplay of Turn Formation and Hydrophobic Interactions on the Early Kinetic Events in Protein Folding." *Chemical Communications (Cambridge, England)* 48 (4): 487–97. doi:10.1039/c1cc13278d.

Jackson, Sophie E., and Alan R. Fersht. 1991. "Folding of Chymotrypsin Inhibitor 2. 1. Evidence for a Two-State Transition Sophie." *Biochemistry* 30 (43): 10428–35.

Jäger, Marcus, Houbi Nguyen, Jason C. Crane, Jeffery W. Kelly, and Martin Gruebele. 2001. "The Folding Mechanism of a Beta-Sheet: The WW Domain." *Journal of Molecular Biology* 311 (2): 373–93. doi:10.1006/jmbi.2001.4873.

Jäger, Marcus, Yan Zhang, Jan Bieschke, Houbi Nguyen, Maria Dendle, Marianne E. Bowman,

Joseph P. Noel, Martin Gruebele, and Jeffery W. Kelly. 2006. “Structure-Function-Folding Relationship in a WW Domain.” *Proceedings of the National Academy of Sciences of the United States of America* 103 (28): 10648–53. doi:10.1073/pnas.0600511103.

Johnsson, N., and A. Varshavsky. 1994. “Split Ubiquitin as a Sensor of Protein Interactions in Vivo.” *Proceedings of the National Academy of Sciences of the United States of America* 91 (22): 10340–44. doi:10.1073/pnas.91.22.10340.

Kelly, Sharon M., Thomas J. Jess, and Nicholas C. Price. 2005. “How to Study Proteins by Circular Dichroism.” *Biochimica et Biophysica Acta* 1751 (2): 119–39. doi:10.1016/j.bbapap.2005.06.005.

Kier, Brandon L., and Niels H. Andersen. 2014. “Captides: Rigid Junctions between Beta Sheets and Small Molecules.” *Journal of Peptide Science* 20 (9): 704–15. doi:10.1002/psc.2657.

Kier, Brandon L., Jordan M. Anderson, and Niels H. Andersen. 2014. “Circular Permutation of a WW Domain: Folding Still Occurs after Excising the Turn of the Folding-Nucleating Hairpin.” *Journal of the American Chemical Society* 136 (2): 741–49. doi:10.1021/ja410824x.

Kier, Brandon L., Irene Shu, Lisa A. Eidenschink, and Niels H. Andersen. 2010. “Stabilizing Capping Motif for Beta-Hairpins and Sheets.” *Proceedings of the National Academy of Sciences of the United States of America* 107 (23): 10466–71. doi:10.1073/pnas.0913534107.

Kier, Brandon L., and Niels H. Andersen. 2014b. “Rigid Peptide Oligomers Via Covalent Assembly: Toward Peptide Legos.” *Journal of Peptide Science* 20 (S1): S71-72.

Kier, Brandon L, Jordan M Anderson, and Niels H Andersen. 2015. “Disulfide-Mediated β‐Strand Dimers: Hyperstable β‐Sheets Lacking Tertiary Interactions and Turns.” *Journal*

of American Chemical Society 137 (16): 5363–71. doi:10.1021/ja5117809.

Kier, Brandon L., Gregory M. Newbloom, Lilo D. Pozzo, and Niels H. Andersen. 2016. "A Structuring Repeat for Peptide Design : Long Beta Ribbons." *ChemBioChem* 17 (3): 224–27. doi:10.1002/cbic.201500618.

Kobayashi, Naohiro, Satoshi Endo, and Eisuke Munekata. 1992. "Conformational Study on the IgG Binding Domain of Protein G." In *Proceesings of the 2nd Japan Symposium on Peptide Chemistry* 278–80.

Koebnik, Ralf. 1999. "Structural and Functional Roles of the Surface-Exposed Loops of the Beta-Barrel Membrane Protein OmpA from Escherichia Coli." *Journal of Bacteriology* 181 (12): 3688–94.

Kubelka, Jan, James Hofrichter, and William A. Eaton. 2004. "The Protein Folding 'Speed Limit'." *Current Opinion in Structural Biology* 14 (1): 76–88. doi:10.1016/j.sbi.2004.01.013.

Lewandowska, Agnieszka, Stanisław Ołdziej, Adam Liwo, and Harold A. Scheraga. 2010. "Beta-Hairpin-Forming Peptides; Models of Early Stages of Protein Folding." *Biophysical Chemistry* 151 (1–2). Elsevier B.V.: 1–9. doi:10.1016/j.bpc.2010.05.001.

Li, Fang, Jung Ho Lee, Alexander Grishaev, Jinfa Ying, and Ad Bax. 2015. "High Accuracy of Karplus Equations for Relating Three-Bond J Couplings to Protein Backbone Torsion Angles." *Chemphyschem* 16 (3): 572–78. doi:10.1002/cphc.201402704.High.

Lin, George Guan-hua, and Jeffrey G. Scott. 2012. "Protein Conformational Switches: From Nature to Design." *Chemisty* 18 (26): 7984–99. doi:10.1016/j.pestbp.2011.02.012.Investigations.

London, Nir, Barak Raveh, and Ora Schueler-furman. 2013. "Druggable Protein – Protein

Interactions – from Hot Spots to Hot Segments." *Current Opinion in Chemical Biology* 17 (6). Elsevier Ltd: 952–59. doi:10.1016/j.cbpa.2013.10.011.

Lovell, Simon C, Ian W. Davis, Bryan W. Arendall, Paul I. W. De Bakker, J. Michael Word, Michael G. Prisant, Jane S. Richardson, and David C. Richardson. 2003. "Structure Validation by Cα Geometry : Φ,Ψ and Cβ Deviation." *Proteins: Structure, Function and Genetics* 50: 437–50. doi:10.1002/prot.10286.

Magliery, Thomas J., Christopher G. M. Wilson, Weilan Pan, Dennis Mishler, Indraneel Ghosh, Andrew D. Hamilton, and Lynne Regan. 2005. "Detecting Protein-Protein Interactions with a Green Fluorescent Protein Fragment Reassembly Trap: Scope and Mechanism." *Journal of the American Chemical Society* 127 (1): 146–57. doi:10.1021/ja046699g.

Malabanan, M. Merced, Tina L. Amyes, and John P. Richard. 2010. "A Role for Flexible Loops in Enzyme Catalysis." *Current Opinion in Structural Biology* 20 (6). Elsevier Ltd: 702–10. doi:10.1016/j.sbi.2010.09.005.

Marx, V. 2005. "Watching Peptide Drugs Grow Up." *Chem. Eng. News* 83: 17–24.

Maurer, Jacoba M., Reinout C. A. Schellekens, Hèlen M. Van Rieke, Christoph Wanke, Ventzeslav Iordanov, Frans Stellaard, Klaus D. Wutzke, et al. 2015. "Gastrointestinal pH and Transit Time Profiling in Healthy Volunteers Using the IntelliCap System Confirms Ileo-Colonic Release of ColoPulse Tablets." *PLoS ONE* 10 (7): 1–17. doi:10.1371/journal.pone.0129076.

Mccallister, Erika L., Eric Alm, and David Baker. 2000. "Critical Role of β-Hairpin Formation in Protein G Folding." *Nature Structural Biology* 7 (8): 669–73.

Merlo, Claudia, Ken A. Dill, and Thomas R. Weikl. 2005. "Phi Values in Protein-Folding Kinetics Have Energetic and Structural Components." *Proceedings of the National*

Academy of Sciences of the United States of America 102 (29): 10171–75. doi:10.1073/pnas.0504171102.

Merrifield, R. B. 1963. "Solid Phase Peptide Synthesis. I. The Synthesis of a Tetrapeptide." *Journal of the American Chemical Society* 85 (14): 2149–54.

Messih, Mario Abdel, Rosalba Lepore, and Anna Tramontano. 2015. "LoopIng: A Template-Based Tool for Predicting the Structure of Protein Loops." *Bioinformatics* 31 (23): 3767–72. doi:10.1093/bioinformatics/btv438.

Mitchell, Alexander R. 2008. "Bruce Merrifield and Solid-Phase Peptide Synthesis: A Historical Assessment." *Biopolymers - Peptide Science* 90 (3): 175–84. doi:10.1002/bip.20925.

Modarres, Hassan Pezeshgi, Boris D. Dorokhov, Vladimir O. Popov, Nikolai V. Ravin, Konstantin G. Skryabin, and Matteo Dal Peraro. 2015. "Understanding and Engineering Thermostability in DNA Ligase from Thermococcus Sp. 1519." *Biochemistry* 54 (19): 3076–85. doi:10.1021/bi501227b.

Muñoz, V., P. A. Thompson, J. Hofrichter, and W. A. Eaton. 1997. "Folding Dynamics and Mechanism of Beta-Hairpin Formation." *Nature* 390 (6656): 196–99. doi:10.1038/36626.

Nagi, Athena D., and Lynne Regan. 1997. "An Inverse Correlation between Loop Length and Stability in a Four-Helix-Bundle Protein." *Folding and Design* 2 (1): 67–75. doi:10.1016/S1359-0278(97)00007-2.

Olsen, Katherine A., R. Matthew Fesinmeyer, James M. Stewart, and Niels H. Andersen. 2005. "Hairpin Folding Rates Reflect Mutations Within and Remote from the Turn Region." *Proceedings of the National Academy of Sciences of the United States of America* 102 (43): 15483–87. doi:10.1073/pnas.0504392102.

Ozbas, Bulent, Juliana Kretsinger, Karthikan Rajagopal, Joel P. Schneider, and Darrin J. Pochan.

2004. “Salt-Triggered Peptide Folding and Consequent Self-Assembly into Hydrogels with Tunable Modulus.” *Macromolecules* 37 (19): 7331–37. doi:10.1021/ma0491762.

Pace, C. Nick, Gerald R. Grimsley, James A. Thomson, and Ben J. Barnett. 1988. “Conformational Stability and Activity of Ribonuclease TI with Zero, One, and Two Intact Disulfide Bonds.” *The Journal of Biological Chemistry* 263 (24): 11820–25.

Panwalkar, Vineet, Philipp Neudecker, Michael Schmitz, Justin Lecher, Marianne Schulte, Karima Medini, Matthias Stoldt, Margaret A. Brimble, Dieter Willbold, and Andrew J. Dingley. 2016. “The Nedd4-1 WW Domain Recognizes the PY Motif Peptide through Coupled Folding and Binding Equilibria.” *Biochemistry* 55 (4): 659–74. doi:10.1021/acs.biochem.5b01028.

Petrovich, Miriana, Amanda L. Jonsson, Neil Ferguson, Valerie Daggett, and Alan R. Fersht. 2006. “Phi-Analysis at the Experimental Limits: Mechanism of Beta-Hairpin Formation.” *Journal of Molecular Biology* 360 (4): 865–81. doi:10.1016/j.jmb.2006.05.050.

Petsko, Gregory A., and Dagmar Ringe. 2004. *Protein Structure and Function*. Sunderland, Ma: New Science Press Ltd.

Pluckthun, Andreas. 2015. “Designed Ankyrin Repeat Proteins (DARPins): Binding Proteins for Research, Diagnostics, and Therapy.” *Annual Review of Pharmacology and Toxixology* 55 (1): 489–511.

Ramachandran, G. N., C. Ramakrishnan, and V. Sasisekharan. 1963. “Stereochemistry of Polypeptide Chain Configurations.” *Journal of Molecular Biology* 7 (1). Academic Press Inc. (London) Ltd.: 95–99. doi:10.1016/S0022-2836(63)80023-6.

Ramsland, P. A., L. Shan, C. R. Moomaw, C. A. Slaughter, Z. Fan, L. W. Guddat, and A. B. Edmundson. 2000. “An Unusual Human IgM Antibody with a Protruding HCDR3 and High

Avidity for Its Peptide Ligands." *Molecular Immunology* 37 (6): 295–310. doi:10.1016/S0161-5890(00)00049-3.

Reja, Rahi M., Mohsina Khan, Sumeet K. Singh, Rajkumar Misra, Anjali Shiras, and Hosahudya N. Gopi. 2016. "pH Sensitive Coiled Coils: A Strategy for Enhanced Liposomal Drug Delivery." *Nanoscale* 8 (9). Royal Society of Chemistry: 5139–45. doi:10.1039/C5NR07734F.

Renner, Christian, and Luis Moroder. 2006. "Azobenzene as Conformational Switch in Model Peptides." *ChemBioChem* 7 (6): 868–78. doi:10.1002/cbic.200500531.

Riemen, Alexander J., and Marcey L. Waters. 2009. "Design of Highly Stabilized Beta-Hairpin Peptides through Cation-Pi Interactions of Lysine and N-Methyllysine with an Aromatic Pocket." *Biochemistry* 48 (7): 1525–31. doi:doi:10.1021/bi801706k.

Robinson, J. A., S. Demarco, F. Gombert, K. Moehle, and D. Obrecht. 2008. "The Design, Structures and Therapeutic Potential of Protein Epitope Mimetics." *Drug Discovery Today* 13 (21–22): 944–51.

Rohonczy, J. 1992. "Total Lineshape Analysis of DNMR Spectra by IBM Personal Computer." *Kem. Kozl.* 74: 161–200.

Rost, Burkhard, Reinhard Schneider, and Chris Sander. 1997. "Protein Fold Recognition by Prediction-Based Threading." *Journal of Molecular Biology* 270 (3): 471–80. doi:10.1006/jmbi.1997.1101.

Santiveri, Clara M., Esther León, Manuel Rico, and M. Angeles Jimønez. 2008. "Context-Dependence of the Contribution of Disulfide Bonds to Beta-Hairpin Stability." *Chemistry - A European Journal.* 14 (2): 488–99. doi:10.1002/chem.200700845.

Scandurra, Roberto, Valerio Consalvi, Roberta Chiaraluce, Laura Politi, and Paul C. Engel.

1998. “Protein Thermostability in Extremophiles.” *Biochimie* 80 (11): 933–41. doi:10.1016/S0300-9084(00)88890-2.

Schlehuber, Lisa D., Iain J. Mcfadyen, Yu Shu, James Carignan, W. Paul Duprex, William R. Forsyth, Jason H. Ho, et al. 2011. “Towards Ambient Temperature-Stable Vaccines : The Identification of Thermally Stabilizing Liquid Formulations for Measles Virus Using an Innovative High-Throughput Infectivity Assay.” *Vaccine* 29 (31). Elsevier Ltd: 5031–39. doi:10.1016/j.vaccine.2011.04.079.

Schneider, Joel P., Darrin J. Pochan, Bulent Ozbas, Karthikan Rajagopal, Lisa Pakstis, and Juliana Kretsinger. 2002. “Responsive Hydrogels from the Intramolecular Folding and Self-Assembly of a Designed Peptide.” *Journal of the American Chemical Society* 124 (50): 15030–37. doi:10.1021/ja027993g.

Searle, Mark S., Dudley H. Williams, and Leonard C. Packman. 1995. “A Short Linear Peptide Derived from the N-Terminal Sequence of Ubiquitin Folds into a Water-Stable Non-Native Beta-Hairpin.” *Nature Structural Biology* 2 (11): 999–1006. doi:10.1038/nsb1195-999.

Shenkin, P. S., D. L. Yarmush, R. M. Fine, H. Wang, and C. Levinthal. 1987. “Predicting Antibody Hypervariable Loop Conformation, 1. Ensembles of Random Conformations for Ring-like Structures.” *Biopolymers* 26: 2053–85. doi:10.1002/bip.360261207.

Sheu, Sheh-Yi, Dah-Yen Yang, H. L. Selzle, E. W. Schlag, R. Jaenicke, Jack D. Dunitz, The Peptide Bond, et al. 2000. “From Sequence to Structure.” *Journal of Biotechnology* 79: 193–203. doi:10.1016/1074-5521(95)90097-7.

Sibanda, B. L., T. L. Blundell, and J. M. Thornton. 1989. “Conformation of Beta-Hairpins in Protein Structures: A Systematic Classification with Applications to Modelling by Homology, Electron Density Fitting and Protein Engineering.” *Journal of Molecular*

Biology 206 (4): 759–77. doi:10.1016/0022-2836(89)90583-4.

Smith, Matthew C., and Jason E. Gestwicki. 2012. "Features of Protein-Protein Interactions That Translate into Potent Inhibitors: Topology, Surface Area and Affinity." *Expert Reviews in Molecular Medicine* 14: e16. doi:10.1017/erm.2012.10.

Song, Jianing, Yongle Li, Changge Ji, and John Z. H. Zhang. 2015. "Functional Loop Dynamics of the Streptavidin-Biotin Complex." *Scientific Reports* 5: 7906. doi:10.1038/srep07906.

Stanger, Heather E., and Samuel H. Gellman. 1998. "Rules for Antiparallel B-Sheet Design: D-Pro-Gly Is Superior to L-Asn-Gly for B-Hairpin Nucleation." *Journal of the American Chemical Society* 120 (7): 4236–37. doi:10.1021/ja973704q.

Tanford, Charles. 1962. "Contribution of Hydrophobic Interactions to the Stability of the Globular Conformation." *Journal of the American Chemical Society.* 84 (86): 4240–47. doi:10.1021/ja00881a009.

———. 1997. "How Protein Chemists Learned about the Hydrophobic Factor." *Protein Science* 6 (6): 1358–66. doi:10.1002/pro.5560060627.

Tsomaia, Natia. 2015. "Peptide Therapeutics: Targeting the Undruggable Space." *European Journal of Medicinal Chemistry* 94. 459–70. doi:10.1016/j.ejmech.2015.01.014.

Venkatachalam, C. M. 1968. "Stereochemical Criteria for Polypeptides and Proteins. V. Conformation of a System of Three Linked Peptide Units." *Biopolymers* 6 (10): 1425–36.

Vieille, Claire, and Gregory J. Zeikus. 2001. "Hyperthermophilic Enzymes: Sources, Uses, and Molecular Mechanisms for Thermostability." *Microbiology and Molecular Biology Reviews* 65 (1): 1–43. doi:10.1128/MMBR.65.1.1.

Vinther, Tine N., Ingrid Pettersson, Kasper Huus, Morten Schlein, Dorte B. Steensgaard, Anders Sørensen, Knud J. Jensen, and Thomas Kjeldsen. 2015. "Additional Disulfide Bonds in

Insulin: Prediction, Recombinant Expression , Receptor Binding Affinity, and Stability." *Protein Science* 24 (5): 779–88. doi:10.1002/pro.2649.

Wang, Guangchuan, Rui-yuan Cao, Rong Chen, Lijuan Mo, Jian-feng Han, Xiaoyu Wang, and Xurong Xu. 2013. "Rational Design of Thermostable Vaccines by Engineered Peptide-Induced Virus Self- Biomineralization under Physiological Conditions." *Proceedings of the National Academy of Sciences* 110 (19): 7619–24. doi:10.1073/pnas.1300233110.

Wang, Li Chun Tommy, and Chih Cheng Chen. 1991. "A Combined Optimization Method for Solving the Inverse Kinematics Problem of Mechanical Manipulators." *IEEE Transactions on Robotics and Automation* 7 (4): 489–99. doi:10.1109/70.86079.

Whitmore, Lee, and B. A. Wallace. 2007. "Protein Secondary Structure Analyses from Circular Dichroism Spectroscopy: Methods and Reference Databases." *Biopolymers* 89 (5): 392–400. doi:10.1002/bip.20853.

Woodman, Robbie, T. H. Johannes Yeh, Sophie Laurenson, and Paul Ferrigno. 2005. "Design and Validation of a Neutral Protein Scaffold for the Presentation of Peptide Aptamers." *Journal of Molecular Biology* 352 (5): 1118–33. doi:10.1016/j.jmp.2005.08.001.

Wright, Caroline F., John Christodoulou, Christopher M. Dobson, and Jane Clarke. 2004. "The Importance of Loop Length in the Folding of an Immunoglobulin Domain." *Protein Engineering, Design and Selection* 17 (5): 443–53. doi:10.1093/protein/gzh052.

Wu, Ling, Dan Mcelheny, Vladimír Setnicka, Jovencio Hilario, and Timothy A. Keiderling. 2012. "Role of Different β-Turns in β-Hairpin Conformation and Stability Studied by Optical Spectroscopy." *Proteins: Structure, Function and Bioinformatics* 80 (1): 44–60. doi:10.1002/prot.23140.

Yarnitzky, Talia, Anat Levit, and Masha Y. Niv. 2010. "Homology Modeling of G-Protein-

Coupled Receptors with X-Ray Structures on the Rise." *Current Opinion in Drug Discovery & Development* 13 (3): 317–25. doi:10.1371/journal.pone.0007011.

Zeikus, J. Gregory, Claire Vieille, and Alexei Savchenko. 1998. "Thermozymes: Biotechnology and Structure-Function Relationships." *Extremophiles* 2 (3): 179–83. doi:10.1007/s007920050058.

Zwanzig, Robert. 1997. "Two-State Models of Protein Folding Kinetics." *Proceedings of the National Academy of Sciences* 94: 148–50.

Appendix A – The natural amino acids, with IUPAC atomic numbering.

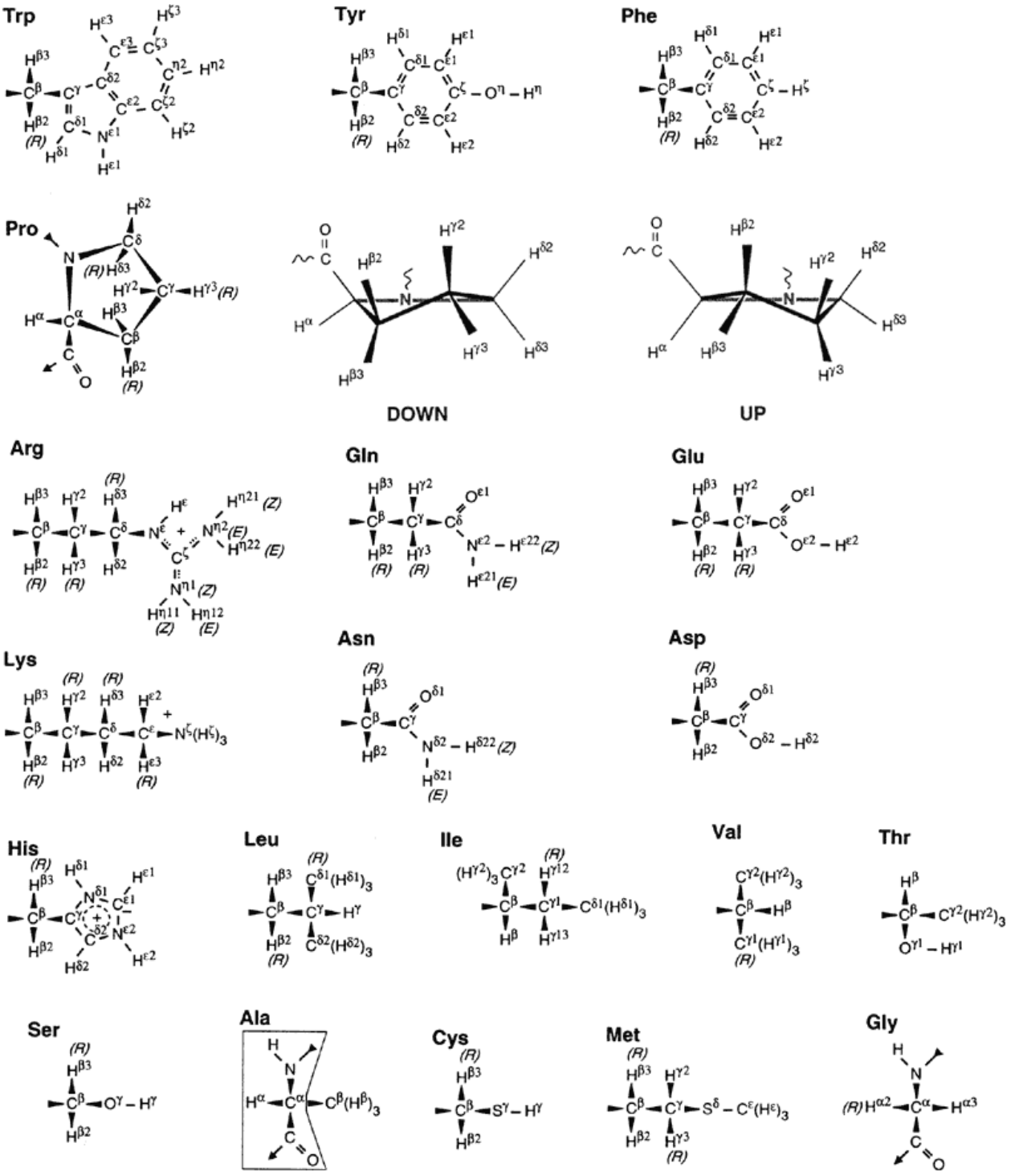

Appendix B – *Peptide List*

The peptide list is organized by chapter and can be used to find the CSDb ascension name, which can be searched in the publically available database at: http://andersenlab.chem.washington.edu/CSDb/. Each peptide in the list that has any Trps participating in an aromatic cluster in bold, and any turns or loops are underlined for clarity.

Chapter 3- β-Cap Optimization

Reference	Sequence	CSDb name
1	RWTTHCHRKWE	R-TurnlessE
2	Ac-WTTHCHRKWTG-NH_2	Turnless WTG
3	KWTTHCHRKWE	Turnless E
4	KWTTHCHRKWT	Turnless T
5	KWTTHCHRKWA	Turnless A
6	KWTTHCHRKWA-NH_2	Turnless A-NH_2
7	TTKWTTHCHRKWETT	TT-TurnlessE-TT
8	GGKWTTHCHRKWEGG	GG-TurnlessE-GG
9	TGKWTTHCHRKWEGT	TG-TurnlessE-GT
10	GTKWTTHCHRKWEGT	GT-TurnlessE-GT
11	TGKWTTHCHRKWETG	TG-TurnlessE-TG
wtWW	KLPPGWEKRMSRSSGRVYYFNHITNASQWERPSGNSSSG	Pin1 WW domain
EXpin1	RWEKRMSRSSGRVYYFNS	WW_Pin1_HP1_wt
Capped pin1	RWEKRMSRSSGRVYYFWD	Cap-WW-pin1

Chapter 4- Turn Optimization

Reference	Sequence	CSDb name
1	RWTV-NPATGK-ITWE	RW-4-WE
2	RWTV-DPATGK-ITWE	
3	RWTV-HPATGK-ITWE	
4	RWTV-CPATGK-ITWE	
5	RWTV-SPATGK-ITWE	
6	RWTV-QPATGK-ITWE	
7	RWTV-APATGK-ITWE	
8	RWTV-GPATGK-ITWE	
9	RWTV-IPATGK-ITWE	
10	RWTV-TPATGK-ITWE	
1-2A	RWTV-NAATGK-ITWE	
1-2A,4A	RWTV-NAAAGK-ITWE	
1-2V	RWTV-NVATGK-ITWE	
1-2G	RWTV-NGATGK-ITWE	
1-3V	RWTV-NPVTGK-ITWE	
1-4N	RWTV-NPANGK-ITWE	

1-4D	RWTV-NPADGK-ITWE
1-4H	RWTV-NPAHGK-ITWE
1-4A	RWTV-NPAAGK-ITWE
1-4A,5T	RWTV-NPAATK-ITWE
1-4G	RWTV-NPAGGK-ITWE
1-4V	RWTV-NPAVGK-ITWE
1-6T	RWTV-NPATGT-ITWE
1-6A	RWTV-NPATGA-ITWE
1-6G	RWTV-NPATGG-ITWE
2-6R	RWTV-DPATGR-ITWE
2-3G	RWTV-DPGTGR-ITWE
2-4S	RWTV-DPASGK-ITWE
2-4S,5T	RWTV-DPASTK-ITWE
2-5N	RWTV-DPATNK-ITWE
1-5A	RWTV-NPATAK-ITWE
1-5H	RWTV-NPATHK-ITWE
3-6R	RWTV-HPATGR-ITWE
3-4A,6R	RWTV-HPAAGR-ITWE

Chapter 5- Loops

Short Loops

Reference	Sequence	CSDb name
G2	RWITVTI-GG-KKIRVWE	R-GG-E
G3	RWITVTI-GGG-KKIRVWE	R-GGG-E
G4	RWITVTI-GGGG-KKIRVWE	RGGGGE
G5	RWITVTI-GGGGG-KKIRVWE	R-GGGGG-E
G6	RWITVTI-GGGGGG-KKIRVWE	R-GGGGGG-E
G7	RWITVTI-GGGGGGG-KKIRVWE	R-G7-E
G8	RWITVTI-GGGGGGGG-KKIRVWE	R-GGGGGGGG-E
G9	RWITVTI-GGGGGGGGG-KKIRVWE	R-G9-E
G10	RWITVTI-GGGGGGGGGG-KKIRVWE	R-G10-E

Long Loops

System	Loop	Sequence	CSDb name
C2	2	RWITVTI-GG-KKIRVWE	R-GG-E
C2	4	RWITVTI-GGGG-KKIRVWE	RGGGGE
C2	10	RWITVTI-GGGGKKGGGG-KKIRVWE	R-Superloop-E
C2	16	RWITVTI-GGGGKKGGGGKKGGGG-KKIRVWE	R-(GGGGKK)3-E
C2	22	RWITVTI-GGGGKKGGGGKKGGGGKKGGGG-KKIRVWE	R-GGGGKK4-E new
C4	4	RWITVRIW-IGGK-WKTIRVWE	RWW-IGGK
C4	10	RWITVRIW-GGGGKKGGGG-WKTIRVWE	RWW-10loop-WWE
C4	16	RWITVRIW-GGGGKKGGGGKKGGGG-WKTIRVWE	RWW-16Loop-WWE
C4	22	RWITVRIW-GGGGKKGGGGKKGGGGKKGGGG-WKTIRVWE	
C4	28	RWITVRIW-GGGGKKGGGGKKGGGGKKGGGGKKGGGG-WKTIRVWE	
C2-6	IpGK	RWITVTI-GIpGKG-KKIRVWE	R-GIpGKG-E

C2-6	IPGK	RWITVTI-GIPGKG-KKIRVWE	R-GIPGKG-E
C2-10	IpGK	RWITVTI-GGGIpGKGGG-KKIRVWE	R-G3IpGKG3-E
C2-10	IPGK	RWITVTI-GGGIPGKGGG-KKIRVWE	R-G3IPGKG3-E
C2-16	IpGK	RWITVTI-GGGGGGIpGKGGGGGG-KKIRVWE	R-G6IpGKG6-E
C2-16	IPGK	RWITVTI-GGGGGGIPGKGGGGGG-KKIRVWE	R-G6IPGKG6-E
C2-16	NPATGK	RWITVTI-GGGGGNPATGKGGGGG-KKIRVWE	R-G5NPATGKG5-E

Chapter 6- pH Switchable β-Sheets

Reference	Sequence	CSDb name
Cntrl	KGWEKRW----NPATGR----WYYYNRITGKRQWERPD-NH_2	WWst29-NPATGR
p1-pHSW	KGWEKRW----HPATGK----WYYYNRITGKRQWERPD-NH_2	WWst29_pHsw
p2-pHSW	KGWEKRW----NPATGR----WYYYHPATGKRQWERPD-NH_2	WWst29-p2-pHSW
G2_pHSW	KGWEKRW--GGHPATGKGG--WYYYNRITGKRQWERPD-NH_2	WWst29-G2HPATGK
G4_pHSW	KGWEKRWGGGGHPATGKGGGGWYYYNRITGKRQWERPD-NH_2	

Appendix C – Full proton assignment for each peptide

Chapter 3- β-Cap Optimization

R-Turnless-E (pH 8 @ 300K**)**

#	Res		Hα	Hβ	Hγ	Hδ	Hε	Hζ	Hη
1	Arg		3.448	1.681, 1.572	1.346, 1.259	3.061,		-----	, , ,
2	Trp	9.011	5.338	3.215, 3.114	-----	7.515	10.339, 7.489	7.443, 7.162	7.267
3	Thr	9.455	4.689	4.046	, 1.039	-----	-----	-----	-----
4	Thr	8.625	4.939	3.943	, 1.117	-----	-----	-----	-----
5	His	8.919	4.807	2.966, 2.759	-----	, 6.847	7.852,	-----	-----
6	Cys	8.745	5.719	2.955, 2.632		-----	-----	-----	-----
7	His	9.011	4.946	3.203,	-----	, 6.983	7.815,	-----	-----
8	Arg	8.746	5.381	1.819, 1.714	1.595, 1.600	2.784, 2.725		-----	, , ,
9	Lys	9.294	4.996	1.849, 1.754	1.399,	1.574,	,		-----
10	Trp	8.892	4.562	2.810, 2.126	-----	6.918	9.989, 5.251	7.418, 6.513	7.090
11	Glu	8.025	4.066	1.814, 1.624	1.986,	-----		-----	-----

R-Turnless-E (pH 5 @ 300K**)**

#	Res		Hα	Hβ	Hγ	Hδ	Hε	Hζ	Hη
1	Arg		3.551	1.747, 1.625	1.382, 1.311	3.088,		-----	, , ,
2	Trp	9.045	5.194	3.216, 3.148	-----	7.499	10.347, 7.451	7.446, 7.150	7.267
3	Thr	9.116	4.720	4.063	, 1.065	-----	-----	-----	-----
4	Thr	8.671	4.847	3.970	, 1.125	-----	-----	-----	-----
5	His	8.704	4.945	3.230, 3.070	-----	, 7.202	8.667,	-----	-----
6	Cys	9.115	5.484	3.013, 2.702		-----	-----	-----	-----
7	His	8.812	4.959	3.348, 3.246	-----	, 7.349	8.692,	-----	-----
8	Arg	8.894	5.257	1.806, 1.707	1.587, 1.546	2.764, 2.684		-----	, , ,
9	Lys	9.153	4.909	1.792,	1.408,	1.621,	,		-----
10	Trp	8.992	4.475	2.846, 2.211	-----	6.935	10.047, 5.407	7.435, 6.572	7.117
11	Glu	7.941	4.140	1.892, 1.640	2.147,	-----		-----	-----

R-Turnless-E (pH 2 @ 300K**)**

#	Res		Hα	Hβ	Hγ	Hδ	Hε	Hζ	Hη
1	Arg		3.735	1.789, 1.720	1.431, 1.407	3.117,	7.131	-----	, , ,
2	Trp	8.975	5.080	3.200,	-----		10.289, 7.471	7.439, 7.149	7.255
3	Thr	8.854	4.657	4.089	, 1.083	-----	-----	-----	-----
4	Thr	8.510	4.721	4.020	, 1.127	-----	-----	-----	-----
5	His	8.649	4.910	3.244, 3.090	-----	, 7.229	8.626,	-----	-----
6	Cys	8.971	5.263	2.992, 2.807		-----	-----	-----	-----
7	His	8.756	4.897	3.326, 3.203	-----	, 7.321	8.650,	-----	-----

8	Arg	8.769	4.997	1.761, 1.679	1.533, 1.533	2.802, 2.733	6.675	-----	, , ,
9	Lys	8.950	4.757	1.767, 1.711	1.377,	1.685, 1.619	2.967,	7.564	-----
10	Trp	8.874	4.452	2.947, 2.508	-----	6.973	10.036, 5.996	7.426, 6.703	7.129
11	Glu	7.892	4.277	1.955, 1.677	2.213,	-----		-----	-----

Turnless WTG (pH 8 @ 300K**)**

#	Res		Hα	Hβ	Hγ	Hδ	Hε	Hζ	Hη
2	Trp	8.265	5.023	3.114,	-----	7.375	10.210, 7.469	7.419, 7.133	7.221
3	Thr	8.950	4.598	4.092	, 1.075	-----	-----	-----	-----
4	Thr	8.434	4.721	3.994	, 1.109	-----	-----	-----	-----
5	His	8.699	4.745	2.984, 2.782	-----	,	,	-----	-----
6	Cys	8.763	5.388	2.893, 2.703		-----	-----	-----	-----
7	His	8.812	4.842	3.153,	-----	,	,	-----	-----
8	Arg	8.600	5.022	1.751, 1.677	1.526,	2.791,		-----	, , ,
9	Lys	9.048	4.761	1.779, 1.696	1.338,	1.559,	2.844,		-----
10	Trp	8.825	4.448	2.979, 2.391	-----	6.822	10.050, 6.313	7.360, 6.792	7.124
11	Thr	8.036	4.213	4.137	, 1.064	-----	-----	-----	-----
12	Gly	6.686	3.540, 3.405	-----	-----	-----	-----	-----	-----

Turnless WTG (pH 2 @ 300K**)**

#	Res		Hα	Hβ	Hγ	Hδ	Hε	Hζ	Hη
2	Trp	8.297	4.728	3.195,	-----	7.274	10.103, 7.419	7.470, 7.052	7.170
3	Thr	8.278	4.377	4.181	, 1.046	-----	-----	-----	-----
4	Thr	8.066	4.351	4.120	, 1.116	-----	-----	-----	-----
5	His	8.323	4.734	3.214, 3.029	-----	, 7.180	8.510,	-----	-----
6	Cys			,		-----	-----	-----	-----
7	His	8.565	4.759	3.259, 3.109	-----	, 7.205	8.518,	-----	-----
8	Arg	8.474	4.441	1.703, 1.635	1.466,	2.923,	6.921	-----	, , ,
9	Lys	8.516	4.393	1.736, 1.681	1.356, 1.296	1.628, 1.623	2.925,	7.528	-----
10	Trp	8.546	4.666	3.189, 2.998	-----	7.130	10.112,	7.424, 7.028	7.176
11	Thr	7.977	4.246	4.169	, 1.085	-----	-----	-----	-----
12	Gly	7.162	3.574, 3.661	-----	-----	-----	-----	-----	-----

Turnless E (pH 2 @ 300K**)**

#	Res		Hα	Hβ	Hγ	Hδ	Hε	Hζ	Hη
1	Lys		3.395	1.663,	1.124,	1.570,	2.859,		-----
2	Trp	8.955	5.318	3.204, 3.110	-----	7.508	10.319, 7.429	7.472, 7.175	7.260
3	Thr	9.426	4.656	4.038	, 1.038	-----	-----	-----	-----

4	Thr	8.650	4.912	3.950	, 1.117	-----	-----	-----	-----
5	His	8.923	4.793	2.953, 2.749	-----	, 6.833	7.803,	-----	-----
6	Cys	9.015	5.693	2.946, 2.640		-----	-----	-----	-----
7	His	9.017	4.939	3.200,	-----	, 6.962	7.772,	-----	-----
8	Arg	8.711	5.358	1.794, 1.698	1.587, 1.562	2.774, 2.727		-----	, , ,
9	Lys	9.278	4.989	1.863, 1.766	1.406,	1.580,	2.878, 2.858		-----
10	Trp	8.870	4.558	2.813, 2.120	-----	6.910	9.972, 5.309	7.403, 6.535	7.092
11	Glu	7.990	4.052	1.815, 1.645	1.986,	-----		-----	-----

Turnless E (pH 5 @ 300K**)**

#	Res		Hα	Hβ	Hγ	Hδ	Hε	Hζ	Hη
1	Lys		3.501	1.705,	1.176,	1.652,	2.885,		-----
2	Trp	8.968	5.179	3.221, 3.144	-----	7.502	10.328, 7.446	7.452, 7.157	7.266
3	Thr	9.115	4.694	4.053	, 1.058	-----	-----	-----	-----
4	Thr	8.675	4.826	3.974	, 1.121	-----	-----	-----	-----
5	His	8.701	4.941	3.236, 3.069	-----	, 7.190	8.668,	-----	-----
6	Cys	9.105	5.477	3.010, 2.708		-----	-----	-----	-----
7	His	8.801	4.956	3.343, 3.241	-----	, 7.340	8.693,	-----	-----
8	Arg	8.880	5.236	1.794, 1.697	1.583, 1.550	2.772, 2.696		-----	, , ,
9	Lys	9.131	4.900	1.803, 1.737	1.406,	,	,		-----
10	Trp	8.943	4.465	2.843, 2.213	-----	6.938	10.026, 5.452	7.422, 6.593	7.114
11	Glu	7.912	4.123	1.886, 1.664	2.141,	-----		-----	-----

Turnless E (pH 2 @ 300K**)**

#	Res	Hα	Hβ	Hγ	Hδ	Hε	Hζ	Hη
1	Lys	3.792	1.775,	1.289,	1.624,	2.927,		-----
2	Trp	4.983	3.214, 3.203	-----	7.371	10.206, 7.450	7.485, 7.129	7.227
3	Thr	4.552	4.101	, 1.087	-----	-----	-----	-----
4	Thr	4.559	4.066	, 1.134	-----	-----	-----	-----
5	His		,	-----	, 7.230	8.584,	-----	-----
6	Cys	4.842	3.245, 3.090		-----	-----	-----	-----
7	His		,	-----	, 7.297	8.606,	-----	-----
8	Arg		1.723, 1.654	1.500, 1.499	2.861, 2.820		-----	, , ,
9	Lys		1.742,	1.365,	1.651,	2.949,		-----
10	Trp	4.506	3.021,	-----	7.038	10.021, 7.567	7.425, 7.111	7.140

11	Glu	4.279	1.982, 1.738	2.223,	-----			-----	-----

Turnless T (pH 8 @ 300K**)**

#	Res		Hα	Hβ	Hγ	Hδ	Hε	Hζ	Hη
1	Lys		3.268	1.539,	1.122,	1.517,	2.860,		-----
2	Trp		5.296	3.195, 3.107	-----	7.496	10.309, 7.436	7.456, 7.172	7.258
3	Thr	9.218	4.631	4.052	, 1.074	-----	-----	-----	-----
4	Thr	8.777	4.847	3.958	, 1.115	-----	-----	-----	-----
5	His	8.918	4.761	2.956, 2.739	-----	, 6.813	7.702,	-----	-----
6	Cys		5.651	2.935, 2.650		-----	-----	-----	-----
7	His	8.976	4.915	3.187,	-----	, 6.942	7.721,	-----	-----
8	Arg	8.697	5.295	1.770, 1.672	1.553, 1.538	2.750, 2.707		-----	, , ,
9	Lys	9.242	4.978	1.858, 1.753	1.403,	1.563,	,		-----
10	Trp	8.933	4.623	2.857, 2.167	-----	7.225	10.062, 5.451	7.398, 6.583	7.094
11	Thr	7.881		4.024	, 1.047	-----	-----	-----	-----

Turnless T (pH 5 @ 300K**)**

#	Res		Hα	Hβ	Hγ	Hδ	Hε	Hζ	Hη
1	Lys		3.471	1.663,	1.152,	1.611,	2.875,		-----
2	Trp	8.972	5.270	3.220, 3.115	-----	7.494	10.324, 7.431	7.441, 7.154	7.257
3	Thr	9.111	4.651	4.042	, 1.095	-----	-----	-----	-----
4	Thr	8.810	4.828	3.974	, 1.119	-----	-----	-----	-----
5	His	8.722	4.947	3.227, 3.075	-----	, 7.211	8.644,	-----	-----
6	Cys	9.105	5.477	3.006, 2.689		-----	-----	-----	-----
7	His	8.793	4.960	3.349, 3.239	-----	, 7.327	8.671,	-----	-----
8	Arg	8.897	5.237	1.781, 1.681	1.573, 1.511	2.742, 2.640		-----	, , ,
9	Lys	9.114	4.937	1.821, 1.744	1.409,	,	,		-----
10	Trp	9.022	4.628	2.860, 2.189	-----	6.932	10.002, 5.408	7.421, 6.568	7.104
11	Thr	7.941		4.059	, 1.038	-----	-----	-----	-----

Turnless T (pH 2 @ 300K**)**

#	Res	Hα	Hβ	Hγ	Hδ	Hε	Hζ	Hη
1	Lys	3.686	1.720,	1.238,	1.600,	2.909,		-----
2	Trp	5.097	3.218, 3.161	-----	7.409	10.229, 7.446	7.460, 7.134	7.236
3	Thr	4.563	4.073	, 1.095	-----	-----	-----	-----
4	Thr	4.636	4.039	, 1.127	-----	-----	-----	-----
5	His	4.877	3.244, 3.106	-----	, 7.233	8.623,	-----	-----

6	Cys	5.187	2.989, 2.881		-----	-----	-----	-----
7	His	4.853	3.290, 3.183	-----	, 7.306	8.643,	-----	-----
8	Arg		1.736, 1.655	1.510, 1.486	2.751, 2.814		-----	, , ,
9	Lys		1.794, 1.722	1.392, 1.347	,	2.937,		-----
10	Trp	4.635	3.001, 2.522	-----	6.968	9.992,	7.419, 6.762	7.124
11	Thr	4.319	4.184	, 1.064	-----	-----	-----	-----

Turnless A (pH 8 @ 300K)

#	Res		Hα	Hβ	Hγ	Hδ	Hε	Hζ	Hη
1	Lys		3.386	1.614,	1.179,	1.577,	2.884,		-----
2	Trp		5.238	3.190, 3.137	-----	7.459	10.305, 7.455	7.464, 7.157	7.253
3	Thr	9.164	4.660	4.079	, 1.082	-----	-----	-----	-----
4	Thr	8.620	4.861	3.966	, 1.121	-----	-----	-----	-----
5	His	8.890	4.783	2.973, 2.770	-----	, 6.834	7.740,	-----	-----
6	Cys		5.597	2.932, 2.676		-----	-----	-----	-----
7	His	8.949	4.903	3.188,	-----	, 6.970	7.773,	-----	-----
8	Arg	8.718		1.771, 1.676	1.539,	2.734, 2.709		-----	, , ,
9	Lys	9.171	4.924	1.841, 1.733	1.390,	1.584,	2.869,		-----
10	Trp	8.880	4.524	2.859, 2.240	-----	6.929	10.014, 5.603	7.401, 6.607	7.103
11	Ala	7.847	3.987	1.148	-----	-----	-----	-----	-----

Turnless A (pH 5 @ 300K)

#	Res		Hα	Hβ	Hγ	Hδ	Hε	Hζ	Hη
1	Lys		3.603	1.713,	1.236,	1.601,	2.914,	7.509	-----
2	Trp	8.914	5.117	3.209, 3.169	-----	7.421	10.274, 7.467	7.457, 7.130	7.241
3	Thr	8.878	4.626	4.086	, 1.097	-----	-----	-----	-----
4	Thr	8.581	4.709	4.007	, 1.123	-----	-----	-----	-----
5	His	8.659	4.893	3.215, 3.076	-----	, 7.202	8.608,	-----	-----
6	Cys	8.979	5.291	2.988, 2.801		-----	-----	-----	-----
7	His	8.762	4.894	3.314, 3.220	-----	, 7.299	8.629,	-----	-----
8	Arg	8.775	5.007	1.750, 1.669	1.525, 1.489	2.775, 2.708	6.643	-----	, , ,
9	Lys	8.927	4.773	1.772,	1.367,	1.710,	2.952,	7.530	-----
10	Trp	8.818	4.509	2.939, 2.432	-----	6.988	10.040, 5.925	7.434, 6.680	7.119
11	Ala	7.859	4.062	1.180	-----	-----	-----	-----	-----

Turnless A (pH 2 @ 300K)

#	Res		Hα	Hβ	Hγ	Hδ	Hε	Hζ	Hη
1	Lys		3.854	1.800,	1.315,	1.626,	2.922,	7.508	-----

2	Trp	8.766	4.917	3.220,	-----	7.304	10.153, 7.446	7.443, 7.200	7.106
3	Thr	8.436	4.464	4.114	, 1.088	-----	-----	-----	-----
4	Thr	8.214	4.438	4.101	, 1.133	-----	-----	-----	-----
5	His	8.544	4.821	3.230, 3.090	-----	, 7.209	8.545,	-----	-----
6	Cys			,		-----	-----	-----	-----
7	His	8.688	4.826	3.255, 3.144	-----	, 7.239	8.551,	-----	-----
8	Arg			1.671, 1.647	1.470, 1.449	2.881, 2.856	6.822	-----	, , ,
9	Lys		3.981	1.842,	1.344,	1.651,	2.937,	7.521	-----
10	Trp			,	-----	7.114	10.038,	7.428, 6.841	7.179
11	Ala	8.049	4.269	1.266	-----	-----	-----	-----	-----

Turnless A-NH_2 (pH 8 @ 300K)

#	Res		Hα	Hβ	Hγ	Hδ	Hε	Hζ	Hη
1	Lys		3.280	1.555, 1.465	1.166,	,	2.881,		-----
2	Trp			,	-----	7.427	10.318, 7.466	7.462, 7.163	7.259
3	Thr	9.152	4.654	4.084	, 1.083	-----	-----	-----	-----
4	Thr	8.563	4.788	3.954	, 1.113	-----	-----	-----	-----
5	His	8.831	4.776	2.986, 2.955	-----	, 6.828	7.753,	-----	-----
6	Cys		5.550	2.924, 2.646		-----	-----	-----	-----
7	His	8.907	4.886	3.195, 3.181	-----	, 6.973	7.798,	-----	-----
8	Arg	8.718		1.773, 1.686	1.561, 1.546	2.757, 2.725		-----	, , ,
9	Lys	9.190	4.900	1.828, 1.731	1.390,	1.590,	2.872,		-----
10	Trp	8.985	4.325	2.911, 2.399	-----	6.914	10.031, 5.685	7.371, 6.593	7.085
11	Ala	8.135	4.227	1.109	-----	-----	-----	-----	-----

Turnless A-NH_2 (pH 5 @ 300K)

#	Res		Hα	Hβ	Hγ	Hδ	Hε	Hζ	Hη
1	Lys	7.538	3.786	1.773, 1.623	1.295,	1.627,	2.924,		-----
2	Trp	8.868	4.992	3.211, 3.191	-----	7.343	10.230, 7.472	7.483, 7.127	7.231
3	Thr	8.660	4.548	4.096	, 1.090	-----	-----	-----	-----
4	Thr	8.401	4.576	4.053	, 1.127	-----	-----	-----	-----
5	His	8.602	4.848	3.215, 3.080	-----	, 7.200	8.574,	-----	-----
6	Cys	8.836	5.080	2.960, 2.910		-----	-----	-----	-----
7	His	8.731	4.825	3.290, 3.173	-----	, 7.269	8.593,	-----	-----
8	Arg	8.662	4.783	1.718, 1.658	1.507, 1.481	2.839, 2.794	6.762	-----	, , ,
9	Lys	8.770	4.801	1.768,	1.384,	1.690,	,		-----
10	Trp	8.740	4.478	3.051, 2.732	-----	7.050	10.088,	7.444, 6.809	7.143
11	Ala	7.943	4.227	1.170	-----	-----	-----	-----	-----

TT-TurnlessE-TT (pH 5 @ 300K)

#	Res	Hα	Hβ	Hγ	Hδ	Hε	Hζ	Hη
1	Thr	4.162	3.983	, 1.283	-----	-----	-----	-----

2	Thr	8.696	4.358	3.994	, 1.026	-----	-----	-----	-----
3	Lys	8.394	4.290	1.654,	1.247,	1.571,	2.874,		-----
4	Trp	8.480	4.739	3.199, 3.055	-----	7.191	10.084, 7.420	7.430, 7.077	7.175
5	Thr	8.082	4.353	4.139	, 1.133	-----	-----	-----	-----
6	Thr	8.694	4.358	3.997	, 1.028	-----	-----	-----	-----
7	His	8.114	4.693	3.234, 3.178	-----	,	,	-----	-----
8	Cys	8.540	4.829	3.395, 3.144		-----	-----	-----	-----
9	His	8.159	4.818	3.219, 3.128	-----	,	,	-----	-----
10	Arg	8.110	4.411	2.224, 2.162	2.019, 1.847	3.256,	8.075	-----	, , ,
11	Lys		4.307	,	1.557, 1.444	,	2.968,	7.010	-----
12	Trp	8.643	4.699	3.222, 3.093	-----	0.000	0.000,	0.000, 0.000	0.000
13	Glu	8.575	4.520	2.165, 2.011	, 2.453	-----		-----	-----
14	Thr	8.205	4.417	4.245	, 1.194	-----	-----	-----	-----
15	Thr	7.911	4.281		, 1.170	-----	-----	-----	-----

GG-TurnlessE-GG (pH 8 @ 300K)

#	Res		Hα	Hβ	Hγ	Hδ	Hε	Hζ	Hη
1	Gly		,	-----	-----	-----	-----	-----	-----
2	Gly		,	-----	-----	-----	-----	-----	-----
3	Lys		4.212	,	1.136, 1.039	1.519,	2.838,		-----
4	Trp	8.392	5.186	3.141, 3.092	-----	7.445	10.193, 7.361	7.357, 7.130	7.210
5	Thr	9.302	4.652	4.062	, 1.063	-----	-----	-----	-----
6	Thr	8.610	4.879	3.958	, 1.123	-----	-----	-----	-----
7	His	8.888	4.774	2.959, 2.756	-----	, 6.834	7.766,	-----	-----
8	Cys		5.642	2.936, 2.653		-----	-----	-----	-----
9	His	8.991	4.920	3.187,	-----	, 6.953	7.744,	-----	-----
10	Arg	8.808	5.288	1.788, 1.696	1.567,	2.772, 2.771		-----	, , ,
11	Lys	9.270	4.932	1.858, 1.743	1.390,	1.590,	,		-----
12	Trp	8.877	4.402	2.779, 2.019	-----	6.739	9.934, 5.609	7.224, 6.521	6.916
13	Glu	8.268	4.340	1.827, 1.662	2.101, 2.045	-----		-----	-----
14	Gly	7.975	3.728, 3.714	-----	-----	-----	-----	-----	-----
15	Gly	7.811	3.725, 3.671	-----	-----	-----	-----	-----	-----

GG-TurnlessE-GG (pH 5 @ 300K)

#	Res		Hα	Hβ	Hγ	Hδ	Hε	Hζ	Hη
1	Gly	8.475	3.977, 3.903	-----	-----	-----	-----	-----	-----
2	Gly	8.428	3.817, 3.583	-----	-----	-----	-----	-----	-----
3	Lys		4.190	,	1.147, 1.064	1.651, 1.568	2.852,	7.447	-----
4	Trp	8.413	5.071	3.169, 3.120	-----	7.447	10.196, 7.395	7.399, 7.117	7.223
5	Thr	9.045	4.649	4.078	, 1.068	-----	-----	-----	-----
6	Thr	8.621	4.760	3.999	, 1.128	-----	-----	-----	-----

7	His	8.703	4.919	3.224, 3.048	-----	, 7.159	8.629,	-----	-----
8	Cys	9.052	5.415	3.004, 2.749		-----	-----	-----	-----
9	His	8.799	4.943	3.347, 3.241	-----	, 7.299	8.629,	-----	-----
10	Arg	8.859	5.136	1.785, 1.689	1.578, 1.565	2.815, 2.797	6.681	-----	, , ,
11	Lys	9.098	4.807	1.811, 1.728	1.395,	1.654,	2.918,	7.493	-----
12	Trp	8.816	4.384	2.836, 2.153	-----	6.802	9.955,	7.245, 6.605	6.967
13	Glu	8.222	4.375	1.887, 1.677	2.162, 2.142	-----		-----	-----
14	Gly	7.957	3.757, 3.715	-----	-----	-----	-----	-----	-----
15	Gly	7.802	3.760, 3.688	-----	-----	-----	-----	-----	-----

GG-TurnlessE-GG (pH 2 @ 300K)

#	Res		Hα	Hβ	Hγ	Hδ	Hε	Hζ	Hη
1	Gly	8.070	3.960,	-----	-----	-----	-----	-----	-----
2	Gly	8.429	3.915, 3.782	-----	-----	-----	-----	-----	-----
3	Lys		4.233	,	1.155, 1.155	1.541,	2.864,	7.449	-----
4	Trp	8.304	4.939	3.238, 3.188	-----	7.340	10.143, 7.418	7.470, 7.102	7.200
5	Thr		4.549	4.131	, 1.088	-----	-----	-----	-----
6	Thr	8.317	4.577	4.080	, 1.133	-----	-----	-----	-----
7	His	8.549	4.847	3.247, 3.093	-----	, 7.216	8.600,	-----	-----
8	Cys	8.751	5.060	2.976, 2.950		-----	-----	-----	-----
9	His	8.702	4.830	3.285, 3.190	-----	, 7.288	8.625,	-----	-----
10	Arg	8.638	4.720	1.754, 1.672	1.533, 1.535	2.875, 2.869	6.804	-----	, , ,
11	Lys	8.746	4.589	,	1.377, 1.339	1.651, 1.638	2.958,	7.512	-----
12	Trp	8.639	4.491	3.006,	-----	6.975	9.989,	7.345, 6.829	7.068
13	Glu	8.129	4.328	1.954, 1.727	2.266,	-----		-----	-----
14	Gly	7.646	3.734,	-----	-----	-----	-----	-----	-----
15	Gly	8.071	3.967,	-----	-----	-----	-----	-----	-----

TG-TurnlessE-GT (pH 8 @ 300K)

#	Res		Hα	Hβ	Hγ	Hδ	Hε	Hζ	Hη
1	Thr	7.618	4.271	4.188	, 1.160	-----	-----	-----	-----
2	Gly	7.687	3.875, 3.776	-----	-----	-----	-----	-----	-----
3	Lys			1.642,	1.143, 1.069	1.516,	,	2.836	-----
4	Trp	8.355	5.162	3.123, 3.087	-----	7.412	10.190, 7.412	7.380, 7.133	7.208
5	Thr	9.295	4.638	4.081	, 1.071	-----	-----	-----	-----
6	Thr	8.572	4.845	3.973	, 1.121	-----	-----	-----	-----
7	His	8.847	4.783	2.955, 2.762	-----	,	,	-----	-----
8	Cys	9.008	5.590	2.945, 2.680		-----	-----	-----	-----
9	His	8.948	4.903	3.190,	-----	,	,	-----	-----
10	Arg	8.659	5.207	1.756, 1.683	1.544,	,	2.764	-----	, , ,
11	Lys	9.192	4.869	1.844, 1.732	1.379,	1.583,	,	2.880	-----

12	Trp	8.821	4.422	2.828, 2.140	-----	6.751	9.915, 5.858	7.233, 6.594	6.952
13	Glu	8.262	4.329	1.849, 1.674	2.103, 2.046	-----		-----	-----
14	Gly	7.925	3.822, 3.821	-----	-----	-----	-----	-----	-----
15	Thr	7.673	4.241	4.159	, 1.126	-----	-----	-----	-----

TG-TurnlessE-GT (pH 5 @ 300K)

#	Res		Hα	Hβ	Hγ	Hδ	Hε	Hζ	Hη
1	Thr	7.739	4.311	4.156	, 1.171	-----	-----	-----	-----
2	Gly	7.546	4.212,	-----	-----	-----	-----	-----	-----
3	Lys		4.217	1.651,	1.138, 1.071	1.533,	2.849,	7.549	-----
4	Trp	8.401	5.042	3.163, 3.133	-----	7.424	10.192, 7.396	7.418, 7.122	7.216
5	Thr	8.943	4.650	4.090	, 1.078	-----	-----	-----	-----
6	Thr	8.581	4.748	4.009	, 1.128	-----	-----	-----	-----
7	His	8.670	4.917	3.225, 3.067	-----	, 7.197	8.627,	-----	-----
8	Cys	9.014	5.362	3.003, 2.779		-----	-----	-----	-----
9	His	8.778	4.926	3.337, 3.231	-----	, 7.321	8.641,	-----	-----
10	Arg	8.815	5.089	1.775, 1.685	1.555, 1.552	2.807, 2.806	6.689	-----	, , ,
11	Lys	9.031	4.777	1.797, 1.721	1.381,	,	2.968,		-----
12	Trp	8.818	4.399	2.856, 2.228	-----	6.802	9.916, 5.968	7.255, 6.645	6.976
13	Glu	8.168	4.375	1.899, 1.698	2.199, 2.184	-----		-----	-----
14	Gly	7.942	3.866, 3.808	-----	-----	-----	-----	-----	-----
15	Thr	7.684	4.276	4.215	, 1.135	-----	-----	-----	-----

TG-TurnlessE-GT (pH 2 @ 300K)

#	Res		Hα	Hβ	Hγ	Hδ	Hε	Hζ	Hη
1	Thr	7.985	4.460		, 1.197	-----	-----	-----	-----
2	Gly	8.658	3.944, 3.754	-----	-----	-----	-----	-----	-----
3	Lys			1.630,	1.145, 1.116	1.538,	2.852,	7.462	-----
4	Trp	8.369	4.989	3.155,	-----	7.375	10.179, 7.411	7.432, 7.112	7.210
5	Thr	8.727	4.620	4.108	, 1.090	-----	-----	-----	-----
6	Thr	8.470	4.686	4.036	, 1.129	-----	-----	-----	-----
7	His	8.622	4.895	3.245, 3.085	-----	, 7.220	8.608,	-----	-----
8	Cys	8.919	5.216	2.984, 2.830		-----	-----	-----	-----
9	His	8.740	4.884	3.315, 3.206	-----	, 7.309	8.633,	-----	-----
10	Arg	8.738	4.936	1.763, 1.683	1.537, 1.537	2.817, 2.817		-----	, , ,
11	Lys	8.906	4.697	1.768, 1.691	1.376,	,	2.965,	7.554	-----
12	Trp	8.781	4.422	2.914,	-----	6.847	9.916, 6.283	7.293, 6.726	7.016
13	Glu	8.113	4.352	1.922, 1.709	2.257,	-----		-----	-----
14	Gly	7.829	3.813,	-----	-----	-----	-----	-----	-----
15	Thr	7.903	4.429		, 1.149	-----	-----	-----	-----

GT-TurnlessE-GT (pH 2 @ 300K)

#	Res		Hα	Hβ	Hγ	Hδ	Hε	Hζ	Hη
1	Gly		,	-----	-----	-----	-----	-----	-----
2	Thr	8.501	4.326	4.043	, 1.070	-----	-----	-----	-----
3	Lys	8.394	4.280	1.636,	1.415,	,	3.056,	7.036	-----
4	Trp	8.176	4.789	3.278, 3.191	-----	7.227	10.097, 7.577	7.462, 7.117	7.209
5	Thr	8.040	4.378	4.164	, 1.092	-----	-----	-----	-----
6	Thr	8.051	4.287	4.166	, 1.161	-----	-----	-----	-----
7	His	8.582	4.717	3.275, 3.154	-----	, 7.235	8.518,	-----	-----
8	Cys	9.667	5.566	,		-----	-----	-----	-----
9	His	8.664	4.732	3.331, 3.200	-----	, 7.258	8.550,	-----	-----
10	Arg	8.309	4.313	1.723,	1.544,	3.092,	7.065	-----	, , ,
11	Lys	8.415	4.289	1.716,	1.368, 1.309	1.637,	2.944,	7.492	-----
12	Trp	8.300	4.647	3.219,	-----	7.227	10.097, 7.579	7.462, 7.117	7.209
13	Glu	8.052	4.275	2.008, 1.773	2.269,	-----		-----	-----
14	Gly	7.558	3.799,	-----	-----	-----	-----	-----	-----
15	Thr	7.972	4.457	4.384	, 1.194	-----	-----	-----	-----

TG-TurnlessE-TG (pH 8 @ 300K)

#	Res		Hα	Hβ	Hγ	Hδ	Hε	Hζ	Hη
1	Thr		3.811	4.162	, 1.335	-----	-----	-----	-----
2	Gly		,	-----	-----	-----	-----	-----	-----
3	Lys	7.333	4.192	1.658, 1.584	,	,	,		-----
4	Trp	8.426	5.233	3.155, 3.084	-----	7.468	10.158, 7.423	7.341, 7.138	7.208
5	Thr	9.357	4.674	4.068	, 1.064	-----	-----	-----	-----
6	Thr	8.645	4.899	3.958	, 1.119	-----	-----	-----	-----
7	His	8.895	4.816	2.991, 2.787	-----	, 6.881	7.919,	-----	-----
8	Cys		5.655	2.948, 2.644		-----	-----	-----	-----
9	His	8.978	4.942	3.221, 3.189	-----	, 6.998	7.876,	-----	-----
10	Arg	8.760	5.321	1.779, 1.691	1.566, 1.566	2.749,		-----	, , ,
11	Lys	9.275	4.941	1.856, 1.750	1.602, 1.392	,	,		-----
12	Trp	8.870	4.454	2.793, 2.009	-----	6.752	9.828, 5.521	7.206, 6.489	6.902
13	Glu	8.396	4.464	1.874, 1.672	2.142, 2.057	-----		-----	-----
14	Thr	8.134	4.208	4.048	, 1.192	-----	-----	-----	-----
15	Gly	7.843	3.684,	-----	-----	-----	-----	-----	-----

Pin1 WW Domain (pH 6.4 @ 285 K)

#	Res		Hα	Hβ	Hγ	Hδ	Hε	Hζ	Hη
1	Lys		4.180	1.990, 1.990	1.540, 1.610	1.800, 1.800	3.100, 3.100		-----
2	Leu	8.860	4.670	1.890, 1.490	2.000	1.130, 0.860	-----	-----	-----
3	Pro	-----	4.660	2.670, 2.670	1.860, 1.720	3.750, 3.090	-----	-----	-----
4	Pro	-----	4.420	2.390, 1.910	2.100, 2.200	3.710, 3.990	-----	-----	-----
5	Gly	8.830	4.090, 3.230	-----	-----	-----	-----	-----	-----

6	Trp	7.440	5.240	3.000, 3.280	-----	7.010	10.570, 7.420	7.470, 7.030	7.050
7	Glu	9.830	4.910	2.280, 2.370	2.620, 2.620	-----		-----	-----
8	Lys	8.980	4.450	1.830, 1.830	1.130, 1.130	1.690, 1.690	3.010, 3.010		-----
9	Arg	8.900	4.450	0.100, 0.100	1.290, 1.470	2.980, 2.690	7.020	-----	, , ,
10	Met	8.280	5.000	2.330, 2.330	2.490, 2.490	-----	1.920	-----	-----
11	Ser	9.120	4.780	4.330, 4.220		-----	-----	-----	-----
12	Arg	9.270	4.200	1.850, 1.780	1.980, 1.980	3.270, 3.270	7.300	-----	, , ,
13	Ser	8.480	4.430	3.980, 3.980		-----	-----	-----	-----
14	Ser	7.950	4.620	3.320, 3.270		-----	-----	-----	-----
15	Gly	8.190	3.990, 4.160	-----	-----	-----	-----	-----	-----
16	Arg	7.750	4.500	2.000, 1.780	1.780, 1.730	2.880, 2.530	6.800	-----	, , ,
17	Val	8.640	4.730	2.040	1.080, 0.840	-----	-----	-----	-----
18	Tyr	8.740	4.960	2.980, 2.560	-----	6.930	6.460	-----	
19	Tyr	9.060	5.330	2.980, 2.710	-----	6.880	6.800	-----	
20	Phe	9.430	5.700	2.970, 2.570	-----	7.010	7.060	7.370	-----
21	Asn	8.230	4.390	-0.640, 2.050	-----	6.700, 4.230	-----	-----	-----
22	His	8.230	4.240	3.230, 3.550	-----	, 7.040	7.710,	-----	-----
23	Ile	8.350	3.920	2.040	1.000, 1.270, 0.790	0.790	-----	-----	-----
24	Thr	7.350	4.290	4.140	, 0.980	-----	-----	-----	-----
25	Asn	8.100	4.160	3.170, 2.960	-----	7.520, 6.900	-----	-----	-----
26	Ala	7.160	4.480	1.290	-----	-----	-----	-----	-----
27	Ser	8.370	6.050	3.770, 3.850		-----	-----	-----	-----
28	Gln	9.410	4.890	2.560, 2.560	2.650, 2.650	-----	6.750, 7.510	-----	-----
29	Trp	8.540	5.000	3.250, 3.670	-----	7.510	10.160, 8.200	7.410, 6.940	7.150
30	Glu	8.140	4.450	1.930, 1.930	2.270, 2.370	-----		-----	-----
31	Arg	8.600	2.680	1.430, 1.430	1.010, 1.240	3.100, 3.100	7.220	-----	, , ,
32	Pro	-----	3.950	0.030, 0.620	0.790, 0.870	2.340, 2.560	-----	-----	-----
33	Ser	8.260	4.370	3.770, 3.850		-----	-----	-----	-----
34	Gly	8.550	4.010, 4.010	-----	-----	-----	-----	-----	-----
35	Asn	8.500	4.840	2.920, 2.830	-----	7.560, 7.230	-----	-----	-----
36	Ser	8.530	4.530	3.940, 3.940		-----	-----	-----	-----
37	Ser	8.470	4.530	3.980, 3.980		-----	-----	-----	-----
38	Ser	8.580	4.560	3.970, 3.970		-----	-----	-----	-----
39	Gly	8.860	4.980, 4.980	-----	-----	-----	-----	-----	-----

WW_Pin1_HP1_wt (pH 3.5 @ 300 K)

#	Res		Hα	Hβ	Hγ	Hδ	Hε	Hζ	Hη
1	Arg		4.007	1.834, 1.807	1.494,	3.114,	7.181	-----	, , ,
2	Trp	8.782	4.766	3.245,	-----	7.242	10.101, 7.527	7.458, 7.114	7.212
3	Glu	8.419	4.608	2.023, 1.925	2.468,	-----		-----	-----
4	Lys	8.265	4.166	1.705, 1.637	1.300, 1.251	,	2.943,		-----
5	Arg	8.454	4.350	1.934,	1.584, 1.527	3.111, 3.056		-----	, , ,

6	Met	8.573	4.616	2.206, 2.093	2.908, 2.851	-----		-----	-----
7	Ser	8.460	4.533	3.899,		-----	-----	-----	-----
8	Arg	8.614	4.390	1.887, 1.781	1.652,	3.169,		-----	, , ,
9	Ser	8.376	4.479	3.890, 3.861		-----	-----	-----	-----
10	Ser	7.915	4.229	3.865, 3.808		-----	-----	-----	-----
11	Gly	8.350	4.016, 3.933	-----	-----	-----	-----	-----	-----
12	Arg	8.004	4.333	1.712, 1.685	1.529, 1.452	3.123,		-----	, , ,
13	Val	8.126	4.161	1.858	0.838, 0.682	-----	-----	-----	-----
14	Tyr	8.339	4.575	2.838, 2.789	-----			-----	
15	Tyr	8.298	4.656	3.086, 2.937	-----			-----	
16	Phe	8.132	4.695	2.848, 2.735	-----				-----
17	Asn	8.344	4.709	2.692, 2.397	-----	6.794, 7.431	-----	-----	-----
18	Ser	7.822	4.245	3.841,		-----	-----	-----	-----

Cap-WW-pin1 (pH 6.5 @ 300 K)

#	Res		Hα	Hβ	Hγ	Hδ	Hε	Hζ	Hη
1	Arg		3.612	1.760, 1.705	1.466, 1.405	3.133,	7.129	-----	, , ,
2	Trp	8.912	5.055	3.218, 3.200	-----	7.446	10.258,	,	
3	Glu		4.647	1.872, 1.440	2.222,	-----		-----	-----
4	Lys	8.447	4.374	1.586,	1.030,	1.552,	2.898,	7.573	-----
5	Arg	8.760	4.506	1.589, 1.486	1.220,	3.095, 2.965	7.029	-----	, , ,
6	Met	8.444	4.862	1.957, 1.885	2.416, 2.357	-----		-----	-----
7	Ser	8.707	4.689	4.065, 4.000		-----	-----	-----	-----
8	Arg	8.951	4.300	1.935, 1.879	1.748, 1.698	3.236,	7.233	-----	, , ,
9	Ser	8.351	4.452	3.907, 3.886		-----	-----	-----	-----
10	Ser	8.078	4.604	3.909,		-----	-----	-----	-----
11	Gly	8.236	4.115, 3.933	-----	-----	-----	-----	-----	-----
12	Arg	7.828	4.433	1.787, 1.740	1.621, 1.550	3.197,	7.159	-----	, , ,
13	Val	8.304	4.513	1.885	0.917, 0.705	-----	-----	-----	-----
14	Tyr	8.716	4.814	2.979, 2.980	-----	7.081	6.663	-----	
15	Tyr	8.485	5.351	2.868, 2.691	-----	6.953	6.714	-----	
16	Phe		5.190	3.083, 3.083	-----	7.148	7.261	7.437	-----
17	Trp	8.589	4.587	2.891, 2.330	-----	6.987	10.011,	7.422, 6.629	7.112
18	Asp	8.042	4.370	2.722, 2.609	-----		-----	-----	-----

Chapter 4. Turn Optimization

RW-4-WE, NPATGK (pH 6.5 @ 300 K)

#	Res		Hα	Hβ	Hγ	Hδ	Hε	Hζ	Hη
1	Arg		3.530	1.723, 1.586	1.367, 1.275	3.076,	7.104	-----	, , ,
2	Trp	8.883	5.277	3.150,	-----	7.465	10.344, 7.532	7.449, 7.231	7.222

3	Thr	9.246	4.683	3.964	, 1.028	-----	-----	-----	-----
4	Val	8.450	4.349	1.898	0.878, 0.699	-----	-----	-----	-----
5	Asn	8.483	4.995	3.279, 2.796	-----	,	-----	-----	-----
6	Pro	-----	4.354	2.368,	2.057,	4.168, 3.891	-----	-----	-----
7	Ala	8.038	4.379	1.518	-----	-----	-----	-----	-----
8	Thr	7.436	4.516	4.371	, 1.171	-----	-----	-----	-----
9	Gly	8.734	4.118, 3.625	-----	-----	-----	-----	-----	-----
10	Lys	7.717	4.411	1.810, 1.706	1.450, 1.393	1.700,	3.035,	7.577	-----
11	Ile	8.637	4.766	1.770	, , 0.884	0.691	-----	-----	-----
12	Thr	9.151	4.900	4.112	, 1.240	-----	-----	-----	-----
13	Trp	8.800	4.632	2.914, 2.443	-----	6.947	10.005, 5.407	7.402, 6.423	7.069
14	Glu	7.954	4.135	1.872, 1.601	2.148,	-----		-----	-----

RW4-DPATGK (pH 6.5 @ 300 K)

#	Res		Hα	Hβ	Hγ	Hδ	Hε	Hζ	Hη
1	Arg		3.548	1.731, 1.602	1.376, 1.288	3.078,	7.096	-----	, , ,
2	Trp	8.839	5.258	3.153,	-----	7.444	10.303, 7.529	7.438, 7.223	7.214
3	Thr	9.205	4.671	3.953	, 1.021	-----	-----	-----	-----
4	Val	8.356	4.336	1.884	0.874, 0.701	-----	-----	-----	-----
5	Asp	8.530	4.955	3.200, 2.738	-----		-----	-----	-----
6	Pro	-----	4.332	2.359, 2.031	2.097, 2.033	4.177, 3.929	-----	-----	-----
7	Ala	8.016	4.339	1.522	-----	-----	-----	-----	-----
8	Thr	7.433	4.511	4.331	, 1.191	-----	-----	-----	-----
9	Gly	8.728	4.104, 3.610	-----	-----	-----	-----	-----	-----
10	Lys	7.753	4.384	1.809,	1.426, 1.389	1.699,	3.026,	7.556	-----
11	Ile	8.553	4.720	1.761	1.608, 1.105, 0.866	0.682	-----	-----	-----
12	Thr	9.128	4.875	4.071	, 1.223	-----	-----	-----	-----
13	Trp	8.708	4.621	2.924, 2.443	-----	6.942	9.985, 5.496	7.398, 6.454	7.075
14	Glu	7.921	4.166	1.897, 1.601	2.176,	-----		-----	-----

RW4-HPATGK (pH 6.5 @ 300 K)

#	Res		Hα	Hβ	Hγ	Hδ	Hε	Hζ	Hη
1	Arg		3.643	1.749, 1.668	1.408,	3.085,	7.096	-----	, , ,
2	Trp	8.814	5.117	3.186,	-----	7.402	10.262, 7.556	7.452, 7.233	7.202
3	Thr	8.989	4.466	3.951	, 0.959	-----	-----	-----	-----
4	Val	8.286	4.221	1.926	0.896, 0.793	-----	-----	-----	-----
5	His	8.624	4.915	3.229,	-----	, 7.245	8.481,	-----	-----

6	Pro	-----	4.310	2.319, 1.950	2.016,	3.851, 3.540	-----	-----	-----
7	Ala	8.739	4.343	1.503	-----	-----	-----	-----	-----
8	Thr	7.794	4.455	4.314	, 1.186	-----	-----	-----	-----
9	Gly	8.454	4.098, 3.780	-----	-----	-----	-----	-----	-----
10	Lys	7.823	4.358	1.759,	1.405, 1.351	1.648,	2.968,		-----
11	Ile	8.451	4.672	1.739	1.558, 1.058, 0.791	0.738	-----	-----	-----
12	Thr	8.682	4.771	4.243	, 1.173	-----	-----	-----	-----
13	Trp	8.537	4.690	3.041, 2.685	-----	7.031	10.028, 6.101	7.438, 6.639	7.117
14	Glu	7.875	4.111	1.914, 1.687	2.087,	-----		-----	-----

RW-CPATGK (pH 12.1 @ 300 K with TCEP)

#	Res		Hα	Hβ	Hγ	Hδ	Hε	Hζ	Hη
1	Arg		3.318	1.446, 1.443	1.280, 1.283	3.027,		-----	, , ,
2	Trp		5.146	2.933, 2.812	-----	7.186	, 7.436	7.385, 7.134	7.179
3	Thr		4.511	4.006	, 1.077	-----	-----	-----	-----
4	Val		4.455	1.852	0.887, 0.755	-----	-----	-----	-----
5	Cys		4.758	3.337, 3.213		-----	-----	-----	-----
6	Pro	-----	4.441	2.348, 2.028	2.091, 2.067	4.159, 4.069	-----	-----	-----
7	Ala		4.480	1.476	-----	-----	-----	-----	-----
8	Thr		4.554	4.338	, 1.289	-----	-----	-----	-----
9	Gly		4.129, 3.696	-----	-----	-----	-----	-----	-----
10	Lys		4.188	1.697, 1.687	1.341, 1.309	1.477,	2.641,		-----
11	Ile		4.813	1.666	, , 0.643		-----	-----	-----
12	Thr		4.762	4.101	, 1.179	-----	-----	-----	-----
13	Trp		4.733	3.102, 2.660	-----	6.993	, 6.342	7.305, 6.639	7.039
14	Glu		4.091	1.891, 1.732	,	-----		-----	-----

RW4-SPATGK (pH 6.5 @ 300 K)

#	Res		Hα	Hβ	Hγ	Hδ	Hε	Hζ	Hη
1	Arg		3.592	1.742, 1.625	1.398, 1.310	3.079,	7.102	-----	, , ,
2	Trp	8.811	5.218	3.166,	-----	7.435	10.299, 7.545	7.448, 7.234	7.224
3	Thr	9.067	4.622	3.964	, 1.024	-----	-----	-----	-----
4	Val	8.335	4.255	1.909	0.891, 0.747	-----	-----	-----	-----
5	Ser	8.408	4.832	4.041,		-----	-----	-----	-----
6	Pro	-----	4.412	2.359, 1.980	2.088, 2.016	4.097, 3.922	-----	-----	-----
7	Ala	7.924	4.339	1.447	-----	-----	-----	-----	-----
8	Thr	7.558	4.491	4.357	, 1.210	-----	-----	-----	-----
9	Gly	8.431	4.111, 3.739	-----	-----	-----	-----	-----	-----
10	Lys	7.829	4.418	1.817,	1.426,	1.684,	3.016,	7.552	-----
11	Ile	8.537	4.601	1.760	1.582, 1.121, 0.840	0.720	-----	-----	-----
12	Thr	9.006	4.803	4.081	, 1.199	-----	-----	-----	-----
13	Trp	8.616	4.660	2.968, 2.570	-----	6.986	10.005, 5.723	7.411, 6.513	7.085

14	Glu	7.915	4.128	1.876, 1.630	2.143,	-----		-----	-----

RW4-QPATGK (pH 6.5 @ 300K)

#	Res		Hα	Hβ	Hγ	Hδ	Hε	Hζ	Hη
1	Arg		3.722	1.780, 1.702	1.439, 1.400	3.101,	7.091	-----	, , ,
2	Trp	8.758	5.057	3.202,	-----	7.369	10.232, 7.564	7.471, 7.192	7.236
3	Thr	8.757	4.495	3.992	, 1.061	-----	-----	-----	-----
4	Val	8.206	4.214	1.928	0.900, 0.802	-----	-----	-----	-----
5	Gln	8.602	4.602	2.204, 1.993	2.411,	-----	,	-----	-----
6	Pro	-----	4.293	2.312, 1.951	2.050,	3.947, 3.717	-----	-----	-----
7	Ala	8.491	4.282	1.469	-----	-----	-----	-----	-----
8	Thr	7.763	4.414	4.285	, 1.208	-----	-----	-----	-----
9	Gly	8.439	4.049, 3.770	-----	-----	-----	-----	-----	-----
10	Lys	7.874	4.304	1.767,	1.397, 1.353	1.661,	2.976,	7.523	-----
11	Ile	8.361	4.476	1.738	1.516, 1.093, 0.751	0.751	-----	-----	-----
12	Thr	8.595	4.657	4.126	, 1.152	-----	-----	-----	-----
13	Trp	8.402	4.661	3.079, 2.803	-----	7.059	10.034, 6.382	7.431, 6.733	7.132
14	Glu	7.897	4.177	1.953, 1.704	2.188,	-----		-----	-----

RW4-APATGK (pH 6.5 @ 300 K)

#	Res		Hα	Hβ	Hγ	Hδ	Hε	Hζ	Hη
1	Arg		3.725	1.790, 1.698	1.439, 1.395	3.103,	7.105	-----	, , ,
2	Trp	8.754	5.083	3.208,	-----	7.373	10.239, 7.568	7.486, 7.185	7.236
3	Thr	8.761	4.514	4.007	, 1.058	-----	-----	-----	-----
4	Val	8.170	4.213	1.928	0.894, 0.805	-----	-----	-----	-----
5	Ala	8.452	4.607	1.426	-----	-----	-----	-----	-----
6	Pro	-----	4.305	2.311, 1.947	2.047, 1.991	3.919, 3.722	-----	-----	-----
7	Ala	8.455	4.281	1.470	-----	-----	-----	-----	-----
8	Thr	7.663	4.420	4.282	, 1.211	-----	-----	-----	-----
9	Gly	8.444	4.047, 3.776	-----	-----	-----	-----	-----	-----
10	Lys	7.863	4.331	1.782, 1.673	1.400, 1.362	1.667,	2.985,	7.522	-----
11	Ile	8.442	4.458	1.750	1.537, 1.113, 0.753	0.755	-----	-----	-----
12	Thr	8.656	4.643	4.106	, 1.176	-----	-----	-----	-----
13	Trp	8.436	4.681	3.078, 2.809	-----	7.062	10.031, 6.357	7.437, 6.722	7.136
14	Glu	7.887	4.159	1.934, 1.698	2.172,	-----		-----	-----

RW4-GPATGK (pH 6.5 @ 300 K)

#	Res		Hα	Hβ	Hγ	Hδ	Hε	Hζ	Hη
1	Arg		3.937	1.853, 1.823	1.529,	3.140,	7.121	-----	, , ,
2	Trp	8.723	4.892	3.268,	-----	7.294	10.137, 7.628	7.484, 7.170	7.244
3	Thr	8.241	4.365	4.064	, 1.087	-----	-----	-----	-----
4	Val	8.027	4.093	2.014	0.916, 0.917	-----	-----	-----	-----

5	Gly	8.302	4.136, 3.970	-----	-----	-----	-----	-----	-----
6	Pro	-----	4.391	2.271,	1.991, 1.936	3.629,	-----	-----	-----
7	Ala	8.445	4.390	1.409	-----	-----	-----	-----	-----
8	Thr	7.965	4.333	4.268	, 1.220	-----	-----	-----	-----
9	Gly	8.331	3.982, 3.947	-----	-----	-----	-----	-----	-----
10	Lys	8.049	4.334	1.776, 1.697	1.376, 1.332	1.641,	2.959,	7.496	-----
11	Ile	8.279	4.179	1.740	, , 0.770	0.655	-----	-----	-----
12	Thr	8.165	4.418	4.157	, 1.140	-----	-----	-----	-----
13	Trp	8.103	4.711	3.229, 3.138	-----	7.195	10.087,	7.495, 7.045	7.197
14	Glu	7.950	4.249	2.032, 1.797	2.221,	-----		-----	-----

RW4-IPATGK (pH 6.5 @ 300 K)

#	Res		Hα	Hβ	Hγ	Hδ	Hε	Hζ	Hη
1	Arg		3.615	1.734, 1.643	1.399, 1.314	3.073,	7.149	-----	, , ,
2	Trp		5.218	3.175,	-----	7.425	10.274, 7.459	7.613, 7.211	7.212
3	Thr	9.070	4.560	3.939	, 1.049	-----	-----	-----	-----
4	Val	8.249	4.449	1.897	0.886, 0.747	-----	-----	-----	-----
5	Ile	8.582	4.433	2.070	1.537, 1.266, 1.006	0.820	-----	-----	-----
6	Pro	-----	4.226	2.340,	2.116, 1.960	4.184, 3.830	-----	-----	-----
7	Ala	8.288	4.210	1.463	-----	-----	-----	-----	-----
8	Thr	7.380	4.507	4.330	, 1.184	-----	-----	-----	-----
9	Gly	8.640	4.081, 3.689	-----	-----	-----	-----	-----	-----
10	Lys	7.672	4.339	1.794,	1.430, 1.357	1.687,	3.001,		-----
11	Ile	8.288	4.688	1.738	, , 0.813		-----	-----	-----
12	Thr	8.834		4.043	, 1.137	-----	-----	-----	-----
13	Trp	8.392		3.011, 2.651	-----	7.019	9.994, 5.932	7.421, 6.556	7.095
14	Glu	7.958	4.095	1.807, 1.673	2.000,	-----		-----	-----

RW4-TPATGK (pH 6.5 @ 300 K)

#	Res		Hα	Hβ	Hγ	Hδ	Hε	Hζ	Hη
1	Arg		3.674	1.758, 1.667	1.416, 1.356	3.083,		-----	, , ,
2	Trp		5.151	3.184,	-----	7.394	10.247, 7.594	7.464, 7.224	7.202
3	Thr	8.915	4.532	3.994	, 1.063	-----	-----	-----	-----
4	Val	8.298	4.414	1.945	0.899, 0.793	-----	-----	-----	-----
5	Thr	7.543	4.455	4.325	, 1.206	-----	-----	-----	-----
6	Pro	-----	4.271	2.330,	2.095, 1.952	4.074, 3.827	-----	-----	-----
7	Ala	8.383	4.231	1.464	-----	-----	-----	-----	-----
8	Thr	8.479	4.602	4.208	, 1.311	-----	-----	-----	-----
9	Gly	8.424	4.058, 3.744	-----	-----	-----	-----	-----	-----
10	Lys	7.767	4.328	1.767,	1.408, 1.349	1.690,	2.980,		-----
11	Ile	8.415	4.589	1.740	, , 0.772	0.704	-----	-----	-----
12	Thr	8.648	4.697	4.100	, 1.154	-----	-----	-----	-----

13	Trp	8.455	4.734	3.061, 2.740	-----	7.052	10.006, 6.199	7.422, 6.652	7.111
14	Glu	7.929	4.094	1.845, 1.688	2.012,	-----		-----	-----

RW4-NAATGK (pH 6.5 @ 300 K)

#	Res		Hα	Hβ	Hγ	Hδ	Hε	Hζ	Hη
1	Arg		3.575	1.733, 1.617	1.384, 1.307	3.083,	7.101	-----	, , ,
2	Trp	8.859	5.232	3.159,	-----	7.454	10.312, 7.543	7.468, 7.221	7.235
3	Thr	9.136	4.652	3.983	, 1.031	-----	-----	-----	-----
4	Val	8.422	4.309	1.920	0.886, 0.729	-----	-----	-----	-----
5	Asn	8.477	4.684	3.130, 2.739	-----	,	-----	-----	-----
6	Ala	8.969	4.087	1.454	-----	-----	-----	-----	-----
7	Ala	8.197	4.352	1.525	-----	-----	-----	-----	-----
8	Thr	7.721	4.475	4.376	, 1.186	-----	-----	-----	-----
9	Gly	8.600	4.121, 3.685	-----	-----	-----	-----	-----	-----
10	Lys	7.719	4.392	1.787,	1.443, 1.370	1.687,	3.020,	7.556	-----
11	Ile	8.592	4.735	1.756	, 1.092, 0.849	0.701	-----	-----	-----
12	Thr	9.033	4.859	4.115	, 1.220	-----	-----	-----	-----
13	Trp	8.752	4.641	2.947, 2.516	-----	6.976	10.009, 5.612	7.410, 6.487	7.080
14	Glu	7.942	4.154	1.884, 1.631	2.169,	-----		-----	-----

RW4-NAAAGK (pH 2.5 @ 300 K)

#	Res		Hα	Hβ	Hγ	Hδ	Hε	Hζ	Hη
1	Arg		3.985	1.862,	1.556,	3.150,	7.132	-----	, , ,
2	Trp	8.754	4.832	3.271,	-----	7.270	10.124, 7.449	7.445, 7.095	7.203
3	Thr	8.086	4.317	4.063	, 1.093	-----	-----	-----	-----
4	Val	8.062	3.960	1.985	0.900,	-----	-----	-----	-----
5	Asn	8.420	4.684	2.835, 2.723	-----	,	-----	-----	-----
6	Ala	8.329	4.233	1.361	-----	-----	-----	-----	-----
7	Ala	8.191	4.270	1.387	-----	-----	-----	-----	-----
8	Ala	8.059	4.294	1.395	-----	-----	-----	-----	-----
9	Gly	8.241	3.928,	-----	-----	-----	-----	-----	-----
10	Lys	7.987	4.339	1.783, 1.705	1.384, 1.324	1.631,	2.951,	7.502	-----
11	Ile	8.217	4.142	1.740	1.422, 1.107, 0.785	0.644	-----	-----	-----
12	Thr	8.123	4.373	4.157	, 1.135	-----	-----	-----	-----
13	Trp	8.074	4.704	3.242, 3.194	-----	7.210	10.105, 7.615	7.489, 7.153	7.239
14	Glu	8.059	4.296	2.053, 1.813	2.239,	-----		-----	-----

RW4-NVATGK (pH 6.5 @ 300 K)

#	Res		Hα	Hβ	Hγ	Hδ	Hε	Hζ	Hη
1	Arg		3.520	1.712, 1.592	1.354, 1.254	3.064,	7.134	-----	, , ,
2	Trp	8.828	5.317	3.152,	-----	7.472	10.337, 7.567	7.449, 7.217	7.213
3	Thr	9.359	4.650	3.969	, 1.032	-----	-----	-----	-----

4	Val	8.409	4.370	1.920	0.725, 0.879	-----	-----	-----	-----
5	Asn	8.489	4.772	3.141, 2.729	-----	,	-----	-----	-----
6	Val	8.730	3.806	2.152	1.024, 0.993	-----	-----	-----	-----
7	Ala	8.154	4.343	1.533	-----	-----	-----	-----	-----
8	Thr	7.713	4.476	4.374	, 1.176	-----	-----	-----	-----
9	Gly	8.643	4.155, 3.676	-----	-----	-----	-----	-----	-----
10	Lys	7.692	4.379	1.786,	1.438, 1.377	1.710,	,		-----
11	Ile	8.606	4.852	1.752	, 1.081, 0.880	0.708	-----	-----	-----
12	Thr	9.098	4.897	4.133	, 1.218	-----	-----	-----	-----
13	Trp	8.754	4.703	2.917, 2.457	-----	6.962	9.996, 5.417	7.402, 6.397	7.052
14	Glu	7.997	4.087	1.785, 1.601	1.977,	-----		-----	-----

RW4-NGATGK (pH 6.5 @ 300 K)

#	Res		Hα	Hβ	Hγ	Hδ	Hε	Hζ	Hη
1	Arg		3.624	1.749, 1.641	1.406, 1.331	3.087,	7.102	-----	, , ,
2	Trp	8.826	5.184	3.172,	-----	7.432	10.289, 7.555	7.465, 7.224	7.217
3	Thr	9.003	4.605	3.989	, 1.031	-----	-----	-----	-----
4	Val	8.372	4.255	1.942	0.895, 0.766	-----	-----	-----	-----
5	Asn	8.517	4.699	3.065, 2.745	-----	,	-----	-----	-----
6	Gly	8.869	3.893,	-----	-----	-----	-----	-----	-----
7	Ala	8.244	4.418	1.498	-----	-----	-----	-----	-----
8	Thr	7.815	4.447	4.353	, 1.194	-----	-----	-----	-----
9	Gly	8.478	4.106, 3.754	-----	-----	-----	-----	-----	-----
10	Lys	7.776	4.382	1.784, 1.704	1.434, 1.365	1.671,	3.006,	7.537	-----
11	Ile	8.527	4.642	1.753	, , 0.816	0.716	-----	-----	-----
12	Thr	8.886	4.792	4.123	, 1.198	-----	-----	-----	-----
13	Trp	8.626	4.670	2.991, 2.605	-----	7.009	10.009, 5.872	7.417, 6.569	7.094
14	Glu	7.920	4.137	1.886, 1.651	2.146,	-----		-----	-----

RW-NPVTGK (pH 6.5 @ 300 K)

#	Res		Hα	Hβ	Hγ	Hδ	Hε	Hζ	Hη
1	Arg		3.509	1.702, 1.582	1.355, 1.254	3.058,	7.116	-----	, , ,
2	Trp	8.821	5.334	3.160, 3.114	-----	7.466	10.324, 7.560	7.441, 7.213	7.215
3	Thr	9.377	4.659	3.972	, 1.031	-----	-----	-----	-----
4	Val	8.450	4.399	1.882	0.878, 0.707	-----	-----	-----	-----
5	Asn	8.582	4.942	3.163, 2.806	-----	,	-----	-----	-----
6	Pro	-----	4.406	2.352, 2.042	2.108, 2.041	4.087, 3.855	-----	-----	-----
7	Val	8.156	3.978	2.207	1.028, 0.951	-----	-----	-----	-----
8	Thr	7.695	4.369		, 1.210	-----	-----	-----	-----
9	Gly	8.442	4.094, 3.668	-----	-----	-----	-----	-----	-----
10	Lys	7.594	4.337	1.775,	1.457, 1.372	1.699,	3.032,		-----
11	Ile	8.643	4.904	1.759	1.666, 1.085, 0.887	0.704	-----	-----	-----

12	Thr	9.156	4.909	4.131	, 1.228	-----	-----	-----	-----
13	Trp	8.786	4.699	2.907, 2.439	-----	6.959	9.977, 5.335	7.399, 6.356	7.052
14	Glu	7.986	4.091	1.791, 1.593	2.006,	-----		-----	-----

RW-NPANGK (pH 6.5 @ 300 K)

#	Res		Hα	Hβ	Hγ	Hδ	Hε	Hζ	Hη
1	Arg		3.541	1.728, 1.600	1.367, 1.262	3.065,	7.132	-----	, , ,
2	Trp	8.820	5.317	3.136,	-----	7.461	10.321, 7.580	7.449, 7.220	7.224
3	Thr	9.342	4.653	3.984	, 1.041	-----	-----	-----	-----
4	Val	8.408	4.453	1.896	0.887, 0.732	-----	-----	-----	-----
5	Asn	8.748	4.709	2.934, 2.492	-----	,	-----	-----	-----
6	Pro	-----	4.381	2.339, 2.049	2.028,	4.140, 3.897	-----	-----	-----
7	Ala	8.130	4.274	1.401	-----	-----	-----	-----	-----
8	Asn	7.198	4.831	3.112, 2.723	-----	,	-----	-----	-----
9	Gly	8.628	4.059, 3.654	-----	-----	-----	-----	-----	-----
10	Lys	8.189	4.291	1.798,	1.346,	1.668,	2.990,		-----
11	Ile	8.568	4.878	1.761	, 1.096, 0.876	0.706	-----	-----	-----
12	Thr	9.086	4.902	4.136	, 1.231	-----	-----	-----	-----
13	Trp	8.749	4.945	3.614, 2.813	-----	6.970	9.990, 5.454	7.396, 6.399	7.058
14	Glu	7.990	4.093	1.795, 1.616	1.995,	-----		-----	-----

RW4-NPADGK (pH 6.5 @ 300 K)

#	Res		Hα	Hβ	Hγ	Hδ	Hε	Hζ	Hη
1	Arg		3.555	1.726, 1.599	1.369, 1.275	3.070, 3.052	7.118	-----	, , ,
2	Trp	8.835	5.285	3.151,	-----	7.461	10.317, 7.567	7.447, 7.220	7.212
3	Thr	9.255	4.653	3.973	, 1.035	-----	-----	-----	-----
4	Val	8.381	4.387	1.899	0.884, 0.727	-----	-----	-----	-----
5	Asn	8.772	4.971	3.601, 2.816	-----	,	-----	-----	-----
6	Pro	-----	4.343	2.341, 1.988	2.047, 1.999	4.135, 3.918	-----	-----	-----
7	Ala	8.049	4.216	1.389	-----	-----	-----	-----	-----
8	Asp	7.257	4.740	2.992, 2.539	-----		-----	-----	-----
9	Gly	8.600	4.031, 3.666	-----	-----	-----	-----	-----	-----
10	Lys	8.246	4.294	1.871, 1.784	1.373, 1.320	1.684,	2.996,	7.554	-----
11	Ile	8.548	4.798	1.759	, , 0.857	0.701	-----	-----	-----
12	Thr	9.071	4.879	4.115	, 1.221	-----	-----	-----	-----
13	Trp	8.738	4.691	2.945, 2.510	-----	6.989	9.993, 5.528	7.401, 6.429	7.064
14	Glu	7.962	4.116	1.834, 1.617	2.086,	-----		-----	-----

RW4-NPAHGK (pH 6.5 @ 300 K)

#	Res		Hα	Hβ	Hγ	Hδ	Hε	Hζ	Hη
1	Arg		3.806	1.787, 1.744	1.469, 1.443	3.099,	7.137	-----	, , ,
2	Trp	8.696	4.934	,	-----	7.330	10.194, 7.584	7.463, 7.171	7.229

3	Thr	8.526	4.393	4.056	, 1.086	-----	-----	-----	-----
4	Val	8.146	4.086	1.968	0.902, 0.838	-----	-----	-----	-----
5	Asn	8.527	4.910	2.799, 2.704	-----	,	-----	-----	-----
6	Pro	-----	4.330	2.227,	1.934,	3.782, 3.698	-----	-----	-----
7	Ala	8.144	4.210	1.283	-----	-----	-----	-----	-----
8	His	8.255	4.727	3.184, 2.957	-----	, 7.179	8.319,	-----	-----
9	Gly	8.285	3.967, 3.903	-----	-----	-----	-----	-----	-----
10	Lys	8.090	4.383	1.799, 1.729	1.389, 1.331	1.622,	2.932,		-----
11	Ile	8.337	4.290	1.752	1.459, 1.089, 0.747		-----	-----	-----
12	Thr	8.240	4.533	4.179	, 1.150	-----	-----	-----	-----
13	Trp	8.068	4.693	3.293, 3.135	-----	7.129	10.045,	7.437, 6.895	7.156
14	Glu	7.869	4.104	1.920, 1.754	2.054,	-----		-----	-----

RW4-NPAAGK (pH 6.5 @ 300 K)

#	Res		Hα	Hβ	Hγ	Hδ	Hε	Hζ	Hη
1	Arg		3.884	1.820, 1.791	1.504,	3.123,	7.112	-----	, , ,
2	Trp	8.720	4.922	3.257,	-----	7.310	10.164, 7.598	7.485, 7.165	7.232
3	Thr	8.388	4.369	4.046	, 1.090	-----	-----	-----	-----
4	Val	8.111	4.026	1.971	0.904, 0.850	-----	-----	-----	-----
5	Asn	8.487	4.941	2.895, 2.713	-----	,	-----	-----	-----
6	Pro	-----	4.336	2.258,	1.988, 1.953	3.794, 3.753	-----	-----	-----
7	Ala	8.068	4.276	1.384	-----	-----	-----	-----	-----
8	Ala	7.881	4.313	1.407	-----	-----	-----	-----	-----
9	Gly	8.228	3.920,	-----	-----	-----	-----	-----	-----
10	Lys	7.845	4.391	1.794, 1.698	1.365, 1.313	1.633,	2.950,	7.503	-----
11	Ile	8.263	4.219	1.738	1.437, 1.092, 0.765	0.667	-----	-----	-----
12	Thr	8.190	4.481	4.177	, 1.145	-----	-----	-----	-----
13	Trp	8.152	4.710	3.200, 3.051	-----	7.163	10.066,	7.472, 6.983	7.180
14	Glu	7.827	4.166	1.987, 1.775	2.178,	-----		-----	-----

RW4-NPAATK (pH 6.5 @ 300 K)

#	Res		Hα	Hβ	Hγ	Hδ	Hε	Hζ	Hη
1	Arg		3.990	1.854,	1.554,	3.147,	7.126	-----	, , ,
2	Trp	8.689	4.831	3.288,	-----	7.266	10.126, 7.620	7.496, 7.155	7.239
3	Thr	8.147	4.295	4.064	, 1.105	-----	-----	-----	-----
4	Val	8.009	3.992	1.965	0.893, 0.878	-----	-----	-----	-----
5	Asn	8.494	4.877	2.851, 2.696	-----	7.634, 6.962	-----	-----	-----
6	Pro	-----	4.347	2.249,	1.979, 1.941	3.754, 3.698	-----	-----	-----
7	Ala	8.119	4.288	1.381	-----	-----	-----	-----	-----
8	Ala	8.041	4.343	1.421	-----	-----	-----	-----	-----
9	Thr	8.008	4.285	4.188	, 1.203	-----	-----	-----	-----
10	Lys	8.196	4.327	1.786, 1.712	1.386, 1.324	1.631,	2.946,	7.493	-----

11	Ile	8.198	4.075	1.722	1.403, 1.095, 0.787	0.614	-----	-----	-----
12	Thr	8.010	4.348	4.175	, 1.131	-----	-----	-----	-----
13	Trp	8.010	4.728	3.259,	-----	7.229	10.111, 7.552	7.490, 7.128	7.220
14	Glu	7.910	4.232	2.041, 1.831	2.222,	-----		-----	-----

RW4-NPAGGK (pH 6.5 @ 300 K)

#	Res		Hα	Hβ	Hγ	Hδ	Hε	Hζ	Hη
1	Arg		3.948	1.837,	1.525,	3.129,		-----	, , ,
2	Trp	8.703	4.905	3.268,	-----		,	,	
3	Thr	8.322	4.351	4.072	, 1.102	-----	-----	-----	-----
4	Val	8.071	4.071	1.965	0.906,	-----	-----	-----	-----
5	Asn	8.554	4.876	2.842, 2.694	-----	,	-----	-----	-----
6	Pro	-----	4.351	2.250,	1.940,	3.770, 3.701	-----	-----	-----
7	Ala	8.213	4.343	1.382	-----	-----	-----	-----	-----
8	Gly	8.216	4.039, 3.906	-----	-----	-----	-----	-----	-----
9	Gly	8.170	3.949,	-----	-----	-----	-----	-----	-----
10	Lys	8.135	4.325	1.763, 1.702	1.388, 1.322	1.613,	,		-----
11	Ile	8.294	4.178	1.746	, , 0.785	0.663	-----	-----	-----
12	Thr	8.182	4.413	4.155	, 1.141	-----	-----	-----	-----
13	Trp	8.144	4.694	3.224, 3.136	-----		, 7.316	, 7.054	
14	Glu	8.066	4.297	2.045, 1.798	2.232,	-----		-----	-----

RW4-NPAVGK (pH 6.5 @ 300 K)

#	Res		Hα	Hβ	Hγ	Hδ	Hε	Hζ	Hη
1	Arg		3.769	1.786, 1.719	1.446, 1.403	3.097,	7.185	-----	, , ,
2	Trp	8.882	5.056	3.230,	-----	7.371	10.308, 7.586	7.467, 7.223	7.195
3	Thr	8.781	4.451	4.019	, 1.083	-----	-----	-----	-----
4	Val	8.331	4.091	1.975	0.910, 0.818	-----	-----	-----	-----
5	Asn	8.649		2.941, 2.764	-----	,	-----	-----	-----
6	Pro	-----	4.356	2.272,	1.987,	3.857, 3.796	-----	-----	-----
7	Ala	8.165	4.281	1.416	-----	-----	-----	-----	-----
8	Val	7.751	4.208	2.158	0.951,	-----	-----	-----	-----
9	Gly	8.480	3.983, 3.843	-----	-----	-----	-----	-----	-----
10	Lys	7.715	4.469	1.808,	1.350,	1.640,	2.942,	7.597	-----
11	Ile	8.529	4.354	1.745	1.494, , 0.743		-----	-----	-----
12	Thr	8.526	4.634	4.202	, 1.175	-----	-----	-----	-----
13	Trp	8.480	4.716	3.125, 2.839	-----	7.100	10.121, 6.542	7.469, 6.799	7.145
14	Glu	7.981	4.096	1.897, 1.727	2.045,	-----		-----	-----

RW4-NPATGT (pH 6.5 @ 300 K)

#	Res		Hα	Hβ	Hγ	Hδ	Hε	Hζ	Hη
1	Arg		3.570	1.736, 1.617	1.390, 1.323	3.090,	7.105	-----	, , ,

2	Trp	8.873	5.257	3.170, 3.133	-----	7.447	10.305, 7.533	7.416, 7.192	7.192
3	Thr	9.227	4.672	3.982	, 1.055	-----	-----	-----	-----
4	Val	8.471	4.406	1.911	0.875, 0.733	-----	-----	-----	-----
5	Asn	8.590	5.022	3.281, 2.761	-----	,	-----	-----	-----
6	Pro	-----	4.362	2.356,	2.048,	4.143, 3.899	-----	-----	-----
7	Ala	8.088	4.375	1.521	-----	-----	-----	-----	-----
8	Thr	7.364	4.519	4.396	, 1.158	-----	-----	-----	-----
9	Gly	8.685	4.149, 3.687	-----	-----	-----	-----	-----	-----
10	Thr	7.769	4.411	4.153	, 1.228	-----	-----	-----	-----
11	Ile	8.598	4.827	1.751	, 1.062, 0.841	0.638	-----	-----	-----
12	Thr	9.013	4.918	4.113	, 1.233	-----	-----	-----	-----
13	Trp	8.736	4.660	2.944, 2.466	-----	6.978	10.007, 5.558	7.408, 6.482	7.085
14	Glu	7.925	4.148	1.889, 1.638	2.169,	-----		-----	-----

RW4-NPATGA (pH 6.5 @ 300 K)

#	Res		Hα	Hβ	Hγ	Hδ	Hε	Hζ	Hη
1	Arg		3.648	1.775, 1.670	1.428, 1.360	3.122,	7.125	-----	, , ,
2	Trp	8.903	5.239	3.162,	-----	7.427	10.248, 7.547	7.418, 7.183	7.183
3	Thr	9.188	4.694	4.029	, 1.076	-----	-----	-----	-----
4	Val	8.399	4.566	1.878	0.867, 0.744	-----	-----	-----	-----
5	Asn	8.740	5.008	3.234, 2.819	-----	,	-----	-----	-----
6	Pro	-----	4.409	2.371,	2.069,	4.163, 3.886	-----	-----	-----
7	Ala	8.143	4.451	1.549	-----	-----	-----	-----	-----
8	Thr	7.445	4.551	4.438	, 1.193	-----	-----	-----	-----
9	Gly	8.698	4.103, 3.600	-----	-----	-----	-----	-----	-----
10	Ala	7.807	4.373	1.388	-----	-----	-----	-----	-----
11	Ile	8.556	4.839	1.743	, 1.058, 0.816	0.626	-----	-----	-----
12	Thr	8.977	4.914	4.137	, 1.240	-----	-----	-----	-----
13	Trp	8.811	4.615	2.967, 2.537	-----	6.969	10.004, 5.672	7.422, 6.517	7.101
14	Glu	7.918	4.258	1.931, 1.660	2.223,	-----		-----	-----

RW4-NPATGG (pH 6.5 @ 300 K)

#	Res		Hα	Hβ	Hγ	Hδ	Hε	Hζ	Hη
1	Arg		3.748	1.792, 1.716	1.443, 1.413	3.119,	7.101	-----	, , ,
2	Trp	8.761	5.114	3.186,	-----	7.382	10.219, 7.567	7.444, 7.179	7.161
3	Thr	8.843	4.559	4.023	, 1.070	-----	-----	-----	-----
4	Val	8.250	4.316	1.922	0.895, 0.787	-----	-----	-----	-----
5	Asn	8.727	4.953	3.121, 2.675	-----	,	-----	-----	-----
6	Pro	-----	4.363	2.316, 2.005	2.037,	4.018, 3.827	-----	-----	-----
7	Ala	8.112	4.367	1.480	-----	-----	-----	-----	-----
8	Thr	7.502	4.489	4.367	, 1.160	-----	-----	-----	-----
9	Gly	8.525	4.132, 3.734	-----	-----	-----	-----	-----	-----

10	Gly	8.348	4.135, 3.782	-----	-----	-----	-----	-----	-----
11	Ile	8.253	4.655	1.745	1.473, 1.077, 0.758	0.638	-----	-----	-----
12	Thr	8.719	4.712	4.123	, 1.186	-----	-----	-----	-----
13	Trp	8.510	4.648	3.059, 2.757	-----	7.046	10.019, 6.288	7.421, 6.702	7.119
14	Glu	7.938	4.260	1.960, 1.695	2.214,	-----		-----	-----

RW4-DPATGR (pH 6.5 @ 300 K)

#	Res		Hα	Hβ	Hγ	Hδ	Hε	Hζ	Hη
1	Arg		3.562	1.732, 1.605	1.379, 1.296	3.084,	7.110	-----	, , ,
2	Trp	8.878	5.262	3.164,	-----	7.463	10.327, 7.544	7.448, 7.221	7.217
3	Thr	9.212	4.682	3.962	, 1.029	-----	-----	-----	-----
4	Val	8.390	4.331	1.893	0.874, 0.702	-----	-----	-----	-----
5	Asp	8.542	4.968	3.198, 2.759	-----		-----	-----	-----
6	Pro	-----	4.341	2.364, 2.035	2.105, 2.037	4.187, 3.941	-----	-----	-----
7	Ala	8.000	4.343	1.528	-----	-----	-----	-----	-----
8	Thr	7.414	4.525	4.331	, 1.194	-----	-----	-----	-----
9	Gly	8.735	4.118, 3.620	-----	-----	-----	-----	-----	-----
10	Arg	7.782	4.407	1.824, 1.732	1.651, 1.598	3.233,	7.235	-----	, , ,
11	Ile	8.624	4.726	1.765	, 1.108, 0.866	0.681	-----	-----	-----
12	Thr	9.139	4.889	4.087	, 1.227	-----	-----	-----	-----
13	Trp	8.740	4.623	2.929, 2.451	-----	6.957	10.008, 5.511	7.409, 6.466	7.080
14	Glu	7.929	4.183	1.900, 1.610	2.194,	-----		-----	-----

RW4-DPGTGR (pH 6.5 @ 300 K)

#	Res		Hα	Hβ	Hγ	Hδ	Hε	Hζ	Hη
1	Arg		3.640	1.751, 1.653	1.413, 1.341	3.095,	7.103	-----	, , ,
2	Trp	8.834	5.184	3.173,	-----	7.429	10.293, 7.553	7.465, 7.198	7.221
3	Thr	9.035	4.613	3.980	, 1.042	-----	-----	-----	-----
4	Val	8.314	4.276	1.916	0.888, 0.746	-----	-----	-----	-----
5	Asp	8.586	4.956	3.106, 2.740	-----		-----	-----	-----
6	Pro	-----	4.361	2.324,	2.083, 2.016	4.092, 3.864	-----	-----	-----
7	Gly	8.368	4.002,	-----	-----	-----	-----	-----	-----
8	Thr	7.683	4.511	4.313	, 1.204	-----	-----	-----	-----
9	Gly	8.593	4.090, 3.714	-----	-----	-----	-----	-----	-----
10	Arg	7.851	4.389	1.811, 1.724	1.632, 1.581	3.211,	7.202	-----	, , ,
11	Ile	8.540	4.630	1.759	1.575, 1.107, 0.823	0.703	-----	-----	-----
12	Thr	8.945	4.794	4.101	, 1.203	-----	-----	-----	-----
13	Trp	8.625	4.631	2.988, 2.582	-----	6.999	10.021, 5.868	7.422, 6.585	7.099
14	Glu	7.936	4.211	1.929, 1.652	2.198,	-----		-----	-----

RW4-DPASGK (pH 6.5 @ 300 K)

#	Res		Hα	Hβ	Hγ	Hδ	Hε	Hζ	Hη

1	Arg		3.679	1.769, 1.679	1.427, 1.370	3.103,	7.106	-----	, , ,
2	Trp	8.808	5.166	3.183,	-----	7.418	10.272, 7.566	7.471, 7.218	7.220
3	Thr	8.964	4.601	3.999	, 1.051	-----	-----	-----	-----
4	Val	8.294	4.279	1.915	0.887, 0.756	-----	-----	-----	-----
5	Asp	8.589	4.961	3.132, 2.773	-----		-----	-----	-----
6	Pro	-----	4.345	2.331,	2.068, 2.013	4.078, 3.871	-----	-----	-----
7	Ala	7.983	4.334	1.462	-----	-----	-----	-----	-----
8	Ser	7.776	4.584	3.995, 3.826		-----	-----	-----	-----
9	Gly	8.591	4.088, 3.701	-----	-----	-----	-----	-----	-----
10	Lys	7.858	4.371	1.797,	1.421, 1.378	1.691,	3.016,	7.543	-----
11	Ile	8.468	4.608	1.755	1.576, 1.106, 0.817	0.710	-----	-----	-----
12	Thr	8.868	4.774	4.115	, 1.205	-----	-----	-----	-----
13	Trp		4.643	3.013, 2.647	-----	7.021	10.024, 6.008	7.426, 6.633	7.112
14	Glu	7.942	4.227	1.945, 1.664	2.202,	-----		-----	-----

RW4-DPASTK (pH 6.5 @ 300 K)

#	Res		Hα	Hβ	Hγ	Hδ	Hε	Hζ	Hη
1	Arg		3.829	1.812, 1.759	1.476,	3.110,	7.116	-----	, , ,
2	Trp	8.735	4.963	3.243,	-----	7.319	10.199, 7.582	7.463, 7.153	7.230
3	Thr	8.474	4.396	4.035	, 1.080	-----	-----	-----	-----
4	Val	8.096	4.105	1.950	0.888, 0.821	-----	-----	-----	-----
5	Asp	8.495	4.812	2.869, 2.615	-----		-----	-----	-----
6	Pro	-----	4.329	2.278,	2.000, 1.956	3.864, 3.786	-----	-----	-----
7	Ala	8.241	4.312	1.422	-----	-----	-----	-----	-----
8	Ser	8.032	4.506	3.968, 3.880		-----	-----	-----	-----
9	Thr	8.147	4.315	4.238	, 1.191	-----	-----	-----	-----
10	Lys	8.104	4.326	1.780, 1.709	1.402, 1.339	1.634,	2.951,	7.502	-----
11	Ile	8.272	4.265	1.732	1.465, 1.093, 0.753	0.684	-----	-----	-----
12	Thr	8.304	4.512	4.140	, 1.149	-----	-----	-----	-----
13	Trp	8.224	4.703	3.172, 2.994	-----	7.129	10.071,	7.435, 6.912	7.156
14	Glu	7.847	4.150	1.969, 1.753	2.172,	-----		-----	-----

RW4-DPATNK (pH 6.5 @ 300 K)

#	Res		Hα	Hβ	Hγ	Hδ	Hε	Hζ	Hη
1	Arg		3.644	1.761, 1.651	1.411, 1.337	3.093,	7.114	-----	, , ,
2	Trp	8.838	5.177	3.194,	-----	7.434	10.289, 7.655	7.465, 7.162	7.232
3	Thr	8.983	4.596	3.972	, 1.040	-----	-----	-----	-----
4	Val	8.317	4.229	1.928	0.887, 0.744	-----	-----	-----	-----
5	Asp	8.498	4.947	3.172, 2.724	-----		-----	-----	-----
6	Pro	-----	4.384	2.330,	2.066, 2.020	4.062, 3.889	-----	-----	-----
7	Ala	8.088	4.327	1.490	-----	-----	-----	-----	-----
8	Thr	7.473	4.399	4.317	, 1.164	-----	-----	-----	-----

9	Asn	8.626	4.365	3.041, 2.810	-----	,	-----	-----	-----
10	Lys	7.753	4.492	1.801,	1.448, 1.388	1.689,	3.020,	7.558	-----
11	Ile	8.517	4.538	1.757	1.543, 1.109, 0.819	0.709	-----	-----	-----
12	Thr	8.943	4.760	4.099	, 1.209	-----	-----	-----	-----
13	Trp	8.578	4.647	3.001, 2.607	-----	7.016	10.032, 5.927	7.421, 6.605	7.103
14	Glu	7.942	4.187	1.928, 1.647	2.190,	-----		-----	-----

RW4-NPATAK (pH 8 @ 300 K)

#	Res		Hα	Hβ	Hγ	Hδ	Hε	Hζ	Hη
1	Arg		3.540	1.625, 1.625	1.372, 1.343	3.053,		-----	, , ,
2	Trp		5.024	3.206,	-----	7.329	10.186, 7.584	7.459, 7.216	7.225
3	Thr	8.646	4.445	4.036	, 1.079	-----	-----	-----	-----
4	Val	8.190	4.182	1.942	0.877, 0.784	-----	-----	-----	-----
5	Asn	8.472	4.919	3.025, 2.717	-----	,	-----	-----	-----
6	Pro	-----	4.340	2.289,	1.987,	3.912, 3.757	-----	-----	-----
7	Ala	8.165	4.345	1.453	-----	-----	-----	-----	-----
8	Thr	7.666	4.323		, 1.170	-----	-----	-----	-----
9	Ala	8.240	4.124	1.430	-----	-----	-----	-----	-----
10	Lys	7.898	4.341	1.766, 1.666	1.414, 1.345	,	2.971,		-----
11	Ile	8.321	4.409	1.729	1.481, 1.072, 0.740	0.716	-----	-----	-----
12	Thr	8.402	4.577	4.145	, 1.159	-----	-----	-----	-----
13	Trp	8.326	4.723	3.153, 2.882	-----	7.090	10.008, 6.668	7.442, 6.807	7.147
14	Glu	7.879	4.095	1.904, 1.732	2.037,	-----		-----	-----

RW4-NPATHK (pH 6.5 @ 300 K)

#	Res		Hα	Hβ	Hγ	Hδ	Hε	Hζ	Hη
1	Arg		3.537	1.720, 1.602	1.373, 1.271	3.064,	7.128	-----	, , ,
2	Trp	8.801	5.300	3.161,	-----	7.457	10.320, 7.562	7.442, 7.228	7.219
3	Thr	9.298	4.634	3.967	, 1.031	-----	-----	-----	-----
4	Val	8.410	4.358	1.907	0.885, 0.697	-----	-----	-----	-----
5	Asn	8.476	4.936	3.163, 2.780	-----	7.783, 7.255	-----	-----	-----
6	Pro	-----	4.262	2.325,	2.036, 1.999	4.059, 3.808	-----	-----	-----
7	Ala	8.013	4.329	1.471	-----	-----	-----	-----	-----
8	Thr	7.555	4.263	4.329	, 1.149	-----	-----	-----	-----
9	His	8.392	4.182	3.528, 3.418	-----	, 7.138	8.528,	-----	-----
10	Lys	7.666	4.513	1.806,	1.476, 1.399	1.699,	3.038,		-----
11	Ile	8.625	4.797	1.763	1.616, 1.094, 0.884	0.716	-----	-----	-----
12	Thr	9.097	4.870	4.133	, 1.222	-----	-----	-----	-----
13	Trp	8.707	4.701	2.940, 2.500	-----	6.963	9.983, 5.491	7.398, 6.417	7.072
14	Glu	7.980	4.086	1.802, 1.613	1.999,	-----		-----	-----

RW4-HPATGR (pH 6.5 @ 300 K)

#	Res		Hα	Hβ	Hγ	Hδ	Hε	Hζ	Hη
1	Arg		3.881	1.805, 1.805	1.515,	3.130,	7.112	-----	, , ,
2	Trp	8.731	4.905	3.246,	-----	7.298	10.159, 7.590	7.474, 7.234	7.237
3	Thr		4.338	3.995	, 1.021	-----	-----	-----	-----
4	Val	8.085	4.031	1.931	0.875, 0.818	-----	-----	-----	-----
5	His	8.531	4.937	3.161,	-----	, 7.260	8.551,	-----	-----
6	Pro	-----	4.358	2.289, 1.933	1.992,	3.756, 3.566	-----	-----	-----
7	Ala	8.551	4.357	1.450	-----	-----	-----	-----	-----
8	Thr	7.945	4.397	4.279	, 1.215	-----	-----	-----	-----
9	Gly	8.390	4.023, 3.899	-----	-----	-----	-----	-----	-----
10	Arg	8.020	4.326	1.771, 1.689	1.580, 1.528	3.126,		-----	, , ,
11	Ile	8.307	4.287	1.736	1.454, 1.085, 0.765	0.677	-----	-----	-----
12	Thr		4.499	4.214	, 1.135	-----	-----	-----	-----
13	Trp	8.177	4.701	3.197, 3.052	-----	7.148	10.064,	7.477, 6.970	7.174
14	Glu	7.863	4.206	2.017, 1.796	2.211,	-----		-----	-----

RW4-HPAAGR (pH 6.5 @ 300 K)

#	Res		Hα	Hβ	Hγ	Hδ	Hε	Hζ	Hη
1	Arg		3.979	1.848,	1.548,	3.134,	7.111	-----	, , ,
2	Trp	8.693	4.823	3.270,	-----	7.249	10.109, 7.599	7.476, 7.138	7.226
3	Thr	8.107	4.271	4.018	, 1.048	-----	-----	-----	-----
4	Val	7.978	3.936	1.916	0.865, 0.817	-----	-----	-----	-----
5	His	8.492	4.918	3.167, 3.070	-----	, 7.255	8.540,	-----	-----
6	Pro	-----	4.354	2.236, 1.892	1.957, 1.900	3.670, 3.505	-----	-----	-----
7	Ala	8.423	4.303	1.391	-----	-----	-----	-----	-----
8	Ala	8.271	4.317	1.397	-----	-----	-----	-----	-----
9	Gly	8.302	3.932,	-----	-----	-----	-----	-----	-----
10	Arg	8.060	4.321	1.781, 1.701	1.551, 1.514	3.113,	7.099	-----	, , ,
11	Ile	8.225	4.085	1.732	1.090, 0.772, 0.618		-----	-----	-----
12	Thr	7.946	4.350	4.174	, 1.118	-----	-----	-----	-----
13	Trp	7.988	4.724	3.264, 3.223	-----	7.206	10.077,	7.463, 7.202	7.111
14	Glu	7.837	4.198	2.024, 1.824	2.204,	-----		-----	-----

Chapter 5. Loops

Short Loops

R-GG-E (pH 6.5 @ 300 K)

#	Res		Hα	Hβ	Hγ	Hδ	Hε	Hζ	Hη
1	Arg		3.499	1.732, 1.616	1.369, 1.226	3.072, 3.027	7.203	-----	, , ,
2	Trp	8.884	5.370	3.206, 3.071	-----	7.515	10.333, 7.491	7.420, 7.165	7.233
3	Ile	9.682	4.696	1.879	1.003, , 0.787	0.674	-----	-----	-----

4	Thr	8.471	5.261	3.964	, 1.100	-----	-----	-----	-----
5	Val	9.175	4.573	2.077	0.890,	-----	-----	-----	-----
6	Thr	8.462	5.160	3.952	, 0.973	-----	-----	-----	-----
7	Ile	8.881	4.364	1.712	1.453, , 1.070	0.874	-----	-----	-----
8	Gly	9.390	3.890, 3.890	-----	-----	-----	-----	-----	-----
9	Gly	8.487	4.127, 3.596	-----	-----	-----	-----	-----	-----
10	Lys	7.744	4.617	1.823,	1.428, 1.374	1.680,	3.009,		-----
11	Lys	8.448	4.864	1.738,	1.288,	1.506, 1.427	2.910,		-----
12	Ile	9.282	4.506	1.852	1.396, 1.173, 0.895	0.798	-----	-----	-----
13	Arg	8.366	5.410	1.767,	1.608,	2.828,	6.614	-----	, , ,
14	Val	9.451	4.854	2.115	0.956, 0.902	-----	-----	-----	-----
15	Trp	8.637	4.567	2.764, 2.078	-----	6.914	9.961, 5.074	7.415, 6.450	7.073
16	Glu	8.047	4.019	1.635,	1.946, 1.562	-----		-----	-----

R-GGG-E (pH 6.5 @ 300 K)

#	Res		Hα	Hβ	Hγ	Hδ	Hε	Hζ	Hη
1	Arg		3.503	1.729, 1.607	1.367, 1.229	3.073, 3.031	7.219	-----	, , ,
2	Trp	8.885	5.346	3.204, 3.068	-----	7.513	10.340, 7.473	7.421, 7.169	7.243
3	Ile	9.683	4.669	1.880	1.022, , 0.792		-----	-----	-----
4	Thr	8.526	5.203	3.990	, 1.126	-----	-----	-----	-----
5	Val	9.188	4.464	1.996	0.871,	-----	-----	-----	-----
6	Thr	8.492	4.884	4.025	, 1.158	-----	-----	-----	-----
7	Ile	8.751	4.633	2.053	, , 0.880		-----	-----	-----
8	Gly	8.294	3.943,	-----	-----	-----	-----	-----	-----
9	Gly	8.819	4.070, 3.843	-----	-----	-----	-----	-----	-----
10	Gly	8.335	4.145, 3.689	-----	-----	-----	-----	-----	-----
11	Lys	7.287	4.305	1.770,	1.455, 1.354	1.670,	2.980,		-----
12	Lys	8.353	5.212	1.664,	1.418, 1.352	1.551,	2.919,		-----
13	Ile	9.012	4.669	1.891	, , 0.890		-----	-----	-----
14	Arg	8.355	5.484	1.757,	1.621, 1.575	2.821,	6.620	-----	, , ,
15	Val	9.386	4.831	2.095	0.960, 0.897	-----	-----	-----	-----
16	Trp	8.667	4.563	2.766, 2.088	-----	6.917	9.961, 5.097	7.418, 6.445	7.083
17	Glu	8.038	4.015	1.635, 1.569	1.942,	-----		-----	-----

RGGGGE (pH 6.5 @ 300 K)

#	Res		Hα	Hβ	Hγ	Hδ	Hε	Hζ	Hη
1	Arg	8.332	3.530	1.737, 1.624	1.424, 1.324	3.048,	7.232	-----	, , ,
2	Trp	8.844	5.308	3.194, 3.071	-----	7.474	10.300, 7.480	7.483, 7.153	7.234
3	Ile	9.553	4.636		, ,	0.796	-----	-----	-----
4	Thr	8.488	5.109	3.997	, 1.123	-----	-----	-----	-----
5	Val	9.061	4.488	2.053	, 0.881	-----	-----	-----	-----
6	Thr	8.403	4.741	4.062	, 1.141	-----	-----	-----	-----

7	Ile	8.508	4.388	1.873	0.894, ,	0.815	-----	-----	-----
8	Gly	8.551	3.975,	-----	-----	-----	-----	-----	-----
9	Gly	8.331	3.989,	-----	-----	-----	-----	-----	-----
10	Gly	8.331	3.989,	-----	-----	-----	-----	-----	-----
11	Gly	8.204	3.940, 3.903	-----	-----	-----	-----	-----	-----
12	Lys		4.307	1.774,	1.428, 1.346	1.665,	2.962, 2.966	7.803	-----
13	Lys		5.003	1.749,	1.381, 1.249	1.567,	2.915, 3.062	7.232	-----
14	Ile	8.886	4.567	1.865	0.887, , 0.889	0.808	-----	-----	-----
15	Arg	8.331	5.343	1.730, 1.646	1.522,	2.806,	6.647	-----	, , ,
16	Val	9.252	4.769		, 0.948	-----	-----	-----	-----
17	Trp	8.601	4.576	2.811, 2.189	-----	6.930	9.959, 5.332	7.410, 6.502	7.083
18	Glu	8.000	4.018	1.959,	1.666, 1.598	-----		-----	-----

R-GGGGG-E (pH 6.5 @ 300 K)

#	Res		Hα	Hβ	Hγ	Hδ	Hε	Hζ	Hη
1	Arg		3.540	1.743, 1.632	1.390, 1.251	3.079, 3.039	7.206	-----	, , ,
2	Trp	8.873	5.328	3.197, 3.086	-----	7.490	10.312, 7.497	7.427, 7.159	7.243
3	Ile	9.592	4.654	1.873	, , 0.801	0.682	-----	-----	-----
4	Thr	8.483	5.146	3.997	, 1.124	-----	-----	-----	-----
5	Val	9.092	4.487	2.048	, 0.880	-----	-----	-----	-----
6	Thr	8.437	4.762	4.011	, 1.086	-----	-----	-----	-----
7	Ile	8.676	4.300	1.876	, , 0.925	0.821	-----	-----	-----
8	Gly	8.714	4.082, 3.915	-----	-----	-----	-----	-----	-----
9	Gly	8.372	4.101, 3.923	-----	-----	-----	-----	-----	-----
10	Gly	8.452	3.933,	-----	-----	-----	-----	-----	-----
11	Gly	8.561	3.969,	-----	-----	-----	-----	-----	-----
12	Gly	8.092	3.999, 3.923	-----	-----	-----	-----	-----	-----
13	Lys	8.074	4.363	1.773,	1.436, 1.379	1.672,	,		-----
14	Lys	8.371	5.066	1.673,	1.440, 1.338	1.578,	,		-----
15	Ile	8.975	4.596	1.864	1.066, , 0.890	0.818	-----	-----	-----
16	Arg	8.331	5.367	1.741,	1.600, 1.538	2.814,	6.627	-----	, , ,
17	Val	9.294	4.800	2.092	0.950, 0.896	-----	-----	-----	-----
18	Trp	8.624	4.581	2.807, 2.168	-----	6.938	9.974, 5.279	7.419, 6.499	7.088
19	Glu	8.014	4.031	1.973,	1.674, 1.587	-----		-----	-----

R-GGGGGG-E (pH 6.5 @ 300 K)

#	Res		Hα	Hβ	Hγ	Hδ	Hε	Hζ	Hη
1	Arg		3.546	1.745, 1.632	1.385, 1.262	3.078, 3.042	7.199	-----	, , ,
2	Trp	8.873	5.320	3.204, 3.085	-----	7.487	10.309, 7.501	7.428, 7.163	7.244
3	Ile	9.564	4.646	1.873	, , 0.801	0.682	-----	-----	-----
4	Thr	8.473	5.131	3.998	, 1.124	-----	-----	-----	-----
5	Val	9.065	4.478	2.047	, 0.875	-----	-----	-----	-----

6	Thr	8.436	4.791	4.014	, 1.090	-----	-----	-----	-----
7	Ile	8.780	4.320	1.902	, , 0.932	0.824	-----	-----	-----
8	Gly	8.558	4.072, 3.981	-----	-----	-----	-----	-----	-----
9	Gly		,	-----	-----	-----	-----	-----	-----
10	Gly		,	-----	-----	-----	-----	-----	-----
11	Gly		,	-----	-----	-----	-----	-----	-----
12	Gly	8.294	4.042, 3.980	-----	-----	-----	-----	-----	-----
13	Gly	8.085	3.955,	-----	-----	-----	-----	-----	-----
14	Lys	8.157	4.428	1.796, 1.745	1.400,	1.667,	,		-----
15	Lys	8.368	5.051	1.684,	1.426, 1.336	1.577,	,		-----
16	Ile	8.964	4.585	1.866	, , 0.888	0.819	-----	-----	-----
17	Arg	8.337	5.345	1.736, 1.595	1.598, 1.535	2.815,	6.632	-----	, , ,
18	Val	9.271	4.782	2.096	0.947, 0.893	-----	-----	-----	-----
19	Trp	8.616	4.583	2.821, 2.187	-----	6.943	9.974, 5.326	7.419, 6.513	7.091
20	Glu	8.012	4.035	1.984,	1.690, 1.591	-----		-----	-----

R-G7-E (pH 6.5 @ 300 K)

#	Res		Hα	Hβ	Hγ	Hδ	Hε	Hζ	Hη
1	Arg		3.537	1.745, 1.596	1.384, 1.282	3.070,	7.089	-----	, , ,
2	Trp	8.907	5.308	3.225, 3.079	-----	7.510	10.310, 7.491	7.443, 7.177	7.253
3	Ile	9.496	4.643	1.877	1.328, 1.046, 0.809	0.677	-----	-----	-----
4	Thr	8.468	5.140	4.009	, 1.128	-----	-----	-----	-----
5	Val	9.078	4.481	2.047	0.880,	-----	-----	-----	-----
6	Thr	8.411	4.850	4.007	1.083, 1.090	-----	-----	-----	-----
7	Ile	8.875	4.388	1.901	, , 0.926	0.823	-----	-----	-----
8	Gly		,	-----	-----	-----	-----	-----	-----
9	Gly		,	-----	-----	-----	-----	-----	-----
10	Gly		,	-----	-----	-----	-----	-----	-----
11	Gly		,	-----	-----	-----	-----	-----	-----
12	Gly		,	-----	-----	-----	-----	-----	-----
13	Gly		,	-----	-----	-----	-----	-----	-----
14	Gly		,	-----	-----	-----	-----	-----	-----
15	Lys	8.249	4.475	1.797, 1.732	1.392, 1.367	1.669,	2.968,	7.546	-----
16	Lys	8.371	5.065	1.683,	1.424, 1.340	1.581,	2.934,	7.478	-----
17	Ile	8.956	4.589	1.870	1.414, , 0.889		-----	-----	-----
18	Arg	8.329	5.353	1.760, 1.632	1.567,	2.836,	6.631	-----	, , ,
19	Val	9.311	4.797	2.094	0.958, 0.915	-----	-----	-----	-----
20	Trp	8.670	4.548	2.810, 2.114	-----	6.931	9.996, 5.311	7.422, 6.552	7.098
21	Glu	8.009	4.137	1.840, 1.557	2.174,	-----		-----	-----

R-GGGGGGGG-E (pH 6.5 @ 300 K)

#	Res		Hα	Hβ	Hγ	Hδ	Hε	Hζ	Hη

1	Arg		3.509	1.742, 1.594	1.380, 1.268	3.064,	7.124	-----	, , ,
2	Trp	8.904	5.326	3.214, 3.080	-----	7.503	10.321, 7.424	7.489, 7.169	7.252
3	Ile	9.562	4.650	1.879	1.325, 1.046, 0.808	0.677	-----	-----	-----
4	Thr	8.490	5.160	4.000	, 1.130	-----	-----	-----	-----
5	Val	9.101	4.496	2.048	, 0.879	-----	-----	-----	-----
6	Thr	8.441	4.880	3.997	, 1.080	-----	-----	-----	-----
7	Ile	8.955	4.412	1.903	1.472, 1.198, 0.925		-----	-----	-----
8	Gly	8.685	4.057, 3.983	-----	-----	-----	-----	-----	-----
9	Gly	8.380	3.933,	-----	-----	-----	-----	-----	-----
10	Gly		,	-----	-----	-----	-----	-----	-----
11	Gly		,	-----	-----	-----	-----	-----	-----
12	Gly		,	-----	-----	-----	-----	-----	-----
13	Gly		,	-----	-----	-----	-----	-----	-----
14	Gly		,	-----	-----	-----	-----	-----	-----
15	Gly		,	-----	-----	-----	-----	-----	-----
16	Lys	8.333	4.495	1.792, 1.736	1.385,	1.661,	2.957,	7.559	-----
17	Lys	8.407	5.079	1.695,	1.427, 1.335	1.574,	2.924,	7.483	-----
18	Ile	9.009	4.602	1.869	1.395, 1.081, 0.893	0.809	-----	-----	-----
19	Arg	8.343	5.379	1.761,	1.572,	2.829,	6.626	-----	, , ,
20	Val	9.345	4.814	2.101	, 0.954	-----	-----	-----	-----
21	Trp	8.656	4.565	2.801, 2.107	-----	6.927	10.000, 5.226	7.423, 6.513	7.093
22	Glu	8.033	4.080	1.772, 1.557	2.107,	-----		-----	-----

R-G9-E (pH 6.5 @ 300 K)

#	Res		Hα	Hβ	Hγ	Hδ	Hε	Hζ	Hη
1	Arg		3.518	1.742, 1.588	1.384, 1.285	3.071,	7.097	-----	, , ,
2	Trp		5.316	3.221, 3.079	-----	7.510	10.298, 7.492	7.452, 7.175	7.246
3	Ile	9.507	4.650	1.882	, , 0.805	0.676	-----	-----	-----
4	Thr	8.467	5.144	4.004	, 1.128	-----	-----	-----	-----
5	Val	9.078	4.484	2.049	, 0.879	-----	-----	-----	-----
6	Thr	8.417	4.864	3.999	, 1.084	-----	-----	-----	-----
7	Ile	8.911	4.398	1.895	, , 0.927		-----	-----	-----
8	Gly		,	-----	-----	-----	-----	-----	-----
9	Gly		,	-----	-----	-----	-----	-----	-----
10	Gly		,	-----	-----	-----	-----	-----	-----
11	Gly		,	-----	-----	-----	-----	-----	-----
12	Gly		,	-----	-----	-----	-----	-----	-----
13	Gly		,	-----	-----	-----	-----	-----	-----
14	Gly		,	-----	-----	-----	-----	-----	-----
15	Gly		,	-----	-----	-----	-----	-----	-----
16	Gly	8.231	3.924,	-----	-----	-----	-----	-----	-----

17	Lys	8.303	4.490	1.799, 1.732	1.389, 1.388	1.669,	2.964,	7.545	-----
18	Lys	8.380	5.073	1.695,	1.414, 1.334	1.579,	2.938,	7.473	-----
19	Ile	8.969	4.595	1.869	, , 0.886		-----	-----	-----
20	Arg	8.328	5.360	1.758, 1.632	1.567,	2.836,	6.628	-----	, , ,
21	Val	9.309	4.803	2.103	0.957, 0.909	-----	-----	-----	-----
22	Trp		4.562	2.805, 2.118	-----	6.941	9.995, 5.283	7.426, 6.539	7.095
23	Glu	8.015	4.106	1.814, 1.558	2.156,	-----		-----	-----

R-G10-E (pH 6.5 @ 300 K)

#	Res		Hα	Hβ	Hγ	Hδ	Hε	Hζ	Hη
1	Arg		3.373	1.592, 1.439	1.229, 1.134	2.916,	6.936	-----	, , ,
2	Trp	8.745	5.156	3.064, 2.933	-----	7.348	10.150, 7.344	7.277, 7.020	7.093
3	Ile	9.343	4.487	1.715	1.166, 0.894, 0.653	0.522	-----	-----	-----
4	Thr	8.307	4.981	3.848	, 0.975	-----	-----	-----	-----
5	Val	8.909	4.352	1.898	0.722, 0.711	-----	-----	-----	-----
6	Thr	8.274	4.708	3.849	, 0.930	-----	-----	-----	-----
7	Ile	8.732	4.246	1.738	1.304, 1.027, 0.765	0.662	-----	-----	-----
8	Gly	8.483	3.908, 3.828	-----	-----	-----	-----	-----	-----
9	Gly		,	-----	-----	-----	-----	-----	-----
10	Gly		,	-----	-----	-----	-----	-----	-----
11	Gly		,	-----	-----	-----	-----	-----	-----
12	Gly		,	-----	-----	-----	-----	-----	-----
13	Gly		,	-----	-----	-----	-----	-----	-----
14	Gly		,	-----	-----	-----	-----	-----	-----
15	Gly		,	-----	-----	-----	-----	-----	-----
16	Gly		,	-----	-----	-----	-----	-----	-----
17	Gly	8.076	3.792, 3.738	-----	-----	-----	-----	-----	-----
18	Lys	8.146	4.320	1.647, 1.575	1.258, 1.206	1.509,	2.804,	7.401	-----
19	Lys	8.220	4.906	1.537,	1.267, 1.184	1.423,	2.770,	7.337	-----
20	Ile	8.804	4.431	1.708	1.245, 0.914, 0.733	0.651	-----	-----	-----
21	Arg	8.186	5.192	1.605, 1.477	1.412,	2.677,	6.477	-----	, , ,
22	Val	9.148	4.655	1.943	0.794, 0.746	-----	-----	-----	-----
23	Trp	8.498	4.406	2.661, 1.971	-----	6.774	9.838, 5.140	7.264, 6.393	6.946
24	Glu	7.854	3.967	1.665, 1.415	2.013,	-----		-----	-----

Long Loops

R-Superloop-E (pH 6.5 @ 300 K)

#	Res		Hα	Hβ	Hγ	Hδ	Hε	Hζ	Hη
1	Arg		4.107	2.078, 2.027	1.851,	,	7.772	-----	, , ,
2	Trp	8.992	5.261	3.194, 3.094	-----	7.455	10.290, 7.493	7.426, 7.153	7.240
3	Ile		4.599	1.858	, , 0.798	0.691	-----	-----	-----

4	Thr	8.438	5.048	4.007	, 1.128	-----	-----	-----	-----
5	Val	8.969	4.439	2.038	0.878, 0.882	-----	-----	-----	-----
6	Thr	8.415	4.797	4.005	, 1.083	-----	-----	-----	-----
7	Ile	8.812	4.358	1.883	1.170, , 0.924	0.825	-----	-----	-----
8	Gly	8.667	4.052, 3.966	-----	-----	-----	-----	-----	-----
9	Gly	8.424	3.991,	-----	-----	-----	-----	-----	-----
10	Gly		,	-----	-----	-----	-----	-----	-----
11	Gly		,	-----	-----	-----	-----	-----	-----
12	Lys	8.425	4.246	,	,	,	,		-----
13	Lys	8.422	4.288	1.878, 1.798	1.450,	1.693,	2.994,		-----
14	Gly	8.294	3.911, 3.901	-----	-----	-----	-----	-----	-----
15	Gly	8.255	4.003,	-----	-----	-----	-----	-----	-----
16	Gly	8.548	3.986,	-----	-----	-----	-----	-----	-----
17	Gly	8.354	3.945,	-----	-----	-----	-----	-----	-----
18	Lys	8.302	4.454	1.793,	1.407,	1.667,	2.972,		-----
19	Lys	8.402	4.970	1.694,	1.433, 1.328	1.585,	2.917,		-----
20	Ile	8.908	4.541	1.863	, , 0.887	0.809	-----	-----	-----
21	Arg	8.325		1.706,	1.522,	2.835,	6.693	-----	, , ,
22	Val	9.142	4.716	2.089	0.930, 0.891	-----	-----	-----	-----
23	Trp	8.551	4.608	2.861, 2.173	-----	6.955	9.975,	7.414, 6.522	7.089
24	Glu	7.982	4.024	1.693, 1.611	1.967,	-----		-----	-----

R-(GGGGKK)3-E (pH 6.5 @ 300K)

#	Res		Hα	Hβ	Hγ	Hδ	Hε	Hζ	Hη
1	Arg		4.113	2.121, 2.058	1.844,	,	7.727	-----	, , ,
2	Trp		5.139	3.203, 3.156	-----	7.401	10.240, 7.548	7.463, 7.169	7.242
3	Ile		4.496	1.831	, , 0.806	0.727	-----	-----	-----
4	Thr	8.384	4.654	4.050	, 1.113	-----	-----	-----	-----
5	Val		4.380	2.050	0.892,	-----	-----	-----	-----
6	Thr	8.253	4.395	4.152	, 1.175	-----	-----	-----	-----
7	Ile	8.634	4.300	1.889	1.199, , 0.917	0.833	-----	-----	-----
8	Gly	8.611	4.029, 3.992	-----	-----	-----	-----	-----	-----
9	Gly		,	-----	-----	-----	-----	-----	-----
10	Gly		,	-----	-----	-----	-----	-----	-----
11	Gly		,	-----	-----	-----	-----	-----	-----
12	Lys			,	,	,	,		-----
13	Lys			,	,	,	,		-----
14	Gly		,	-----	-----	-----	-----	-----	-----
15	Gly		,	-----	-----	-----	-----	-----	-----
16	Gly		,	-----	-----	-----	-----	-----	-----
17	Gly		,	-----	-----	-----	-----	-----	-----
18	Lys			,	,	,	,		-----

19	Lys			,	,	,	,		-----
20	Gly		,	-----	-----	-----	-----	-----	-----
21	Gly		,	-----	-----	-----	-----	-----	-----
22	Gly		,	-----	-----	-----	-----	-----	-----
23	Gly		,	-----	-----	-----	-----	-----	-----
24	Lys		4.401	1.797,	1.401,	1.662,	,		-----
25	Lys	8.371	4.775	1.687,	1.420, 1.340	1.605,	2.944,		-----
26	Ile		4.422	1.853	, , 0.871	0.811	-----	-----	-----
27	Arg	8.312		1.659,	1.586, 1.485	2.887,		-----	, , ,
28	Val				,	-----	-----	-----	-----
29	Trp			,	-----	7.048	10.016,	7.461, 6.741	7.147
30	Glu	7.903	4.055	1.786, 1.681	2.008,	-----		-----	-----

R-GGGGKK4-E new (pH 6.5 @ 300 K)

#	Res		Hα	Hβ	Hγ	Hδ	Hε	Hζ	Hη
1	Arg		3.773	1.811, 1.755	1.485, 1.421	3.122,		-----	, , ,
2	Trp		5.017	3.206,	-----	7.339	10.207, 7.603	7.481, 7.169	7.246
3	Ile		4.384		, , 0.812	0.758	-----	-----	-----
4	Thr	8.380	4.542	4.073	, 1.135	-----	-----	-----	-----
5	Val	8.047	4.307	2.056	0.901, 0.849	-----	-----	-----	-----
6	Thr	8.350	4.378	4.123	, 1.164	-----	-----	-----	-----
7	Ile	8.525	4.252	1.871	, , 0.916	0.844	-----	-----	-----
8	Gly	8.606	4.007,	-----	-----	-----	-----	-----	-----
9	Gly		,	-----	-----	-----	-----	-----	-----
10	Gly		,	-----	-----	-----	-----	-----	-----
11	Gly		,	-----	-----	-----	-----	-----	-----
12	Lys			,	,	,	,		-----
13	Lys			,	,	,	,		-----
14	Gly		,	-----	-----	-----	-----	-----	-----
15	Gly		,	-----	-----	-----	-----	-----	-----
16	Gly		,	-----	-----	-----	-----	-----	-----
17	Gly		,	-----	-----	-----	-----	-----	-----
18	Lys			,	,	,	,		-----
19	Lys			,	,	,	,		-----
20	Gly		,	-----	-----	-----	-----	-----	-----
21	Gly		,	-----	-----	-----	-----	-----	-----
22	Gly		,	-----	-----	-----	-----	-----	-----
23	Gly		,	-----	-----	-----	-----	-----	-----
24	Lys			,	,	,	,		-----
25	Lys			,	,	,	,		-----
26	Gly		,	-----	-----	-----	-----	-----	-----

27	Gly		,	-----	-----	-----	-----	-----	-----
28	Gly		,	-----	-----	-----	-----	-----	-----
29	Gly		,	-----	-----	-----	-----	-----	-----
30	Lys			,	,	,	,		-----
31	Lys	8.384	4.610	1.706, 1.612	1.427, 1.351	,	,		-----
32	Ile	8.197	4.197	2.058	, , 0.902	0.825	-----	-----	-----
33	Arg		3.941	1.832,	1.536,	3.153,		-----	, , ,
34	Val	8.078	4.048	1.984	0.871, 0.835	-----	-----	-----	-----
35	Trp	8.089	4.727	3.325, 3.220	-----	7.113	10.059,	7.473, 6.867	7.161
36	Glu	7.859	4.073	1.858, 1.737	2.033,	-----		-----	-----

RWW-IGGK (pH 6.5 @ 300 K)

#	Res		Hα	Hβ	Hγ	Hδ	Hε	Hζ	Hη
1	Arg		3.492	1.738, 1.585	1.373, 1.258	3.085, 3.045	7.134	-----	, , ,
2	Trp	8.948	5.349	3.232, 3.082	-----	7.544	10.353, 7.429	7.427, 7.147	7.286
3	Ile	9.704	4.691	1.915	1.335, 1.078, 0.829	0.681	-----	-----	-----
4	Thr	8.500	5.224	4.032	, 1.149	-----	-----	-----	-----
5	Val	9.158	4.577	2.086	0.942, 0.906	-----	-----	-----	-----
6	Arg	8.441	5.504	1.788,	1.586,	2.822,		-----	, , ,
7	Ile	9.404	5.021	1.873	1.577, 1.153, 0.988	0.882	-----	-----	-----
8	Trp	8.665	4.638	2.864, 1.752	-----	6.684	9.798, 5.471	7.210, 6.476	6.924
9	Ile	8.563	4.240	1.638	1.388, 0.999, 0.826	0.764	-----	-----	-----
10	Gly	8.616	3.612, 3.612	-----	-----	-----	-----	-----	-----
11	Gly	7.333	3.733, 3.044	-----	-----	-----	-----	-----	-----
12	Lys	6.473	4.087	1.709,	1.197, 1.132	1.526,	2.951,		-----
13	Trp	8.273	5.286	3.149, 3.027	-----	7.487	10.119,	7.264,	7.203
14	Lys	9.787	4.777	1.850, 1.693	1.333,	1.628, 1.441	2.935,		-----
15	Thr	8.621	5.221	4.042	, 1.148	-----	-----	-----	-----
16	Ile	9.246	4.710	1.923	1.409, 1.115, 0.929	0.828	-----	-----	-----
17	Arg	8.367	5.520	1.789, 1.636	1.598,	2.824,	6.627	-----	, , ,
18	Val	9.427	4.893	2.126	0.990, 0.933	-----	-----	-----	-----

19	Trp	8.755	4.565	2.786, 2.061	-----	6.906	9.998, 5.088	7.423, 6.491	7.098	
20	Glu	8.047	4.084	1.747, 1.543	2.100,	-----		-----	-----	

RWW-10loop-WWE (pH 6.5 @ 300 K)

#	Res		Hα	Hβ	Hγ	Hδ	Hε	Hζ	Hη
-1	Arg		3.494	1.729, 1.585	1.370, 1.250	3.070, 3.059	7.136	-----	, , ,
1	Trp	8.917	5.352	3.219, 3.076	-----	7.528	10.336, 7.491	7.429, 7.185	7.252
2	Ile	9.688	4.686	1.907	1.059, , 0.812		-----	-----	-----
3	Thr	8.451	5.199	4.012	, 1.132	-----	-----	-----	-----
4	Val	9.142	4.496	2.040	0.924, 0.891	-----	-----	-----	-----
5	Arg	8.399	5.391	1.716,	1.591,	2.733,	6.581	-----	, , ,
6	Ile	9.303	4.913	1.877	, , 0.945		-----	-----	-----
7	Trp	8.959	4.303	2.887, 2.237	-----	6.751	9.966, 5.620	7.262, 6.476	7.010
8	Gly	7.910	3.992, 3.461	-----	-----	-----	-----	-----	-----
9	Gly	7.185	3.826, 3.675	-----	-----	-----	-----	-----	-----
10	Gly	8.290	3.881,	-----	-----	-----	-----	-----	-----
11	Gly	8.397	3.976,	-----	-----	-----	-----	-----	-----
12	Lys	8.367	4.223	,	,	,	,		-----
13	Lys	8.396	4.273	,	,	,	,		-----
14	Gly	8.124	4.108, 3.885	-----	-----	-----	-----	-----	-----
15	Gly	8.247	3.988,	-----	-----	-----	-----	-----	-----
16	Gly	8.156	3.688,	-----	-----	-----	-----	-----	-----
17	Gly	7.089	3.664, 3.160	-----	-----	-----	-----	-----	-----
18	Trp	8.223	5.029	3.076,	-----	7.441	10.266, 7.497	7.433, 7.156	7.221
19	Lys	9.451	4.776	1.823, 1.759	1.344,	,	,		-----
20	Thr	8.532	5.268	4.015	, 1.121	-----	-----	-----	-----
21	Ile	9.127	4.697	1.912	, , 0.906		-----	-----	-----
22	Arg	8.317	5.514	1.771,	1.592,	2.829,	6.621	-----	, , ,
23	Val	9.384	4.857	2.113	0.976, 0.920	-----	-----	-----	-----
24	Trp	8.703	4.568	2.774, 2.054	-----	6.912	9.988, 5.088	7.423, 6.478	7.085
25	Glu	8.038	4.080	1.759, 1.558	2.099,	-----		-----	-----

RWW-16Loop-WWE (pH 6.5 @ 300 K)

#	Res		Hα	Hβ	Hγ	Hδ	Hε	Hζ	Hη
1	Arg		3.486	1.735, 1.576	1.379, 1.259	3.064, 3.065	7.103	-----	, , ,
2	Trp	8.900	5.329	3.218, 3.067	-----	7.521	10.320,	7.428,	7.162
3	Ile	9.639	4.668	1.902	, , 0.816	0.680	-----	-----	-----
4	Thr	8.427	5.170	4.012	, 1.130	-----	-----	-----	-----
5	Val	9.125	4.468	2.027	0.917, 0.894	-----	-----	-----	-----
6	Arg	8.376	5.331	1.769, 1.656	1.388,	2.714,		-----	, , ,
7	Ile	9.261	4.864	1.866	, 1.149, 0.933	0.852	-----	-----	-----

8	Trp	8.938	4.316	2.926, 2.333	-----	6.798	9.973, 5.791	7.285, 6.540	7.041
9	Gly	7.940	3.941, 3.458	-----	-----	-----	-----	-----	-----
10	Gly	6.745	3.726, 3.702	-----	-----	-----	-----	-----	-----
11	Gly	7.326	3.648, 3.252	-----	-----	-----	-----	-----	-----
12	Gly		,	-----	-----	-----	-----	-----	-----
13	Lys			,	,	,	,		-----
14	Lys			,	,	,	,		-----
15	Gly		,	-----	-----	-----	-----	-----	-----
16	Gly		,	-----	-----	-----	-----	-----	-----
17	Gly		,	-----	-----	-----	-----	-----	-----
18	Gly		,	-----	-----	-----	-----	-----	-----
19	Lys			,	,	,	,		-----
20	Lys			,	,	,	,		-----
21	Gly		,	-----	-----	-----	-----	-----	-----
22	Gly		,	-----	-----	-----	-----	-----	-----
23	Gly		,	-----	-----	-----	-----	-----	-----
24	Gly	8.381	4.161,	-----	-----	-----	-----	-----	-----
25	Trp	8.097	4.995	3.068,	-----	7.401	10.237, 7.486	7.434, 7.152	7.225
26	Lys	9.364	4.762	1.765,	1.341,	1.605, 2.844	2.973, 2.863		-----
27	Thr	8.496	5.248	4.012	, 1.121	-----	-----	-----	-----
28	Ile	9.088	4.679	1.907	, , 0.906	0.817	-----	-----	-----
29	Arg	8.300	5.484	1.767, 1.653	1.395,	2.973, 2.820		-----	, , ,
30	Val	9.360	4.833	2.101	0.970, 0.929	-----	-----	-----	-----
31	Trp	8.681	4.551	2.777, 2.048	-----	6.905	9.985, 5.117	7.422, 6.491	7.092
32	Glu	8.025	4.088	1.805, 1.551	2.143,	-----		-----	-----

R-GIpGKG-E (pH 6.5 @ 300 K)

#	Res		Hα	Hβ	Hγ	Hδ	Hε	Hζ	Hη
1	Arg		3.491	1.735, 1.572	1.372, 1.272	3.058,	7.090	-----	, , ,
2	Trp	8.924	5.343	3.219, 3.080	-----	7.519	10.326, 7.481	7.417, 7.171	7.245
3	Ile	9.615	4.676	1.877	1.326, 1.048, 0.807	0.668	-----	-----	-----
4	Thr	8.499	5.223	3.993	, 1.128	-----	-----	-----	-----
5	Val	9.148	4.575	2.052	, 0.875	-----	-----	-----	-----
6	Thr	8.465	4.998	3.970	, 1.011	-----	-----	-----	-----
7	Ile	9.006	4.551	1.877	1.456, 1.183, 0.902	0.820	-----	-----	-----
8	Gly	8.534	4.198,	-----	-----	-----	-----	-----	-----
9	Ile	8.314	4.656	1.816	1.491, 1.129, 0.882		-----	-----	-----
10	dPro	-----	4.363	2.325,	2.035, 1.944	3.814,	-----	-----	-----
11	Gly	8.712	3.991, 3.858	-----	-----	-----	-----	-----	-----
12	Lys	7.758	4.548	1.945, 1.840	1.465, 1.434	1.702,	3.017,	7.545	-----
13	Gly	8.155	4.376, 3.591	-----	-----	-----	-----	-----	-----
14	Lys	8.703	4.560	1.799,	1.391,	1.690,	2.960,	7.597	-----

15	Lys	8.451	5.095	1.705,	1.420,	1.576,	2.912,	7.498	-----
16	Ile	9.149	4.624	1.871	, , 0.883	0.795	-----	-----	-----
17	Arg	8.365	5.432	1.773,	1.595,	2.812,	6.603	-----	, , ,
18	Val	9.424	4.870	2.106	0.956, 0.910	-----	-----	-----	-----
19	Trp	8.709	4.542	2.785, 2.045	-----	6.890	9.993, 5.119	7.414, 6.491	7.089
20	Glu	8.039	4.112	1.794, 1.535	2.148,	-----		-----	-----

R-GIPGKG-E (pH 6.5 @ 300 K)

#	Res		Hα	Hβ	Hγ	Hδ	Hε	Hζ	Hη
1	Arg		3.526	1.744, 1.622	1.384, 1.249	3.076, 3.042	7.183	-----	, , ,
2	Trp	8.874	5.328	3.206, 3.081	-----	7.494	10.312, 7.486	7.414, 7.165	7.249
3	Ile	9.584	4.656	1.869	, , 0.797		-----	-----	-----
4	Thr	8.472	5.171	3.991	, 1.123	-----	-----	-----	-----
5	Val	9.063	4.502	2.038	0.860,	-----	-----	-----	-----
6	Thr	8.449	4.851	3.974	, 0.993	-----	-----	-----	-----
7	Ile	8.858	4.435	1.890	1.181, , 0.895	0.818	-----	-----	-----
8	Gly	8.546	4.348, 3.780	-----	-----	-----	-----	-----	-----
9	Ile	8.116	4.367	1.814	1.204, , 0.961		-----	-----	-----
10	Pro	-----	4.219	2.279, 1.899	2.120, 1.954	3.988, 3.650	-----	-----	-----
11	Gly	8.679	4.264, 3.721	-----	-----	-----	-----	-----	-----
12	Lys	8.181	4.572	1.949, 1.628	1.394, 1.348	1.688,	2.984,		-----
13	Gly	8.229	4.208, 3.806	-----	-----	-----	-----	-----	-----
14	Lys	8.296	4.500	1.805, 1.736	1.408, 1.373	1.661,	,		-----
15	Lys	8.378	5.070	1.674,	1.411, 1.310	1.571,	2.908,		-----
16	Ile	9.028	4.605	1.870	1.080, 1.051, 0.886	0.805	-----	-----	-----
17	Arg	8.320	5.383	1.745, 1.609	1.558,	2.820,		-----	, , ,
18	Val	9.316	4.811	2.101	0.950, 0.893	-----	-----	-----	-----
19	Trp	8.621	4.579	2.800, 2.152	-----	6.934	9.972, 5.213	7.411, 6.493	7.083
20	Glu	8.025	4.036	1.990,	1.678, 1.580	-----		-----	-----

R-G3IpGKG3-E (pH 6.5 @ 300 K)

#	Res		Hα	Hβ	Hγ	Hδ	Hε	Hζ	Hη
1	Arg		3.518	1.745, 1.620	1.384, 1.243	3.069, 3.029		-----	, , ,
2	Trp	8.871	5.342	3.202, 3.079	-----	7.491	10.313, 7.489	7.414, 7.151	7.229
3	Ile	9.610	4.659	1.872	1.316, 1.013, 0.800	0.682	-----	-----	-----
4	Thr	8.476	5.185	3.988	, 1.124	-----	-----	-----	-----
5	Val	9.087	4.495	2.039	, 0.878	-----	-----	-----	-----
6	Thr	8.445	4.887	3.983	, 1.063	-----	-----	-----	-----
7	Ile	8.962	4.417	1.898	, , 0.922	0.831	-----	-----	-----
8	Gly	8.695	4.067, 3.941	-----	-----	-----	-----	-----	-----
9	Gly	8.290	3.957, 3.839	-----	-----	-----	-----	-----	-----
10	Gly	8.218	3.988, 3.912	-----	-----	-----	-----	-----	-----

11	Ile	8.287	4.456	1.856	, , 0.923		-----	-----	-----
12	dPro	-----	4.431	2.312,	2.031,	3.970, 3.766	-----	-----	-----
13	Gly	8.181	3.940, 3.869	-----	-----	-----	-----	-----	-----
14	Lys	7.847	4.349	1.832,	1.470, 1.425	1.687,	3.001,		-----
15	Gly	8.509	3.961,	-----	-----	-----	-----	-----	-----
16	Gly		,	-----	-----	-----	-----	-----	-----
17	Gly		,	-----	-----	-----	-----	-----	-----
18	Lys	8.320	4.492	1.751,	1.376,	1.653,	2.948,		-----
19	Lys	8.412	5.088	1.692,	1.420, 1.322	1.561,	2.918,		-----
20	Ile	9.037	4.614	1.866	, , 0.887		-----	-----	-----
21	Arg	8.327	5.403	1.747,	1.565,	2.821,		-----	, , ,
22	Val	9.331	4.815	2.102	0.958, 0.901	-----	-----	-----	-----
23	Trp	8.626	4.575	2.793, 2.134	-----	6.921	9.968, 5.204	7.412, 6.474	7.082
24	Glu	8.025	4.028	1.668, 1.577	1.975,	-----		-----	-----

R-G3IPGKG3-E (pH 6.5 @ 300 K)

#	Res		Hα	Hβ	Hγ	Hδ	Hε	Hζ	Hη
1	Arg		3.555	1.748, 1.642	1.398, 1.276	3.088, 3.040		-----	, , ,
2	Trp		5.284	3.200, 3.079	-----	7.460	10.278, 7.501	7.429, 7.155	7.238
3	Ile	9.466	4.614	1.863	1.332, 1.022, 0.802	0.696	-----	-----	-----
4	Thr	8.420	5.088	4.001	, 1.125	-----	-----	-----	-----
5	Val	8.989	4.459	2.042	0.935, 0.882	-----	-----	-----	-----
6	Thr	8.411	4.799	4.007	, 1.080	-----	-----	-----	-----
7	Ile	8.825	4.364	1.893	1.462, 1.192, 0.921	0.823	-----	-----	-----
8	Gly	8.646	4.055, 3.937	-----	-----	-----	-----	-----	-----
9	Gly	8.294	3.975, 3.914	-----	-----	-----	-----	-----	-----
10	Gly	8.256	3.926, 3.884	-----	-----	-----	-----	-----	-----
11	Ile	7.998	4.477	1.836	1.477, 1.149, 0.935	0.850	-----	-----	-----
12	Pro	-----	4.341	2.298, 1.916	2.101, 1.964	3.967, 3.697	-----	-----	-----
13	Gly	8.558	4.142, 3.831	-----	-----	-----	-----	-----	-----
14	Lys	8.040	4.487	1.760, 1.670	1.424, 1.358	1.931,	2.985,		-----
15	Gly		,	-----	-----	-----	-----	-----	-----
16	Gly		,	-----	-----	-----	-----	-----	-----
17	Gly		,	-----	-----	-----	-----	-----	-----
18	Lys	8.298	4.454	1.659,	1.402, 1.360	1.776,	2.949,		-----
19	Lys	8.371	5.012	1.582,	1.416, 1.317	1.685,	2.912,		-----
20	Ile	8.927	4.564	1.863	1.066, 1.037, 0.807	0.882	-----	-----	-----
21	Arg	8.301	5.284	1.725, 1.572	1.533,	2.826,		-----	, , ,
22	Val	9.189	4.736	2.088	0.934, 0.886	-----	-----	-----	-----
23	Trp	8.547	4.591	2.842, 2.253	-----	6.945	9.960,	7.410, 6.502	7.085
24	Glu	7.974	4.030	1.701, 1.604	1.977,	-----		-----	-----

R-G6IpGKG6-E (pH 6.5 @ 300 K)

#	Res		Hα	Hβ	Hγ	Hδ	Hε	Hζ	Hη
1	Arg		3.584	,	,	3.074, 3.074		-----	, , ,
2	Trp	8.892	5.204	,	-----	7.450	10.271, 7.509	7.431, 7.157	7.239
3	Ile				, ,		-----	-----	-----
4	Thr	8.405	5.043	4.011	, 1.131	-----	-----	-----	-----
5	Val	8.930	4.445	2.050	, 0.885	-----	-----	-----	-----
6	Thr	8.391	4.750	4.007	, 1.093	-----	-----	-----	-----
7	Ile	8.769	4.356	1.886	, , 0.921		-----	-----	-----
8	Gly		,	-----	-----	-----	-----	-----	-----
9	Gly		,	-----	-----	-----	-----	-----	-----
10	Gly		,	-----	-----	-----	-----	-----	-----
11	Gly		,	-----	-----	-----	-----	-----	-----
12	Gly		,	-----	-----	-----	-----	-----	-----
13	Gly		,	-----	-----	-----	-----	-----	-----
14	Ile	8.201	4.487	1.856	, , 0.914		-----	-----	-----
15	dPro	-----	4.429	2.310,	2.025,	3.929, 3.764	-----	-----	-----
16	Gly		,	-----	-----	-----	-----	-----	-----
17	Lys	7.971	4.368	1.888, 1.813	1.463, 1.445	1.685,	3.000,		-----
18	Gly	8.621	4.041, 3.965	-----	-----	-----	-----	-----	-----
19	Gly		,	-----	-----	-----	-----	-----	-----
20	Gly		,	-----	-----	-----	-----	-----	-----
21	Gly		,	-----	-----	-----	-----	-----	-----
22	Gly		,	-----	-----	-----	-----	-----	-----
23	Gly		,	-----	-----	-----	-----	-----	-----
24	Lys			,	,	,	,		-----
25	Lys			,	,	,	,		-----
26	Ile	8.846	4.506		, , 0.881		-----	-----	-----
27	Arg	8.300	2.840	1.708,	1.531,	,	6.670	-----	, , ,
28	Val				,	-----	-----	-----	-----
29	Trp	8.517	4.598	2.883, 2.314	-----	6.967	9.972,	7.427, 6.584	7.104
30	Glu	7.959	4.037	1.726, 1.626	1.986,	-----		-----	-----

R-G6IPGKG6-E (pH 6.5 @ 300 K)

#	Res		Hα	Hβ	Hγ	Hδ	Hε	Hζ	Hη
1	Arg		3.624	1.769, 1.674	1.420, 1.317	3.076, 3.057	7.172	-----	, , ,
2	Trp		5.195	3.205, 3.114	-----	7.415	10.246, 7.525	7.441, 7.155	7.236
3	Ile		4.534	1.843	1.330, 1.025, 0.803	0.705	-----	-----	-----
4	Thr	8.361	4.935	4.004	, 1.128	-----	-----	-----	-----
5	Val	8.828	4.407	2.046	0.880,	-----	-----	-----	-----
6	Thr	8.371	4.707	4.022	, 1.101	-----	-----	-----	-----
7	Ile	8.678	4.317	1.876	, , 0.913	0.829	-----	-----	-----

8	Gly	8.595	4.017, 3.981	-----	-----	-----	-----	-----	-----
9	Gly		,	-----	-----	-----	-----	-----	-----
10	Gly		,	-----	-----	-----	-----	-----	-----
11	Gly		,	-----	-----	-----	-----	-----	-----
12	Gly		,	-----	-----	-----	-----	-----	-----
13	Gly	8.255	3.931,	-----	-----	-----	-----	-----	-----
14	Ile	8.030	4.457	1.842	1.491, 1.170, 0.933	0.848	-----	-----	-----
15	Pro	-----	4.376	2.288, 1.924	2.068, 1.959	3.926, 3.691	-----	-----	-----
16	Gly	8.457	4.013, 3.924	-----	-----	-----	-----	-----	-----
17	Lys	8.161	4.394	1.886,	1.424, 1.391	1.755, 1.667	2.979,		-----
18	Gly	8.513	3.982,	-----	-----	-----	-----	-----	-----
19	Gly		,	-----	-----	-----	-----	-----	-----
20	Gly		,	-----	-----	-----	-----	-----	-----
21	Gly		,	-----	-----	-----	-----	-----	-----
22	Gly		,	-----	-----	-----	-----	-----	-----
23	Gly	8.291	3.989,	-----	-----	-----	-----	-----	-----
24	Lys	8.248	4.413	1.796, 1.728	1.396, 1.368	1.660,	2.957,		-----
25	Lys	8.342	4.875	1.673,	1.417, 1.333	1.597,	2.926,		-----
26	Ile	8.762	4.462	1.850	, , 0.874	0.813	-----	-----	-----
27	Arg	8.299	5.106	1.687, 1.598	1.504, 1.498	2.852,	6.710	-----	, , ,
28	Val		4.610	2.070	0.913, 0.888	-----	-----	-----	-----
29	Trp	8.459	4.607	2.926, 2.394	-----	6.994	9.985,	7.418, 6.638	7.112
30	Glu	7.924	4.042	1.748, 1.641	2.004,	-----		-----	-----

R-G5NPATGKG5-E (pH 6.5 @ 300 K)

#	Res		Hα	Hβ	Hγ	Hδ	Hε	Hζ	Hη
1	Arg		3.583	1.764, 1.633	1.413, 1.316	3.101, 3.080	7.129	-----	, , ,
2	Trp	8.896	5.252	3.223, 3.119	-----	7.469	10.299, 7.514	7.446, 7.177	7.254
3	Ile	9.547	4.587	1.867	1.332, 1.054, 0.813	0.701	-----	-----	-----
4	Thr	8.494	5.160	4.022	, 1.145	-----	-----	-----	-----
5	Val	8.950	4.464	2.054	0.889,	-----	-----	-----	-----
6	Thr	8.414	4.765	4.025	, 1.111	-----	-----	-----	-----
7	Ile	8.784	4.355	1.893	, , 0.925	0.841	-----	-----	-----
8	Gly	8.650	4.060, 3.992	-----	-----	-----	-----	-----	-----
9	Gly	8.345	3.972,	-----	-----	-----	-----	-----	-----
10	Gly	8.184	4.128,	-----	-----	-----	-----	-----	-----
11	Gly	8.391	3.995,	-----	-----	-----	-----	-----	-----
12	Gly		,	-----	-----	-----	-----	-----	-----
13	Asn	8.281	4.996	2.918, 2.725	-----	,	-----	-----	-----
14	Pro	-----	4.420	2.305, 1.981	2.018,	3.845, 3.759	-----	-----	-----
15	Ala	8.329	4.354	1.431	-----	-----	-----	-----	-----

16	Thr	7.874	4.360	4.301	, 1.216	-----	-----	-----	-----
17	Gly	8.532	3.984,	-----	-----	-----	-----	-----	-----
18	Lys	8.217	4.367	1.882,	1.680,	1.758,	2.995,	7.524	-----
19	Gly	8.289	3.992,	-----	-----	-----	-----	-----	-----
20	Gly	8.289	3.992,	-----	-----	-----	-----	-----	-----
21	Gly		,	-----	-----	-----	-----	-----	-----
22	Gly		,	-----	-----	-----	-----	-----	-----
23	Gly		,	-----	-----	-----	-----	-----	-----
24	Lys	8.304	4.448	1.809,	1.675,	1.740,	2.969,	7.561	-----
25	Lys	8.378	4.958	1.697,	1.434,	1.598,	2.937,	7.495	-----
26	Ile	8.879	4.527	1.869	, , 0.889		-----	-----	-----
27	Arg	8.346	5.222	1.743, 1.637	1.543,	2.859,	6.702	-----	, , ,
28	Val	9.328	4.768	2.079	0.941, 0.905	-----	-----	-----	-----
29	Trp	8.601	4.587	2.888,	-----	6.980	10.025,	7.432, 6.626	7.117
30	Glu	8.029	4.113	1.851, 1.604	2.165,	-----		-----	-----

WWst29-NPATGR (pH 8 @ 300 K)

#	Res		Hα	Hβ	Hγ	Hδ	Hε	Hζ	Hη
1	Lys			,	,	,	,		-----
2	Gly		,	-----	-----	-----	-----	-----	-----
3	Trp	8.124	5.081	3.258, 3.097	-----	7.289	10.365, 7.427	7.492, 6.974	6.946
4	Glu	9.706	4.887	2.242, 2.134	2.482, 2.334	-----		-----	-----
5	Lys	8.749	4.714	1.699,	1.084, 0.851	1.490,	,		-----
6	Arg	9.140	4.827	0.546,	,	,		-----	, , ,
7	Trp	8.670	4.399	2.720, 2.069	-----	6.679	9.993, 5.465	7.306, 6.331	6.890
8	Asn	7.978	5.224	3.281, 2.501	-----	,	-----	-----	-----
9	Pro	-----		,	,	,	-----	-----	-----
10	Ala	7.686	4.145	1.440	-----	-----	-----	-----	-----
11	Thr	6.933	4.305	4.058	,	-----	-----	-----	-----
12	Gly	7.811	3.732, 3.238	-----	-----	-----	-----	-----	-----
13	Arg	6.559	4.547	1.994,	1.542,	,		-----	, , ,
14	Trp	8.615	5.408	3.206, 3.029	-----	7.650	10.272, 7.490	7.272, 7.056	7.124
15	Tyr	9.580	5.070	2.862, 2.647	-----	6.918	6.385	-----	
16	Tyr	9.083	5.331	2.912, 2.666	-----			-----	
17	Tyr	9.601	5.619	2.960, 2.740	-----			-----	
18	Asn	8.368	4.286	2.233, -0.082	-----	,	-----	-----	-----
19	Arg	8.344	3.837	,	,	,		-----	, , ,
20	Ile	8.028	3.885	1.984	, , 0.821		-----	-----	-----
21	Thr	7.615	4.211		,	-----	-----	-----	-----
22	Gly	8.269	4.087, 3.635	-----	-----	-----	-----	-----	-----
23	Lys	7.087	4.296	1.823,	1.462,	1.591,	,		-----

24	Arg	8.372	5.935	,	,	,		-----	, , ,
25	Gln	9.304	4.819	,	2.407,	-----	,	-----	-----
26	Trp	8.618	5.018	3.610, 3.206	-----	7.500	10.156, 8.030	7.427, 6.883	6.983
27	Glu	8.029	4.250	,	,	-----		-----	-----
28	Arg	8.159	4.425	,	,	,		-----	, , ,
29	Pro	-----	3.880	1.078, 0.940	0.776, 0.258	2.471,	-----	-----	-----
30	Asp			,	-----		-----	-----	-----

WWst29-NPATGR (pH 2.5 @ 300 K)

#	Res		Hα	Hβ	Hγ	Hδ	Hε	Hζ	Hη
1	Lys			,	,	,	,		-----
2	Gly	8.973	4.078, 3.766	-----	-----	-----	-----	-----	-----
3	Trp	8.047	4.995	3.243, 3.137	-----	7.305	10.303,	,	
4	Glu	9.476	4.847	2.243, 2.122	2.649, 2.501	-----		-----	-----
5	Lys	8.756	4.747	1.704, 1.512	1.119, 0.919	,	,		-----
6	Arg	9.101	4.828	1.518,	0.760,	,		-----	, , ,
7	Trp	8.689	4.385	2.744, 2.112	-----	6.703	10.010, 5.543	7.320, 6.418	6.928
8	Asn	7.943	5.175	3.275, 2.463	-----	,	-----	-----	-----
9	Pro	-----	3.847	2.428,	2.101, 2.035	,	-----	-----	-----
10	Ala	7.712	4.166	1.437	-----	-----	-----	-----	-----
11	Thr	6.910	4.318		, 1.039	-----	-----	-----	-----
12	Gly	7.853	3.754, 3.275	-----	-----	-----	-----	-----	-----
13	Arg	6.607	4.542	1.957,	1.540,	,		-----	, , ,
14	Trp	8.555	5.326	3.195, 3.015	-----	7.634	10.285, 7.449	7.303, 7.077	7.139
15	Tyr	9.492	5.019	2.891, 2.756	-----			-----	
16	Tyr	8.945	5.302	2.919, 2.701	-----	6.900	6.748	-----	
17	Tyr	9.403	5.519	2.991, 2.746	-----			-----	
18	Asn	8.385	4.319	2.319,	-----	,	-----	-----	-----
19	Arg	8.231	3.909	,	,	,		-----	, , ,
20	Ile	8.061	3.946	1.973	, , 0.843		-----	-----	-----
21	Thr				,	-----	-----	-----	-----
22	Gly		,	-----	-----	-----	-----	-----	-----
23	Lys	7.245	4.334	,	,	,	,		-----
24	Arg	8.388	5.694	2.022,	1.946, 1.952	,		-----	, , ,
25	Gln	9.205	4.786	2.149,	2.362,	-----	,	-----	-----
26	Trp	8.484	4.996	3.537, 3.312	-----	7.451	10.170, 7.893	7.449, 6.975	7.077
27	Glu	7.904	4.441	1.889,	2.351, 2.256	-----		-----	-----
28	Arg			,	,	,		-----	, , ,
29	Pro	-----	4.835	1.508,	, 0.743	3.013, 2.961	-----	-----	-----
30	Asp			,	-----		-----	-----	-----

WWst29_pHsw (pH 8 @ 300 K)

#	Res		Hα	Hβ	Hγ	Hδ	Hε	Hζ	Hη
1	Lys			,	,	,	,		-----
2	Gly		,	-----	-----	-----	-----	-----	-----
3	Trp	8.166	5.081	3.267, 3.107	-----	7.296	10.383, 7.493	7.436, 6.952	6.992
4	Glu	9.741	4.902	2.334, 2.145	2.496, 2.249	-----		-----	-----
5	Lys	8.749	4.762	1.677, 1.485	1.041, 0.899	1.206, 1.206	,		-----
6	Arg	9.161	4.827	1.544, 2.792	, 0.544	3.074,		-----	, , ,
7	Trp	8.667	4.297	2.765, 2.209	-----	6.648	9.996, 5.506	7.330, 6.342	6.935
8	His			,	-----	,	,	-----	-----
9	Pro	-----		,	,	,	-----	-----	-----
10	Ala	8.223	4.476		-----	-----	-----	-----	-----
11	Thr	7.289	4.380		,	-----	-----	-----	-----
12	Gly	8.028	3.781, 3.258	-----	-----	-----	-----	-----	-----
13	Lys	6.680	4.548	2.023,	,	,	,		-----
14	Trp	8.496	5.414	3.155, 2.985	-----	7.621	10.358, 7.475	7.318, 7.136	7.142
15	Tyr	9.418	5.017	2.370,	-----			-----	
16	Tyr	9.014	5.298	2.900, 2.656	-----	6.855	6.770	-----	
17	Tyr	9.640	5.601	2.936, 2.753	-----	6.883	6.683	-----	
18	Asn	8.393	4.281	2.253, -0.062	-----	,	-----	-----	-----
19	Arg	8.369	3.849	,	,	,		-----	, , ,
20	Ile	8.037	3.884		, , 0.823		-----	-----	-----
21	Thr	7.624	4.211		,	-----	-----	-----	-----
22	Gly	8.281	4.089, 3.622	-----	-----	-----	-----	-----	-----
23	Lys	7.078	4.310	1.831,	,	1.463,	,		-----
24	Arg	8.409	5.926	,	,	,		-----	, , ,
25	Gln	9.347	4.870	2.146,	2.439,	-----	6.648, 7.282	-----	-----
26	Trp	8.797	4.913	3.644, 3.170	-----	7.281	10.181, 8.054	7.067, 6.804	6.435
27	Glu	8.119	4.479	,	,	-----		-----	-----
28	Arg	8.410	4.552	,	,	,		-----	, , ,
29	Pro	-----	3.875	1.108, 1.036	0.701, 0.173	2.445,	-----	-----	-----
30	Asp			,	-----		-----	-----	-----

WWst29_pHsw (pH 2.5 @ 300 K)

#	Res	Hα	Hβ	Hγ	Hδ	Hε	Hζ	Hη
1	Lys		,	,	,	,		-----
2	Gly	8.673 3.981,	-----	-----	-----	-----	-----	-----
3	Trp		,	-----		,	,	
4	Glu	8.528 4.422	,	,	-----		-----	-----
5	Lys		,	,	,	,		-----
6	Arg		,	,	,		-----	, , ,
7	Trp		,	-----		,	,	

8	His			,	-----	,	,	-----	-----
9	Pro	-----		,	,	,	-----	-----	-----
10	Ala	8.395	4.294	1.355	-----	-----	-----	-----	-----
11	Thr	7.938	4.310		, 1.166	-----	-----	-----	-----
12	Gly		,	-----	-----	-----	-----	-----	-----
13	Lys			,	,	,	,	-----	
14	Trp	8.299	4.708	,	-----		,	,	
15	Tyr	8.370	4.581	,	-----		-----		
16	Tyr			,	-----		-----		
17	Tyr	8.459	4.609	,	-----		-----		
18	Asn			,	-----	,	-----	-----	-----
19	Arg			,	,	,	-----	, , ,	
20	Ile	8.145	4.107	1.949	, , 0.870		-----	-----	-----
21	Thr	8.031	4.317		, 1.171	-----	-----	-----	-----
22	Gly		,	-----	-----	-----	-----	-----	-----
23	Lys			,	,	,	,	-----	
24	Arg			,	,	,	-----	, , ,	
25	Gln	8.355	4.281	,	,	-----	,	-----	-----
26	Trp			,	-----		,	,	
27	Glu			,	,	-----		-----	-----
28	Arg			,	,	,	-----	, , ,	
29	Pro	-----		,	,	,	-----	-----	-----
30	Asp			,	-----		-----	-----	-----

WWst29-p2-pHSW (pH 8 @ 300 K)

#	Res		Hα	Hβ	Hγ	Hδ	Hε	Hζ	Hη
1	Lys			,	,	,	,		-----
2	Gly		,	-----	-----	-----	-----	-----	-----
3	Trp	8.216	4.877	3.188,	-----	7.355	10.189,	,	
4	Glu	9.776	4.886	2.317, 2.075	2.387, 2.212	-----		-----	-----
5	Lys	8.722	4.759	1.708, 1.496	1.076, 0.862	,	,		-----
6	Arg	9.119	4.839	1.542, 1.485	1.408, 0.555	,		-----	, , ,
7	Trp	8.663	4.383	2.715, 2.046	-----	6.678	9.994, 5.461	, 6.349	
8	Asn	7.966	5.210	3.293, 2.502	-----	,	-----	-----	-----
9	Pro	-----	3.886	2.429,	2.105, 2.023	,	-----	-----	-----
10	Ala	7.685	4.148	1.440	-----	-----	-----	-----	-----
11	Thr	6.925	4.306		,	-----	-----	-----	-----
12	Gly	7.815	3.734, 3.238	-----	-----	-----	-----	-----	-----
13	Arg	6.556	4.548	1.987,	1.537,	,		-----	, , ,
14	Trp	8.613	5.403	3.199, 3.024	-----	7.651	10.266,	,	
15	Tyr	9.584	5.080	2.867, 2.678	-----			-----	

16	Tyr	9.121	5.416	2.982, 2.688	-----			-----	
17	Tyr	9.750	5.848	3.021, 2.717	-----			-----	
18	His	8.331	4.490	2.402, 0.345	-----	,	,	-----	-----
19	Pro	-----	3.795	2.314,	, 1.827	3.664,	-----	-----	-----
20	Ala				-----	-----	-----	-----	-----
21	Thr	7.375	4.495		,	-----	-----	-----	-----
22	Gly	8.607	4.201,	-----	-----	-----	-----	-----	-----
23	Lys	7.340	4.297	,	,	,	,		-----
24	Arg	8.349	5.908	,	,	,		-----	, , ,
25	Gln	9.276	4.790	2.379, 2.132	,	-----	,	-----	-----
26	Trp	8.611	5.024	3.636, 3.269	-----	7.497	10.158, 8.019	, 7.003	
27	Glu	8.153	4.449	,	,	-----		-----	-----
28	Arg	8.372	4.547	,	,	,		-----	, , ,
29	Pro	-----	3.879	1.120, 1.034	0.836, 0.416	2.537,	-----	-----	-----
30	Asp	7.981	4.419	2.603,	-----		-----	-----	-----

WWst29-p2-pHSW (pH 2.5 @ 300 K)

#	Res		Hα	Hβ	Hγ	Hδ	Hε	Hζ	Hη
1	Lys			,	,	,	,		-----
2	Gly	8.692	4.017, 3.906	-----	-----	-----	-----	-----	-----
3	Trp	8.140	4.843	3.257, 3.097	-----		,	,	
4	Glu	8.882	4.611	2.115, 1.809	2.449,	-----		-----	-----
5	Lys	8.542	4.972	1.608, 1.478	1.115, 1.049	,	,		-----
6	Arg	9.062	4.869	1.655, 1.551	1.302,	,		-----	, , ,
7	Trp	8.791	4.277	2.752, 2.093	-----	6.706	10.003, 5.630	7.305, 6.459	6.937
8	Asn	7.783	5.053	3.258, 2.326	-----	,	-----	-----	-----
9	Pro	-----	3.891	2.415,	2.079, 2.020	3.831,	-----	-----	-----
10	Ala	7.765	4.184	1.412	-----	-----	-----	-----	-----
11	Thr	6.876	4.303		, 1.019	-----	-----	-----	-----
12	Gly	7.952	3.766, 3.303	-----	-----	-----	-----	-----	-----
13	Arg	6.691	4.464	1.825,	1.489,	,		-----	, , ,
14	Trp	8.353	5.124	3.109, 2.901	-----	7.563	10.275, 7.341	7.348, 7.064	7.174
15	Tyr	9.386	4.891	2.999,	-----	7.061	6.596	-----	
16	Tyr	8.585	5.133	2.811, 2.748	-----	7.038	6.747	-----	
17	Tyr	8.923	4.848	2.850,	-----			-----	
18	His	8.426	4.794	2.819, 2.437	-----	, 6.736	8.139,	-----	-----
19	Pro	-----	4.279	2.290,	, 1.905	3.487, 3.342	-----	-----	-----
20	Ala	8.450	4.391	1.417	-----	-----	-----	-----	-----
21	Thr	8.129	4.394		, 1.227	-----	-----	-----	-----
22	Gly	8.394	4.007,	-----	-----	-----	-----	-----	-----
23	Lys	8.176	4.321	,	,	,	,		-----
24	Arg	8.203	4.304	,	,	,		-----	, , ,

25	Gln	8.460	4.368	2.040, 1.953	2.287,	-----	,	-----	-----
26	Trp	8.246	4.678	3.265,	-----		,	,	
27	Glu	7.954	4.312	1.968, 1.800	2.291,	-----		-----	-----
28	Arg	8.388	4.348	1.710, 1.528	1.580,	,		-----	, , ,
29	Pro	-----	4.387	2.281,	2.028,	3.765, 3.647	-----	-----	-----
30	Asp	8.455	4.648	,	-----		-----	-----	-----

WWst29-G2HPATGK (pH 8 @ 300 K)

#	Res		Hα	Hβ	Hγ	Hδ	Hε	Hζ	Hη
1	Lys			,	,	,	,		-----
2	Gly		,	-----	-----	-----	-----	-----	-----
3	Trp	8.094	5.050	3.227, 3.110	-----	7.271	10.325, 7.424	7.477, 6.949	7.007
4	Glu			,	,	-----		-----	-----
5	Lys	8.621	4.640	1.599,	0.949,	1.433,	,		-----
6	Arg	8.889	4.724	1.491, 1.464	0.560,	,		-----	, , ,
7	Trp	8.606	4.628	2.865, 2.338	-----	6.798	9.957, 5.320	7.228, 6.342	6.976
8	Gly	8.440	4.238, 3.873	-----	-----	-----	-----	-----	-----
9	Gly		,	-----	-----	-----	-----	-----	-----
10	His			,	-----	,	,	-----	-----
11	Pro	-----		,	,	,	-----	-----	-----
12	Ala	8.046	4.417		-----	-----	-----	-----	-----
13	Thr	7.689	4.358		,	-----	-----	-----	-----
14	Gly	8.319	4.087, 3.745	-----	-----	-----	-----	-----	-----
15	Lys	7.820	4.308	1.676,	1.301,	1.536,	,		-----
16	Gly	8.443	3.474,	-----	-----	-----	-----	-----	-----
17	Gly	7.684	3.786, 3.189	-----	-----	-----	-----	-----	-----
18	Trp	8.148	5.232	3.122, 2.855	-----	7.529	10.366,	7.442,	7.194
19	Tyr	9.269	4.639	,	-----			-----	
20	Tyr	8.799	5.180	2.880, 2.642	-----	6.825	6.704	-----	
21	Tyr		5.539	2.886, 2.746	-----	6.872	6.675	-----	
22	Asn	8.327	4.288	2.300,	-----	,	-----	-----	-----
23	Arg	8.417	3.882	1.821,	1.698,	,		-----	, , ,
24	Ile	8.025	3.886	2.093	, 1.117, 0.818		-----	-----	-----
25	Thr	7.609	4.211		, 1.058	-----	-----	-----	-----
26	Gly	8.276	4.079, 3.641	-----	-----	-----	-----	-----	-----
27	Lys	7.116	4.319	1.834,	,	1.598,	,		-----
28	Arg	8.422	5.888	,	,	,		-----	, , ,
29	Gln	9.342	4.919	,	,	-----	,	-----	-----
30	Trp	9.069	4.723	3.615, 3.135	-----	7.335	9.909, 7.813	7.010, 6.776	6.782
31	Glu	8.041	4.471	1.966,	2.336, 2.248	-----		-----	-----
32	Arg			,	,	,		-----	, , ,

33	Pro	-----	4.518	,	0.981, 0.836	,	-----	-----	-----
34	Asp			,	-----		-----	-----	-----

Appendix D – Coupling Constants of Tryptophan.

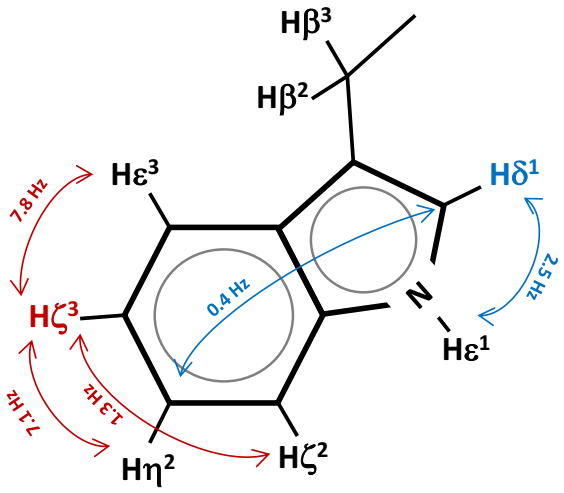

	Hδ1	Hε1	Hζ2	Hη2	Hζ3	Hε3
Hδ1		2.5	-	0.4	-	-
Hε1	2.5		-	-	-	0.8
Hζ2	-	-		8.1	1.3	0.9
Hη2	0.4	-	8.1		7.1	1.2
Hζ3	-	-	1.3	7.1		7.8
Hε3	-	0.8	0.9	1.2	7.8	

Appendix E – $\Delta\Delta G_F$ for each point mutation in Chapter 4.

	Position	Reference Number	Mutation	Parent	Free Energy of Unfolding ΔG_U (kJ/mol)			Parent - Mutated $\Delta\Delta G_F$ (kJ/mol)		
					pH 2.5	pH 6.5	pH 8	pH 2.5	pH 6.5	pH 8
Single Point Mutations	S-1	1	NPATGK	---	2.0	4.1	4.0			
		2	DPATGK	NPATGK	1.4	3.6	6.9	0.6	0.5	-2.9
		3	HPATGK	NPATGK	-7.9	0.9	5.5	9.9	3.2	-1.5
		4	CPATGK	NPATGK	-0.4	n.s.	4.5	2.4	n.s.	-0.6
		5	SPATGK	NPATGK	-1.2	2.2	-0.2	3.2	1.9	4.2
		6	QPATGK	NPATGK	-3.5	0.6	1.1	5.5	3.5	2.8
		7	APATGK	NPATGK	-3.8	-0.3	-0.4	5.8	4.4	4.4
		8	GPATGK	NPATGK	-3.0	-5.0	n.s.	5.0	9.1	n.s.
		9	IPATGK	NPATGK	-2.2	1.9	-0.1	4.2	2.3	4.1
		10	TPATGK	NPATGK	-4.7	0.5	-1.5	6.7	3.6	5.5
	T1	1-2a	NAATGK	NPATGK	0.5	3.0	4.0	1.5	1.1	0.0
		1-2v	NVATGK	NPATGK	-0.1	5.0	n.s.	2.1	-0.8	n.s.
		1-2g	NGATGK	NPATGK	-1.9	1.7	2.2	3.9	2.5	1.7
	T2	1-3v	NPVTGK	NPATGK	2.5	6.1	5.5	-0.5	-2.0	-1.5
	T3	1-4n	NPANGK	NPATGK	0.5	5.0	2.9	1.5	-0.8	1.1
		1-4d	NPADGK	NPATGK	-0.5	4.0	4.3	2.5	0.2	-0.4
		1-4h	NPAHGK	NPATGK	-7.9	-1.5	-4.3	9.9	5.7	8.3
		1-4a	NPAAGK	NPATGK	-7.3	-4.3	-6.5	9.3	8.5	10.4
		1-4g	NPAGGK	NPATGK	n.s.	-4.7	-0.8	n.s.	8.9	4.8
		1-4v	NPAVGK	NPATGK	-9.7	-2.1	-2.6	11.7	6.3	6.6
	T4	1-5a	NPATAK	NPATGK	n.s.	n.s.	-1.3	n.s.	n.s.	5.3
		1-5h	NPATHK	NPATGK	0.6	4.3	2.0	1.4	-0.2	2.0
	S+1	1-6g	NPATGG	NPATGK	-0.8	0.5	3.8	2.8	3.6	0.2
		1-6t	NPATGT	NPATGK	0.5	3.6	n.s.	1.5	0.5	n.s.
		1-6a	NPATGA	NPATGK	1.7	3.3	6.5	0.3	0.8	-2.5
Multiple Point Mutations		1-2a	NAATGK	---	0.5	3.0	4.0			
		+T4A	NAAAGK	NAATGK	-8.7	n.s.	n.s.	9.2	n.s.	n.s.
		1-4a	NPAAGK	---	-7.3	-4.3	-6.5			
		+G5T	NPAATK	NPAAGK	-7.3	-7.9	-9.7	0.0	3.6	3.3
		2	DPATGK	---	1.4	3.6	6.9			
		2-6r	DPATGR	DPATGK	1.3	3.8	7.9	0.1	-0.2	-1.1
		2-3g	DPGTGR	DPATGK	-0.8	1.9	7.9	2.2	1.7	-1.1
		2-5n	DPATNK	DPATGK	-3.0	1.4	n.s.	4.4	2.2	n.s.
		2-4s	DPASGK	DPATGK	-1.0	1.3	5.5	2.4	2.3	1.4
		+G5T	DPASTK	DPASGK	n.s.	-3.6	-3.3	n.s.	7.2	10.2
		3	HPATGK	---	-7.9	0.9	5.5			
		3R	HPATGR	HPATGK	-7.9	-3.0	4.1	0.0	3.9	1.3
		3R-4a	HPAAGR	HPATGR	-7.3	-7.3	n.s.	-0.6	8.3	n.s.

Appendix F – Concentration Dependence of **C4-22**

CD. CD spectra were taken from 6.25-100 μM to verify that the exciton couplet observed is from a monomeric species. (A) Raw CD spectra. (B) Signal at 228 nm vs. peptide concentration.

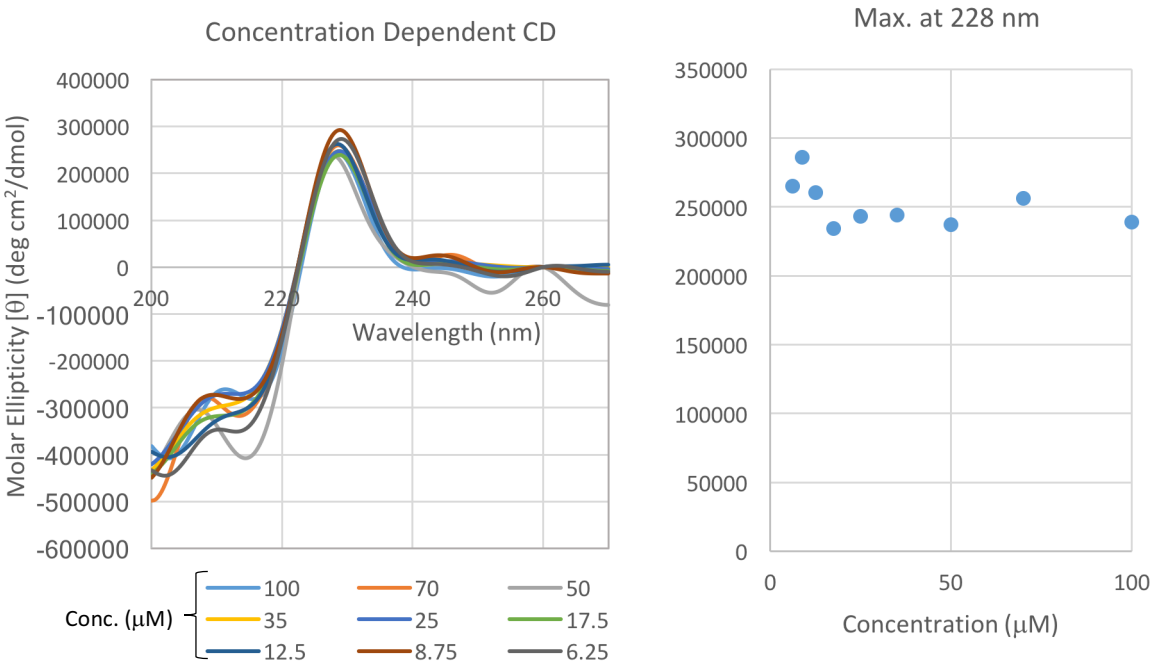

NMR. Concentration dependent NMR spectra of Peptide **C4-22** loop: NMR spectra of the aromatic and amide H_N region, taken at 30 (red) and 700 μM (blue). Peak position and broadening appear similar. The broadening seen, particularly at highly shifted resonances, is due to slow exchange between the folded and unfolded states.

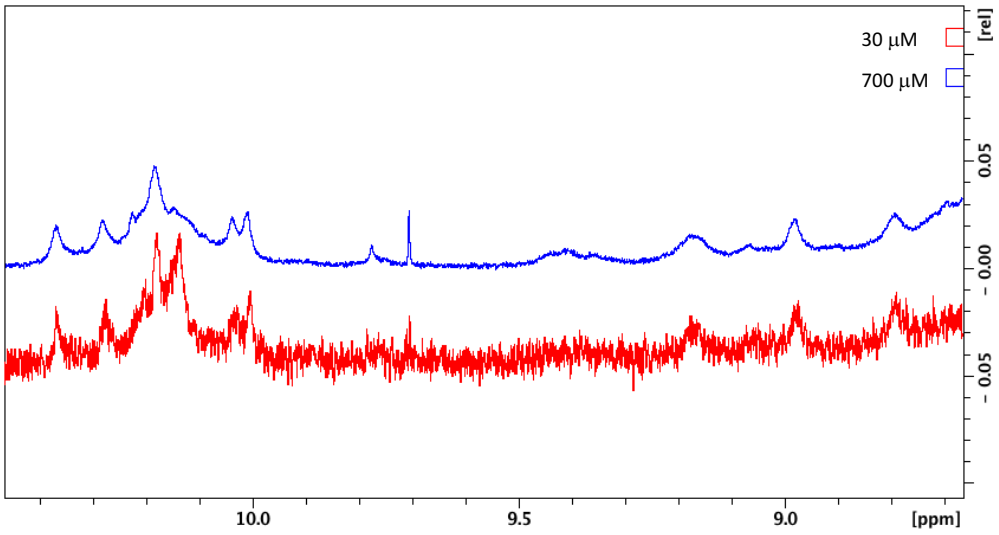

Appendix G – Loop CSDs for **G2-G4**.

H_N CSDs in Loop region of peptide **G2**.

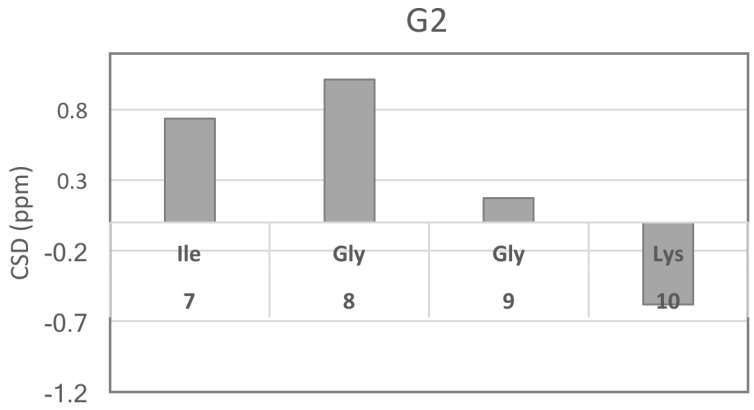

H_N CSDs in Loop region of peptide **G3**.

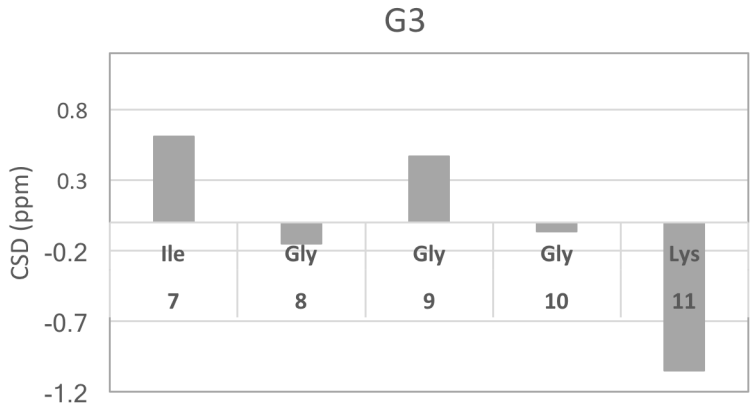

H_N CSDs in Loop region of peptide **G4**.

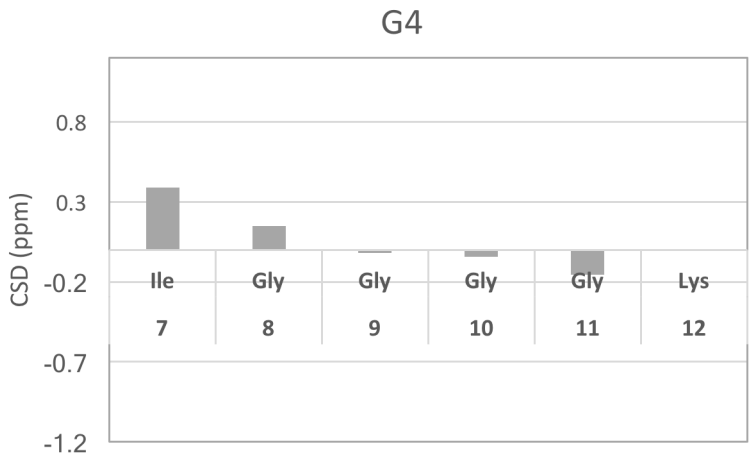

Appendix H – Maximum molar ellipticity at 228 nm for Loops **G2-G10**

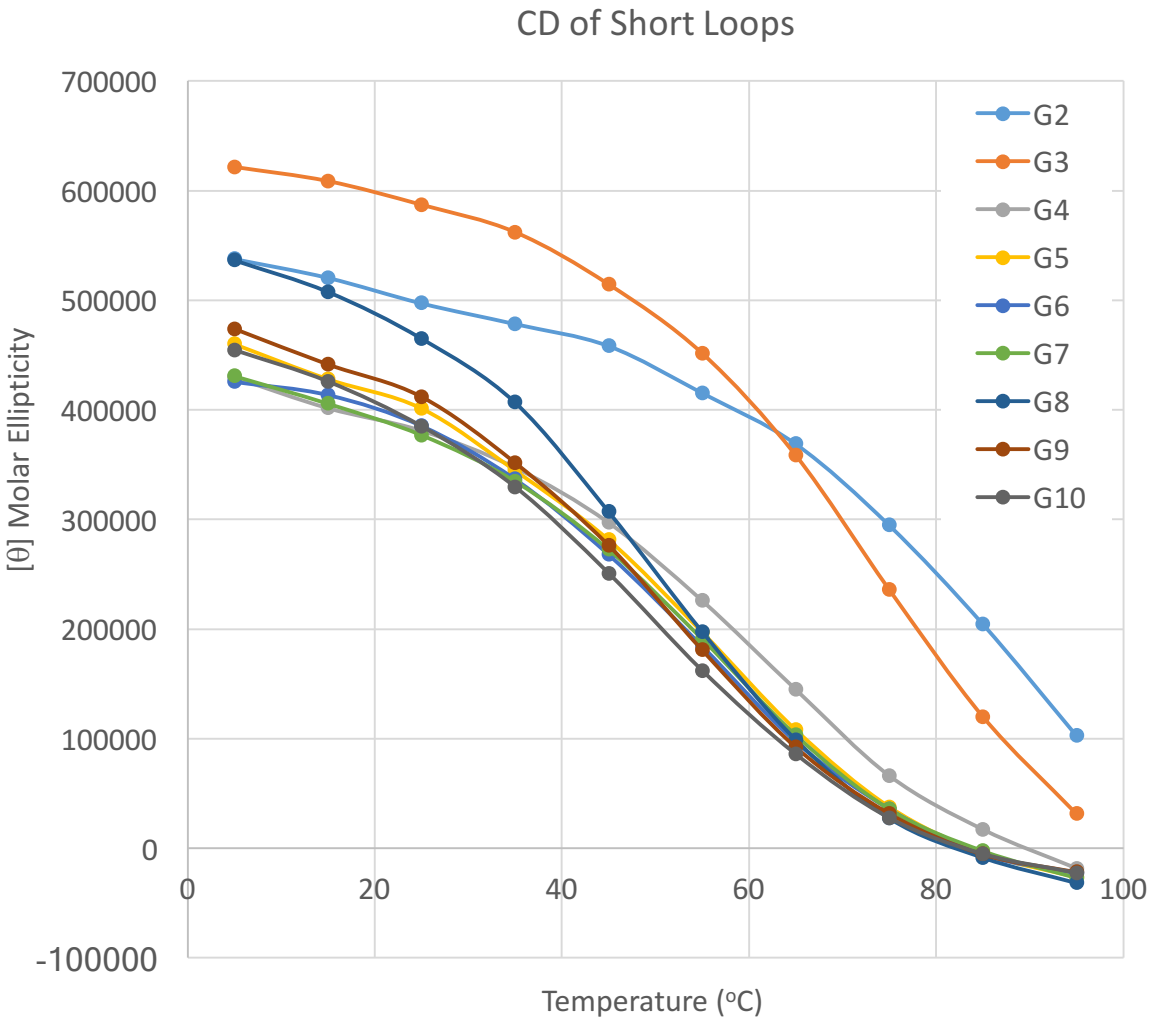

Appendix I – CD of Long Loops

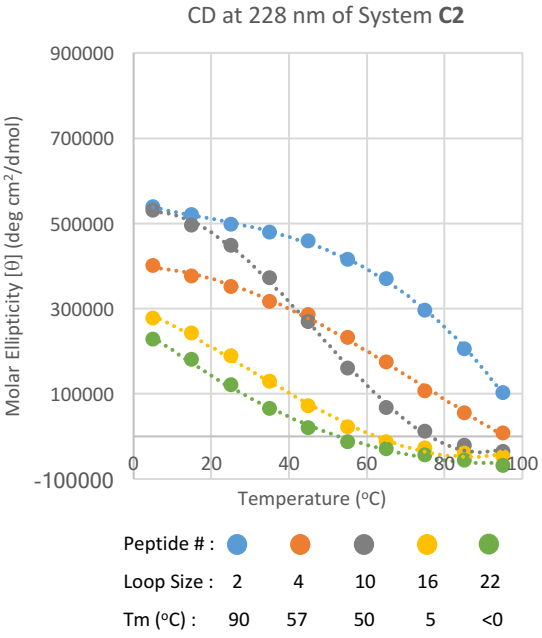

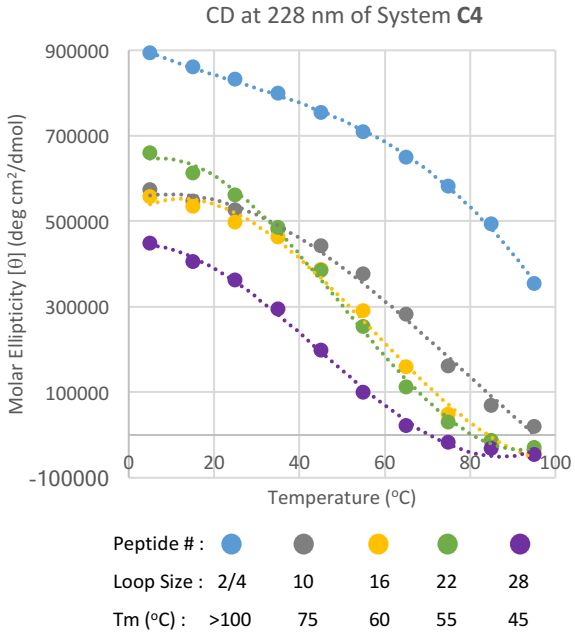

Appendix J – Supplemental information for pH switch WW domains.

Residue	Proton	CSD (ppm)	Reason for shift
E4	H_N	1.452	β-Strand amide anisotropy, H-bonding + Y17 sidechain ring current
W7	Hε3	-2.115	Ring current from W14 sidechain
R13	H_N	-1.685	Ring current from W7 and W14
Y15	H_N	1.586	β-Strand amide anisotropy, H-bonding
Y16	H_N	1.129	β-Strand amide anisotropy
Y16	Hα	0.926	β-Strand amide anisotropy
Y17	H_N	1.607	β-Strand amide anisotropy, H-bonding
N18	Hβ3	-2.882	Ring current from W3 sidechain
K23	H_N	-1.147	β-Strand amide anisotropy
R24	Hα	1.644	β-Strand amide anisotropy + Y17 sidechain ring current
Q25	H_N	0.98	β-Strand amide anisotropy, H-bonding
P29	Hγ3	-1.702	Ring current from W3 sidechain
W26	Hε3	0.45	Ring current from Y15 sidechain

Dependence of the CD of **p1-pHSW** upon pH. The value at the 228 nm maximum is plotted versus pH at 25 °C; the solid line is a fit of the Henderson-Hasselbalch equation to the data, for pKa = 4.8.